BIOMOLECULAR STUDIES ON CARNIITNE OCTANOYLTRANSFERASE

CARNITINE

By

Sitheswaran Nainamalai

University of St Andrews

St Andrews

Scotland

A thesis presented for the degree of Doctor of Philosophy at the University of St Andrews, October 2005.

DECLARATION

I, Sitheswaran Nainamalai, hereby certify that this thesis, which is approximately 31000 words in length, has been written by me, that it is the record of my work carried out by me and that it has not been submitted in any previous application for a higher degree.

Date 17/05/06... Signature of candidate ...

I was admitted as a research student in September 2001 and as a candidate for the degree of Doctor of Philosophy in September 2001; the higher study for which this record was carried out in the University of St. Andrews between 2001 and 2005.

Date 17/05/06.... Signature of candidate .

I hereby certify that the candidate has fulfilled the conditions of the Resolution and Regulations appropriate for the degree of Doctor of Philosophy in the University of St. Andrews and that the candidate is qualified to submit this thesis in application for that degree.

Date 16/05/06... Signature of supervisor

In submitting this thesis to the University of St. Andrews I understand that I am giving permission for it to be made available for use in accordance with the regulations of the University Library for the time being in force, subject to any copyright vested in the work not being affected thereby. I also understand that the title and abstract will be published, and that a copy of the work may be made and supplied to any *bona fide* library or research worker.

Date 17/05/06... Signature of candidate .

ACKNOWLEDGEMENTS

A journey is easier when you travel together. Interdependence is certainly more valuable than independence. I have been accompanied and supported by many people. It is a pleasant aspect that I have now the opportunity to express my gratitude for all of them.

The first person I would like to thank is my direct supervisor Dr Rona R Ramsay as a sympathetic and principle-centered person. Her overly enthusiasm and integral view on research and her mission for providing 'only high-quality work and not less', has made a deep impression on me. I owe her lots of gratitude for having me shown this way of research. She could not even realize how much I have learned from her. Besides of being an excellent supervisor, Rona was as close as a relative, advisor and a good friend to me. I am really glad that I have come to get know Rona Ramsay in my life.

Many thanks to Dr Nigel T Price for helping me in molecular biology and his friendly approach. I would also express my gratitude towards Professor Victor A Zammit for giving me the opportunity to work in his lab and his friendly advice. In addition I would also like to thank Professor Jim Naismith and his group for allowing me to access his lab and also helping me in crystallisation especially Dr.Kannan for his kind help throughout this PhD. A special thanks to Dr Naomi Fawcett, her friendly companionship in the lab over the last three years was much appreciated.

Sincere thanks go to everyone I have worked alongside throughout this PhD. My friend, Gildas Deniau for helping me in chemistry as well as a good friend and being a good flatmate I thank him a lot. In the course of writing this thesis I have acquired many new friends without whom the thesis would undoubtedly have been completed somewhat quicker a special thanks to Tanja Quintas, Annik and Matthieu Coliboeuf, also Mayca Onega, and Saraha Parveen. When I am not in the lab I was more than like playing golf. For making this such a pleasurable and successful pastime I am in debt to Martin, Richard, Vincent Brunet, Matthieu, Graham and Luke. Finally, thanks to all my friends I have made in St Andrews.

I feel a deep sense of gratitude for my late father and who formed part of my vision and taught me the good things that really matter in life. The happy memory of my father still provides a persistent inspiration for my journey in this life. I am grateful to my mother, sister and my family member's. Without the unconditional love and support I have received from them I would not be where I am today. I only hope I can repay them one day.

to my father…..

ABBREVIATIONS

Abs	-	Absorbance
ACC	-	Acetyl-CoA carboxylase
AP	-	Alkaline Phosphatase
ATP	-	Adenosine triphosphate
BCA	-	Bicinchonic acid
BSA	-	Bovine serum albumin
C75	-	α-methylene-γ-butyrolactone
CACT	-	Carnitine; acylcarnitine transporter
CAT	-	Carnitine acetyltransferase
cDNA	-	Complementary DNA
CIAP	-	Calf Intestine Alkaline Phosphatase
CoA	-	Coenzyme A
COT	-	Carnitine Octanoyltransferase
CPT	-	Carnitine Palmitoyltransferase
CPT1	-	Carnitine Palmitoyltransferase 1
CPT2	-	Carnitine Palmitoyltransferase2
DEAE	-	Diethylaminoethyl
DEPC	-	Diethylpyrocarbonate
DMSO	-	Dimethylsulphoxide
DNA	-	Deoxyribonucleic acid
dNTP	-	Deoxynucleotide triphosphate
DTT	-	Dithiothreitol
EDTA	-	Ethylenediaminetetracetic acid
ER	-	Endoplasmic reticulum

FAD	-	Flavin adenine dinucleotide
FADH	-	Flavin adenine dinucleotide, reduced form
FAO	-	Fatty acid oxidation
FAS	-	Fatty acid synthase
FFA	-	Free fatty acid
His	-	Histidine
IC_{50}	-	50% Inhibition Constant
IDDM	-	Insulin dependent diabetes mellitus
IPTG	-	Isopropyl-β-D-thiogalactopyranose
Kd	-	Dissociation constant
Ki	-	Inhibition constant
Km	-	Kinetic Constant
KPi	-	Potassium phosphate buffer
LB	-	Luria broth
LB	-	Luria-Bertani broth
LCFA	-	Long chain fatty acid
L-CPT1	-	Liver-Carnitine palmitoyltransferase1
LSLB	-	Low salt LB
M-CPT1	-	Muscle-Carnitine palmitoyltranferase1
NAD	-	Nicotinamide adenine dinucleotide
NADH	-	Nicotinamide adenine dinucleotide, reduced form
NIDDM	-	Non- Insulin dependent diabetes mellitus
OCTN	-	Organic Cation Transporter
PCR	-	Polymerase chain reactiom
PMSF	-	Phenyl Methane Sulphonylfluoride

S	-	Substrate
SDS-PAGE	-	Sodiumdodecyl sulphate-Polyacrylamide Gel Electrophoresis
TPB	-	Tryptone Phosphate Buffer
VLCFA	-	Very long chain fatty acid
Vmax	-	Maximum velocity
WHO	-	World health organisation
YPD	-	Yeast peptone dextrose

INDEX

ABSTRACT

Carnitine acyltransferases play an important role in fatty acid metabolism. These enzymes catalyses the reversible transfer of acyl groups between CoA and L-carnitine. Carnitine octanoyltransferase plays a crucial role in transferring medium chain fatty acids to carnitine for transport to the mitochondria for complete oxidation. The aim of this project is to analyse bovine, human and rat COT, and the bovine G553M and human Y340H mutants.

COT clones from rat, human, and cow were expressed and purified but only small crystals were obtained. Histidine-tagged clones afforded efficient and effective purification but no better crystals. Crystals were obtained for carnitine acyltransferase2 after expression in *E.coli*.

Functional studies established that the cloned bovine COT had kinetic properties identical to the enzyme purified from bovine liver. Human COT was characterised for the first time, revealing Km values of 1.5 μM for decanoyl-CoA, 58 μM for L-carnitine, 16 μM for CoA and 7.4 μM for palmitoyl-l-carnitine, similar to bovine COT. The acyl chain-length specificity was the greatest difference between species, with human COT having optimum selectivity for 10 and 16 carbons.

From its crystal structure, it was proposed that the short acyl-chain specificity of CAT was determined by methionine 554 which blocks access to a putative acyl-binding region. When G553 in bovine COT was altered to the methionine found in CAT, it

catalysed transfer only with acetyl-CoA. However, saturable hydrolysis of the ester also occurred indicating perturbation of the active site.

Inhibition studies demonstrated that conformationally constrained acetyl-L-carnitine analogues competed with both the acyl-CoA and L-carnitine substrates with Ki values around 10 μM. Acyl-aminocarnitine analogues designed for antiketotic action by inhibiting carnitine palmitoyltransferase1 (CPT1) were also highly effective inhibitors of COT, competing against both acyl-CoA and L-carnitine. The Ki values were submicromolar with 12 carbon derivative being the most effective at 30 nM. The CPT1 inhibitor, etomoxiryl-CoA, and the fatty acid synthase inhibitor, C75, were also shown to inhibit COT.

Neither rCOT nor hCOT in purified form were inhibited by malonyl-CoA when assayed with saturating acyl-CoA, although it is a competitive inhibitor with sub-saturating substrate. The same lack of inhibition was found with the Y340H mutant of hCOT demonstrating that a histidine at position 340 in hCOT does not alter the sensitivity to malonyl-CoA. Thus, consistent with its intra-peroxisomal location, COT is not regulated by malonyl-CoA.

1 INTRODUCTION

1.1 Carnitine

"Carnitine" (L-3-hydroxy-4-N,N,N-trimethylammoniumbutyrate) is a zwitterionic compound formed from lysine and widely distributed in nature, it acts as a co-enzyme in the process of turning fat into energy. It is not normally considered an essential nutrient because the body can manufacture all it needs. However, supplemental carnitine may improve the ability of certain tissues to produce energy. This effect has led to the use of carnitine in various muscle diseases as well as for heart conditions (Horne and Broquist, 1973).

Carnitine was discovered at the beginning of the last century, but its importance in metabolism was only established 50 years later. Carnitine is essential metabolite involved in a number of indispensable roles in intermediary metabolism one of which is to stimulate fatty acid oxidation (Fritz et al., 1955). This led to the discovery of the carnitine acyltransferases and the carnitine esters intermediates in the β-oxidation of fatty acids (reviewed in Bremer 1983). As interest in the function of carnitine increased, it became apparent that carnitine had more than one role in intermediary metabolism from the multi-organelle and multi-enzyme distribution of carnitine acyltransferases (Bieber *et al.*, 1982).

During the past decades, several roles for carnitine in metabolism have been proposed most of which are involved in conjugation of acyl residues to the β-hydroxyl group of carnitine to form esters, with subsequent translocation of activated long chain

fatty acids from the cytosol to the mitochondrial matrix, where β-oxidation takes place and excrete the acyl groups. Carnitine is also involved in transfer of the products of peroxisomal β-oxidation, including acetyl-CoA to the mitochondria for oxidation to CO_2 and H_2O in the Kreb's cycle (Verhoeven *et al.*, 1998).

Carnitine is present in most animal species, microorganism and plants. Animal tissues has high amount of carnitine from 0.2-6 $\mu mol.g^{-1}$ with highest concentration in heart, skeletal muscle, kidney and liver and with lowest amounts found in the brain and blood serum. Although, carnitine can be obtained from the diet, most mammals are capable of synthesizing carnitine endogenously. Carnitine is synthesized from lysine and methionine in which lysine in a protein provides the carbon backbone of carnitine and the 4-N-methyl group originates from methionine (Tanphaichitr *et al.*, 1971; Cox and Hopel.,1973). The general molecular structure of carnitine in shown in figure 1.1.

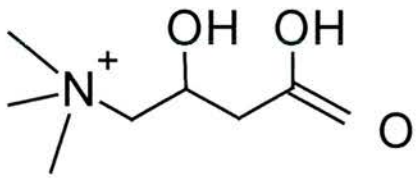

Figure 1.1 : Molecular structure of the carnitine

Carnitine does not help in protein synthesis, nor is it used as a neurotransmitter. Its main function seems to be transporting long chain fatty acids that will be eventually used for energy. Carnitine is made from protein-bound lysine and is dependent upon adequate amounts of Vitamin C, iron, thiamin (B1), and Vitamin B6 being present for

the process. Since carnitine is an alcohol and contains nitrogen, it is soluble in water. Carnitine comes in two forms; L-carnitine, the active form found in body tissues; and the "D" form, which is the inactive mirror image. The L form is the only one of value to supplement the normal serum concentration for uptake into the cell.

1.2 Fatty Acid Oxidation

The fatty acid oxidation pathways are located in the peroxisome, mitochondria, and endoplasmic reticulum. The oxidation of fatty acids is an important source of energy for ATP production in mitochondria through the entry of acetyl-CoA into the Krebs cycle. Fatty acids are completely oxidized inside the mitochondrial matrix but the fatty acids come from the cytosol. The cytosolic fatty acids are activated by esterification of coenzyme A (CoA) to form acyl-CoA. The CoA ester formation makes the metabolite impermeant through cellular membranes, and reduces the free CoA available in the limited pools of each subcellular compartment. Long-chain acyl-CoA synthesised in the cytosol is used for fatty acid oxidation in mitochondria or peroxisomes and also for complex lipid synthesis in the cytosol and endoplasmic reticulum. Some acyl-CoA esters also have regulatory activity such as regulation of gene expression, membrane trafficking and modulation of ion-channel activities (Zammit, 1999). Thus, the cell has two requirements: (i) a mechanism for the control of CoA ester concentrations that is rapid and does not involve the energetically expensive cycle of hydrolysis and resynthesis between the esters and the free acids, and (ii) a system that, after the initial synthesis of the CoA ester, enables the acyl moiety to permeate membranes without the need to re-expend energy. Diverse function and location means that ester must be regulated and moved between compartments. This is achieved through a reversible reaction between CoA esters and

L-carnitine to form carnitine ester and regenerate unesterified CoA by carnitine acyltransferases (Zammit, 1999, Ramsay and Zammit, 2004)

1.3 Reversible acyl transfer

The reversible transfer of acyl group between CoA and L-carnitine is catalysed by a family of enzymes carnitine acyltransferases (Chase and Tubbs, 1970; Bieber 1998; Ramsay *et al.*, 2001).

In carnitine acyltransferases the histidine residue in the active site acts as a general base in the catalysis (McGarry and Brown 1997, and Ramsay *et al.*, 2001). It extracts the proton from the 3-hydroxyl group of carnitine or the thiol group of CoA, depending on the direction of the reaction. The activated hydroxyl or thiol group can then directly attack the carbonyl carbon in acyl-CoA or acylcarnintine, and the reaction proceeds without the formation of an acyl-enzyme intermediate as shown in figure 1.2. (Jogl G and Tong, 2003)

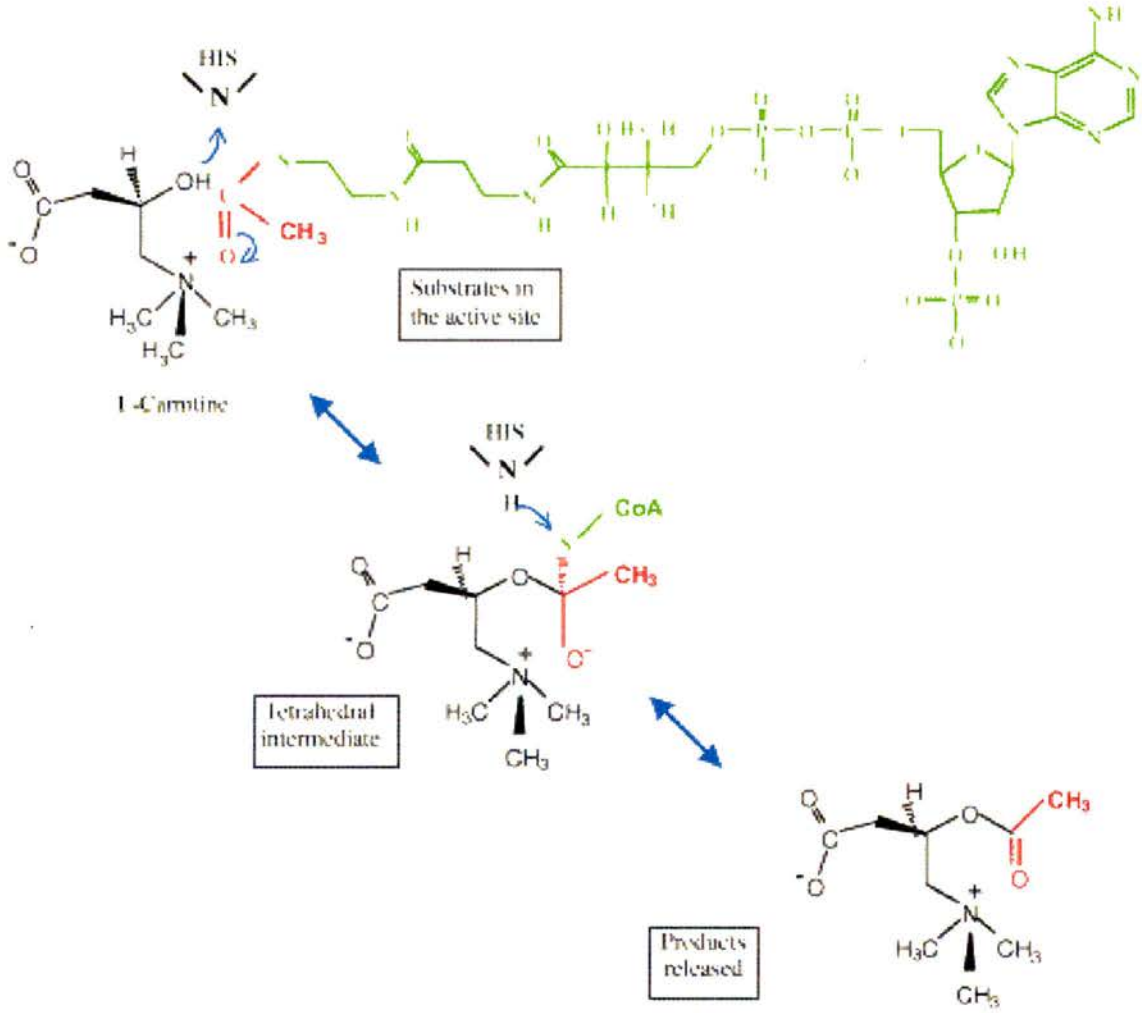

Figure 1.2: The general mechanism of carnitine acyltransferases. The histidine residue in the active site acts as a general base for the catalysis. L-Carnitine is shown in black, CoA in green, and the acetate group in red. In the active site, the catalytic base is positioned so that it can pull a proton from either carnitine or CoA depending on the direction of the freely reversible reaction. (Ramsay, 2004)

1.4 Carnitine Acyltransferases

Carnitine and carnitine acyltransferases are important for the transfer of activated long-chain fatty acids from the peroxisomes to the mitochondrion for β-oxidation (Fritz et al., 1955, McGarry and Brown, 1997, Ramsay et al., 2001). These enzymes are carnitine acetyltransferases (CAT), carnitine octanoyltransferase (COT), and carnitine palmitoyltransferase (CPT1A, CPT1B, and CPT 2). These have optimum activity with short, medium and long-chain fatty acids respectively (Ramsay *et al.*,

2001, Faye et al., 2005). All these enzymes are belongs to the carnitine acyltransferase family and generally contain 600 amino acid residues (shown in appendix), with molecular weights of about 70 kDa. These enzymes have different properties with respect to intracellular location, substrate specificity, kinetics, and physiological function (Feike *et al.*, 2000). The carnitine acyltransferases are organelle specific and location of carnitine-dependent enzyme activities are shown in figure 1.3.

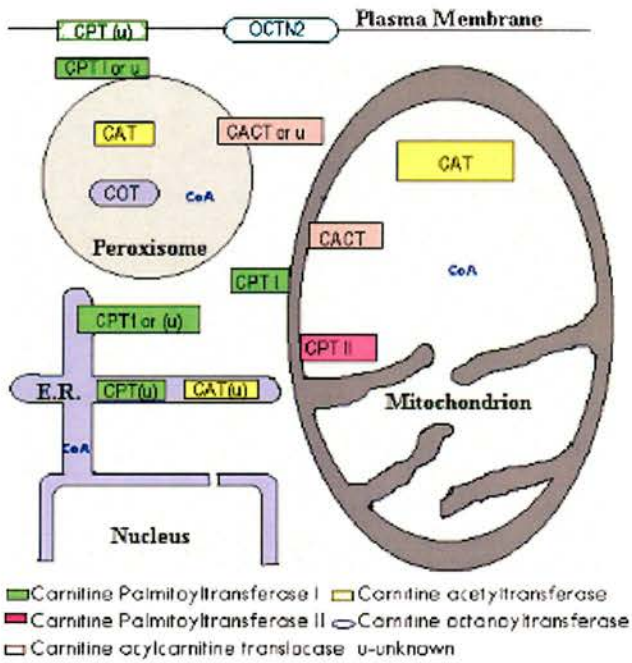

Figure 1.3: Proteins of the carnitine system connect pools of acetyl-CoA. Malonyl-CoA sensitive enzymes such as CPT 1, shown as green squres, act on cytosolic long-chain substrates. CAT is found only inside the organelles. The mitochondrial carniitine acylcarnitine translocase (CACT, pink squres) transfers carnitine and its esters across the membranes. The sodium-dependent organic cation transporter (OCTN2) is the high affinity carnitine transporter in the plasma membrane for uptake of carnitine into the cell (Ramsay, 2001).

1.4.1 Carnitine Acetyltransferase (CAT)

Carnitine acetyltransferase(CAT), catalyses the interconversion between acetyl-CoA and acetylcarnitine with carnitine and CoA as the co-substrate. CAT found in mitochondria, peroxisomes and mitochondrial preparations, is a single gene product with multiple targeting signals. In yeast, the peroxisomal CAT exports acetyl and propionyl moieties out of peroxisome, formed during the partial β-oxidation of very long-chain fatty acids and transports the acetyl moieties to the mitochondria for oxidation (Zammit, 1999). The mitochondrial CAT plays an important role in modulating matrix acetyl-CoA concentration the free CoA that is essential for Citric acid cycle.

1.4.2 Carnitine Palmitoyltransferase 1 (CPT1)

Carnitine palmitoyltransferase 1 (CPT1) is an integral membrane enzyme located on the mitochondrial outer membrane (Figure 1.4). The membrane topology of CPT1 predicts exposure of the CPTI N- and C-terminal domains crucial for activity and malonyl CoA sensitivity on the cytosolic side of the outer mitochondrial membrane (Fraser et al., 1997). The CPT1 has direct access to the cytosolic pool of acyl-CoA and its most distinguishing kinetic characteristic is binding of malonyl-CoA that regulates its activity. Mammalian tissues express three different isoforms of CPT 1, a liver isoform (L-CPT 1), muscle isoform (M-CPT1) and a third isoform abundant in brain (CPT1-C), (Britton et al., 1995; Yamazaki et al., 1996; Price et al., 2002). L-CPT1 is the major one expressed in the liver, kidney, pancreatic islets, ovary, spleen, intestine and brain, M-CPT1 is expressed in heart/skeletal muscle, (Yamazaki et al., 1995; Morillas *et al.*, 2001, Faye et al.,2005).

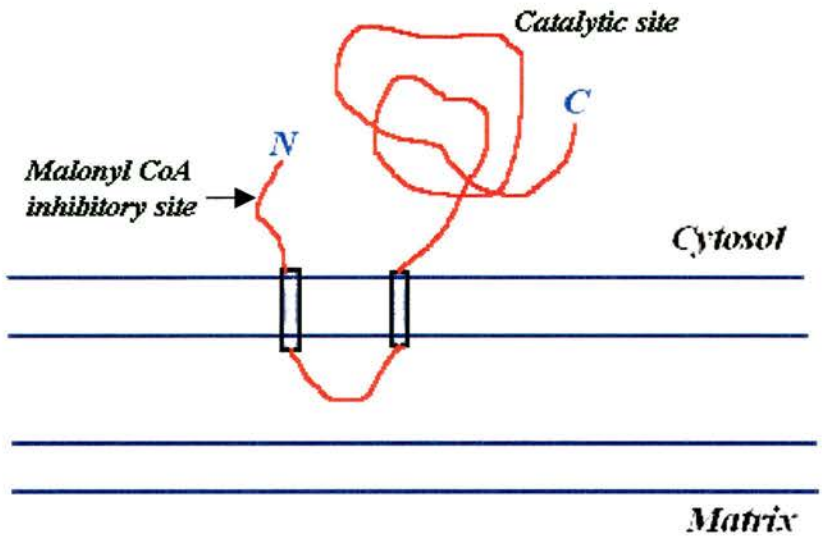

Figure1.4: Schematic representations of CPT1 membrane topology. The N and C terminal domain is exposed in the cytosol and the malonyl-CoA sensitive site in the N-terminal domain is indicated

1.4.3 Carnitine Palmitoyltransferase 2 (CPT2) and transporters

Another long-chain specific enzyme, carnitine palmitoyltransferase (CPT II), is localised on the mitochondrial inner membrane with its catalytic site is facing the matrix. Two additional proteins are required for the mitochondrial transport of LCFA: a plasma membrane carnitine transporter (OCTN2) dedicated to the maintenance of the intracellular level of carnitine, and a carnitine acylcarnitine translocase(CACT), that shuttles long-chain acylcarnitines across the inner mitochondrial membrane in exchange for free carnitine (Ramsay et al., 2001). The peroxisomal COT and mitochondrial CPT follows different kinetics and they are different gene product (Ramsay, 2000).

1.4.4 Enzymes in the endoplasmic reticulum (ER)

The identity of the enzymes in the endoplasmic reticulum (ER) remains uncertain. Isolated ER has malonyl-CoA-sensitive CPT activity but immunoblotting failed to detect CPT 1. Recently, lumenal palmitoyl-CoA formation from added palmitoyl-carnitine was demonstrated. The synthesis of complex lipids (via, e.g., diacylglycerol acyltransferase and acyl cholesterol acyltransferase) inside the lumen of ER means that active acyl groups must be delivered there but the flux rate may be less critical than in mitochondria where the demands for fat breakdown and ketone body synthesis must be rapid and tightly regulated (Ramsay 2001).

1.5 Mitochondrial β-oxidation

Mitochondrial fatty acid oxidation (FAO) is essential for energy homeostasis in situations that require simultaneous glucose sparing and major energy supply, such as prolonged fasting or exercise. Fatty acids are catabolized mostly in the mitochondria through the beta-oxidation pathway. The activated fatty acids from peroxisome are transported into the mitochondria for complete oxidation. The pathway proceeds as a spiral successively removing two carbons at a time. This is a cyclic series of reactions occurring within the mitochondria with the end result of two carbon units being hydrolysed from the fatty acid chain with each cycle (figure1.5). These two carbon units are molecules of acetyl CoA with each oxidation cycle, a molecule of NAD is reduced to NADH and one FAD is reduced to FADH. These are re-oxidised by the electron transport chain with the energy released coupled to ATP synthesis. The acetyl CoA molecules formed in each cycle are oxidised to CO_2 in the citric acid cycle, with

the oxidation/reduction reactions coupled to the electron transport chain and further ATP synthesis. These events occur in liver and muscle (Berg et al., 2002).

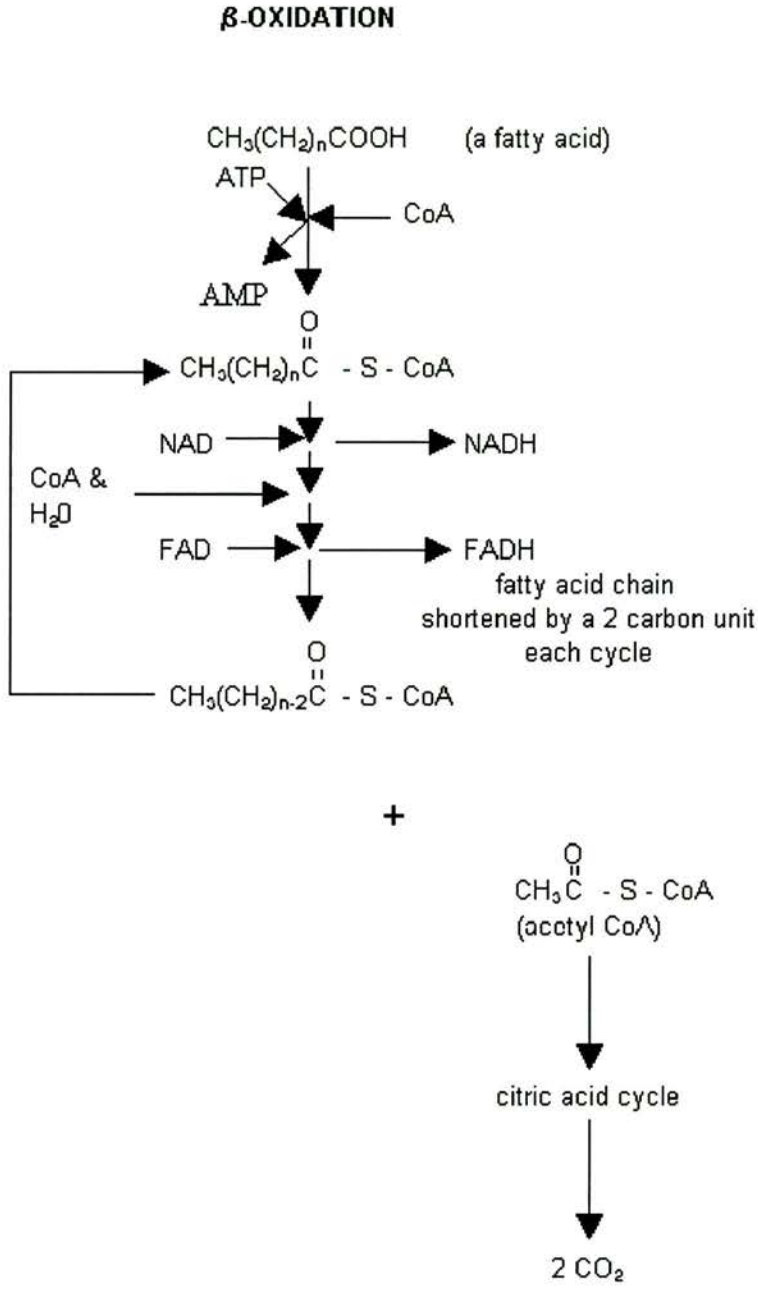

Figure 1.5: Schematic representation of mitochondrial fatty acid oxidation of long chain fatty acids. The removal of two carbon units in each cycles is indicated and the final product acetyl CoA occurs in the mitochondrial matrix.

Long-chain fatty acids (LCFA), the major fraction of fatty acids delivered to target tissues, cannot enter the mitochondria by simple diffusion, in contrast to medium- or short-chain fatty acids. After their activation by a long-chain fatty acyl-CoA synthetase on the outer mitochondrial membrane, long-chain fatty acyl-CoAs are imported into the mitochondrial matrix by the carnitine palmitoyltransferase (CPT) system. This enzymatic complex is made up of two distinct enzymes named carnitine palmitoyltransferase 1 (CPT1) and 2 (CPT2) (McGarry and Brown, 1997).

1.5.1 Functions of CPT system

CPT plays an important role in modulating long-chain acyl trafficking involved in homeostatis of the complex lipid fatty acid turnover in cells where mitochondrial fatty acid oxidation is either present (as in liver and muscle) or is not present (as in red cells) or minimally expressed (as in brain cells).

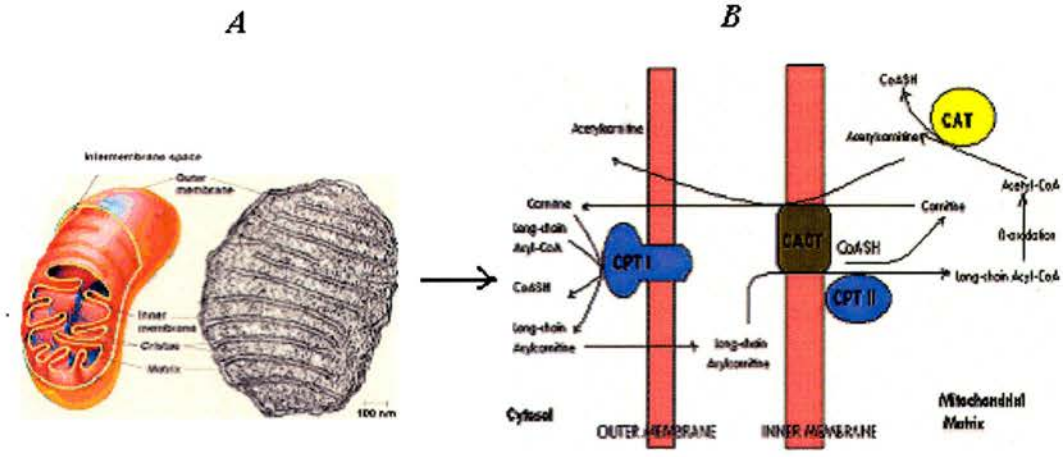

Figure 1.6: The structure and function of mitochondria. A. Structure of mitochondria and B shows mitochondrial β–oxidation (Wanders, 2002).

The first step in the pathway is the activation of the fatty acid to fatty acyl-coenzyme A (CoA). Long chain fatty acids must be activated in the cytosol before

being oxidised in the mitochondria (Figure 1.6), although medium and short chain acids can be activated in the matrix. Activation is catalysed by acyl-CoA synthetase. Activation occurs in two steps. First, the fatty acid reacts with ATP to form an acyl adenylate. The sulphydryl group of CoA then attacks the acyl adenylate, which is tightly bound to the enzyme, to form acyl-CoA and AMP (Fritz and Marquis, 1965). Activated long-chain fatty acids are carried across the inner mitochondrial membrane as their L-carnitine esters. The acyl group is transferred from the sulphur group in CoA to the hydroxyl group in L-carnitine, forming acyl-L-carnitine. This reaction is catalysed by carnitine palmitoyltransferase 1 (CPT1), (Ramsay and Tubbs, 1987).

The long chain acyl-carnitine is transported into the matrix by CACT in the inner mitochondrial membrane. Once the long chain acyl-carnitine is inside the matrix, CPT2 exchanges CoA for carnitine to produce fatty acid-CoA again, ready to enter fatty acid oxidation in the matrix to produce energy. The free carnitine is transported back out to renew the cytoplasmic pool of carnitine and allow the transfer process to continue.

The CPT1 and CPT2 couple mediate the transport of long-chain fatty acids by transesterification of long chain acyl CoA into long-chain acylcarnitine in the cytosol and vice versa in the mitochondrial matrix (Figure 1.6). The CPT1 isoforms are located in the mitochondrial outer membrane and are sensistive for inhibition by malonyl-CoA, which makes these enzymes important sites for metabolic regulation. Malonyl-CoA is the product of a reaction catalysed by acetyl-CoA carboxylases. This reaction is the first step in fatty acid biogenesis from acetyl-CoA and is preserved in nonlipogenic tissues such as skeletal and heart muscles (van der Leij *et al.*,2000).

Overall, the net mitochondrial uptake of activated long-chain fatty acids, i.e., long-chain acyl-CoA, is facilitate through the temporary replacement of the CoA group by carnitine. The CPT1 and CPT2 enzymes therefore have a clearcut function that is essential to allow mitochondrial β-oxidation of the long-chain fatty acids. The product of this process, acetyl-CoA, is the central substrate for many processes, most importantly the Kreb's cycle and, in the liver, ketogenesis.

1.5.3 Liver Ketogenesis

Ketosis is a physiological response to a diverse group of hormonal or nutritional perturbations. Ketotic states are characterized by increased rates of both hepatic ketogenesis and extrahepatic ketone body utilization. Since hepatic mitochondria are the major sites of ketone body formation, considerable attention has been focused on the factors controlling mitochondrial function. The mitochondrial sites implicated have included the transport of acyl groups (Shepherd et al.,1966), and product formation, (citrate and acetoacetate) (Garland et al., 1969).

Increased carnitine palmitoyltransferase activity (CPT1) has been described in the ketosis of diabetes and starvation (Harano et al., 1972). Excess acetyl-CoA is formed by mitochondrial β-oxidation and diverted to the formation of acetoacetate, D-3-hydroxybutyrate and acetone, called ketone bodies (Figure1.7). The accumulation of ketone bodies in the bloodstream is a consequence of a relative imbalance between production and removal rates. While the liver is the only organ in humans that makes a net contribution of ketone bodies to the bloodstream, muscle, kidney, and brain are quantitatively the most important tissues that remove ketone bodies from the blood.

Abnormally elevated levels of ketone bodies were observed in diabetic conditions (McGarry, and Foster. 1972).

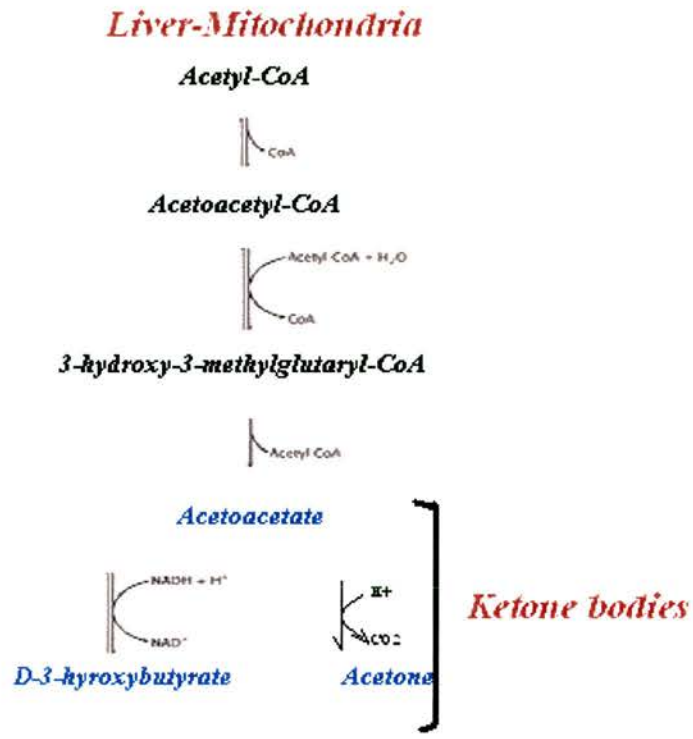

Figure 1.7: Schematic illustration of liver ketogenesis. Acetyl-CoA is the product of mitochondrial β-oxidation. When acetyl-CoA is produced faster than it is metabolised, ketone bodies are made in the liver.

1.5.4 Regulation of mitochondrial β-oxidation

The main site of regulation of mitochondrial β–oxidation in mammals is the reaction catalysed by carnitine palmitoyltransferase 1(CPT1). As the enzyme that catalyses the rate limiting step in fatty acid oxidation. CPT1 is regulated tightly by its physiological inhibitor, malonyl-CoA the first intermediate in fatty acid synthesis (McGarry et al., 1987). Malonyl-CoA is synthesised from acetyl-CoA through the catalytic activity of two isoforms of acetyl-CoA carboxylase: ACC-α and ACC-β. Whereas ACC-α appears to give rise to the bulk of the pool of malonyl-CoA within the cytosol that is used as a precursor for fatty acid synthesis, ACC-β appears to supply a

specific pool of malonyl-CoA that regulates the rate of mitochondrial fatty acid oxidation. The malonyl-CoA inhibition is an important regulatory mechanism in fatty acid oxidation and suggests coordinated control of fatty acid oxidation and synthesis (Brandt et al., 1998, Mascaro et al., 1998,Yu et al., 1998).

Understanding the molecular mechanism of the regulation of the CPT system by malonyl-CoA and long-chain fatty acids is crucial in the design of drugs for control of excessive fatty acid oxidation in diabetes mellitus (Prentki and Corkey 1996), in myocardial ischemia in which accumulation of acylcarnitines has been associated with arrhythmias (Corr and Yamada 1995) and in human inherited CPT deficiency diseases (Bonnefont et al., 1996). The inhibition of CPT1 by malonyl-CoA ensures that the flux through the two enzymes is closely regulated by the relative availability of glucose and fatty acids to the cell, as well as by hormonal (e.g., insulin, glucagon, leptin, adiponectin) and neuronal (e.g., sympathetic) inputs to the tissues. Therefore, the source of cytosolic malonyl-CoA to which CPT1 sensitivity is considerable importance.

1.6 Carnitine Octanoyltransferase (COT)

Carnitine octanoyltransferase (COT) catalyses the reversible transfer of medium chain fatty acyl-CoA to acyl-L-carnitine. COT is predominantly present in the peroxisomes and facilitates the transport of medium chain fatty acids from peroxisome to mitochondria (Figure 1.8). Peroxisomes are small (0.1-1μm), subcellular organelle bound by a single membrane, which are found in almost all eukaryotic cells (Figure1.8). Although the enzyme expressed can vary by tissue and species, the majority of these organelles contain some oxidases and all have catalase to dispose of the H_2O_2 produced by oxidases (Ramsay, 1999). In mammals, one of the most important metabolic processes of the peroxisome is the β-oxidation of long and very

long chain fatty acids. The peroxisome is also involved in bile acid synthesis, cholesterol synthesis, plasmalogen synthesis, amino acid and purine metabolism.

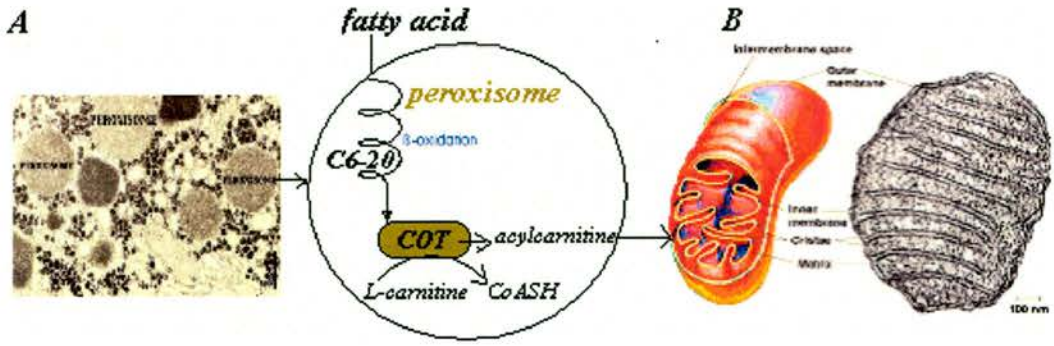

Figure 1.8: A. Picture of human liver (peroxisome) section and schematic representation of peroxisome showing the chain shortening long and medium chain fatty acids to acylcarnitine and transport to the mitochondria (B), where it undergoes further oxidation

The existence of carnitine octanoyltransferase(COT) was first discovered after separation of CAT, COT and CPT activities from calf liver (Solberg, 1971). A CPT protein purified from calf liver showed a best activity with octanoyl carnitine. In extracts of mitochondrial protein from beef heart concluded the presence of an "intermediary chain length carnitine acyltransferase different from CPT and CrAT (Kopec and Fritz, 1971). The activity of carnitine acyltransferase in liver organelles have shown in peroxisomes and in microsomes in the absence of detectable CPT activity, while at the same time, COT activity from which CrAT was successfully separated and partially purified (Markwell et al., 1976).

A survey of CrAT, COT, and CPT activities in homogenates from 10 rat tissues has significant COT activity in all tissues assayed except brain. However highest activity of COT was reported in the ovary, intestine, and liver (Choi et al., 1977). Medium chain length fatty acids are rare in the normal diet and medium chain

fatty acids such as octanoate are able to cross the mitochondrial inner membrane and activated for β-oxidation by thiokinases within the matrix (McGarry et al., 1974). It was proposed that mitochondrial β-oxidation of long chain fatty acids to medium chain lengths was followed by transfer to carnitine and export from different organelle. Significant intracellular concentrations of medium chain acyl esters of CoA have been reported in rat liver (Williamsons et al., 1979).

1.6.1 Peroxisomal β-oxidation

The peroxisome handles the β-oxidation of many substrates. These include very long chain fatty acids (VLCFAs; both saturated and unsaturated), some long chain fatty acids, and long chain dicarboxylic acids (products of ω-oxidation). Peroxisomes can also oxidize the side chains of eicosanoids, which are molecules important in short-range signaling and are derived from arachidonic acid. The eicosanoid family includes prostaglandins (involved in the regulation of cAMP, and therefore implicated in numerous pathways, thromboxanes (involved in blood clotting), and leukotrienes (involved in muscle contraction). Peroxisomal (β-oxidation also plays a role in bile acid synthesis (Ramsay, 1999).

In the first step in the peroxisomal β-oxidation the fatty acyl-CoA synthetases ligate CoA to a free fatty acid. This step requires ATP and magnesium, as well as the CoASH (Figure1.9). There are a two cloned human peroxisomal synthetases, a very long chain fatty acyl-CoA synthetase (VLCFA), and a long chain fatty acyl-CoA synthetase (LCFA) (Wanders *et al.*, 1992). The flavoenzyme acyl-CoA oxidases introduce a double bond between the carbons of the acyl-CoA and passes the electrons to oxygen, producing hydrogen peroxide (H_2O_2). There are at least 3 human acyl-CoA

oxidases, named for substrate specificity. These include a straight chain acyl-CoA oxidase (oxidase 1: there are two isoforms, A, and B), a branched chain oxidase, and a pristanoyl-CoA oxidase. However, there are six putative peroxisomal acyl-CoA oxidases apparent in the completed genome of *C.elegans*, suggesting that there may be at least three more in humans which have not yet been identified (Aoyama *et al.*,1994).

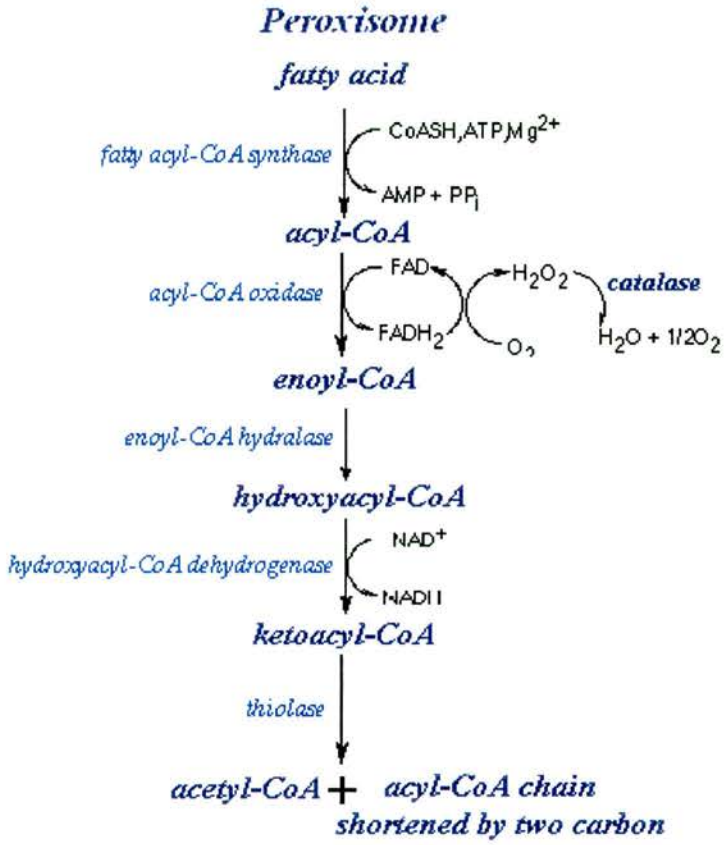

Figure 1.9: Schematic diagram of peroxisomal b-oxidation

Enoyl-CoA hydrolase adds water across the double bond of enoyl-CoA, producing hydroxyacyl-CoA. Hydroxyacyl-CoA dehydrogenase then oxidizes the hydroxyacyl-CoA to ketoacyl-CoA and passes the hydrogen to NAD^+. These two enzymatic activities exist on a single protein, known as the multifunctional enzyme. There are two known human multifunctional enzymes, multifunctional enzyme 1 (MFE1) and multifunctional enzyme 2 (MFE2, also known as 17-β-hydroxysteroid

dehydrogenase). These enzymes have different substrate specifities, with MFE1 reacting with straight chain enoyl-CoA esters, and MFE2 reacting with both straight chain enoyl-CoAs as well as branched chain enoyl-CoAs (Leenders *et al.*, 1996).

Finally thiolase cleaves the ketoacyl-CoA to acetyl-CoA and an acyl-CoA shortened by two carbons (Miyazawa et al 1981). Humans contain at least two distinct peroxisomal thiolases (1) and (2), also known as SCPX. Thiolase 1, is imported by the less utilized peroxisome targeting signal type 2 (PTS2) pathway, and this signal is cleaved once inside the peroxisome. SCPX contains the more common PTS1 (Seedorf *et al.*, 1991).

1.6.2 Distinctions between mitochondrial and peroxisomal β-oxidation

There are two major differences between mitochondrial and peroxisomal β-oxidation: specificity and mechanism. In mammals, the mitochondria oxidize short, medium, and most long chain fatty acids, while peroxisomes oxidize some long chain, but mostly very long chain fatty acids.

The mechanistic distinction between the two pathways lies in the enzymatic step following fatty acid activation to its CoA ester. Mitochondria have an acyl-CoA dehydrogenase to convert the acyl-CoA to enoyl-CoA. This enzyme transfers the electrons to FAD, and then into the electron transport pathway. However, peroxisomes have an acyl-CoA oxidase, which finally transfers the electrons to oxygen, producing hydrogen peroxide, a product converted to water and oxygen by catalase. The mechanism of the rest of the β-oxidation pathway is identical between the

mitochondria and peroxisomes but the peroxisomal and mitochondrial, enzymes are encoded by distinct genes.

1.6.3 Homology study of COT sequence from different species

The cDNA sequence of peroxisomal COT from human (Ferdinandusse et al., 1999), rat (Chatterjee et al., 1988, Choi et al., 1995) and bovine (Cronin, 1997a), COT encode proteins of 612 amino acids with a deduced molecular weight of about 70 kDa. The active site has conserved histidine in all the enymes in carnitine acyltransferase family. The C-terminal sequence contains THL, AHL and PHL respectively and serve as a peroxisomal targeting signal (PTS). However, other signals may also be involved or the folded state of the protein may contain specific information for sorting (Ramsay et al., 2001). The C-terminal THL, AHL or PHL sequence indicates that, like CrAT, the COT will be imported by the same transporter (with the PTS-1 receptor) as the β-oxidation enzymes. Although more is now known about defects in the human peroxisomal β-oxidation system, no human disease-causing mutations in COT are yet known (Wanders et al., 2001).

1.6.4 Mutations of COT

Mutational studies in heterologously expressed COT proteins from different species have identified the function of several of the conserved residues (reviewed in Ramsay et al., 2001). The catalytic histidine in bCOT is H327 and this residue is conserved throughout the family. The STS motif is also found in all the transferases and mutations in bovine COT established that these residues are important for carnitine binding (Cronin, 1997b), and Arg 505 is important in binding the carboxylate

group of carnitine (Cronin, 1997a). The mutants of COT and their effects are given in table 1.1.

Mutations that affect the activity of CPT1 and CPT2 have mild to severe effects on muscle and liver function in humans and so have been identified. Some have been functionally characterised after expression in yeast. The most common mutation in CPT2 is S113L, which has only mild muscular consequences (Taroni et al., 1992). L-CPT1 deficiency presents as recurrent attacks of fasting hypoketotic hypoglycemia (Bonnefont et al., 1999). One mutation causing it was G710E which, by comparing the sequence to CrAT and its structure, is now thought to block the acyl binding site (Gobin et al., 2003). Changing this residue in COT is reported in this thesis.

Sequence comparisons of COT with the malonyl-CoA sensitive CPT1 led to the suggestion that two histidines in COT would contribute to malonyl-CoA sensitivity. When rat COT was expressed in yeast, malonyl-CoA sensitivity was found which disappeared in these mutations. In particular, the H131 that is Y in bovine COT was thought to explain the lack of malonyl-CoA sensitivity there. However, recent work in our lab (reported in chapter 4) has shown that none of the purified COT proteins (rat with H131 and human and cow with Y131) have any sensitivity to malonyl-CoA except as a competitive inhibitor and the Y340H mutation makes no difference.

Substitution	Enzyme	Decrease in	References
1. H327A	rat COT	Activity	Morillas et al., 2000
2. R505A	bovine COT	carnitine binding	Cronin, 1997
3. S542A	bovine COT	carnitine binding	Cronin, 1997
T543A	bovine COT	carnitine binding	Cronin, 1997
S544A	bovine COT	carnitine binding increase	Cronin, 1997
4. G553M	rat COT	Acyl chain length specificity	Cordente et al., 2004

Table 1.1: Mutations in mammalian carnitine octanoyltransferase and their effects on activity and binding.

1.6.5 Kinetics of COT

Kinetic studies of COT showed that it followed a rapid equilibrium, random mechanism with an equillibrium constant close to 1.0 (Nic a' Bhaird et al., 1993). This suggest that the role of COT, like CrAT, is to maintain the equilibrium between the acylation state of the CoA and carnitine pools in the peroxisomes (Ramsay, 1999). After perturbation of the system, the rate at which the equilibrium is achieved will

depend on the level of expression of the activity and the kinetic parameters (Ramsay 2000).

1.6.6 Substrate specificity of COT

The substrate specificity of COT varies among different species. The specificity of the COT present in the peroxisomes may play a role in determining the point of chain termination (Ramsay 1999). The relative substrate specificity expressed as the V_{max}/K_M for acyl-CoA revealed that the COT from mouse liver has highest activity with C_6 acyl-CoA chain-length and almost no activity with C_{16} or longer (Farrell et al., 1984), whereas rat liver COT has an optimum at C_8 and shows good activity with C_{16} and C_{18} acyl-CoA (Miyazawa et al., 1983).

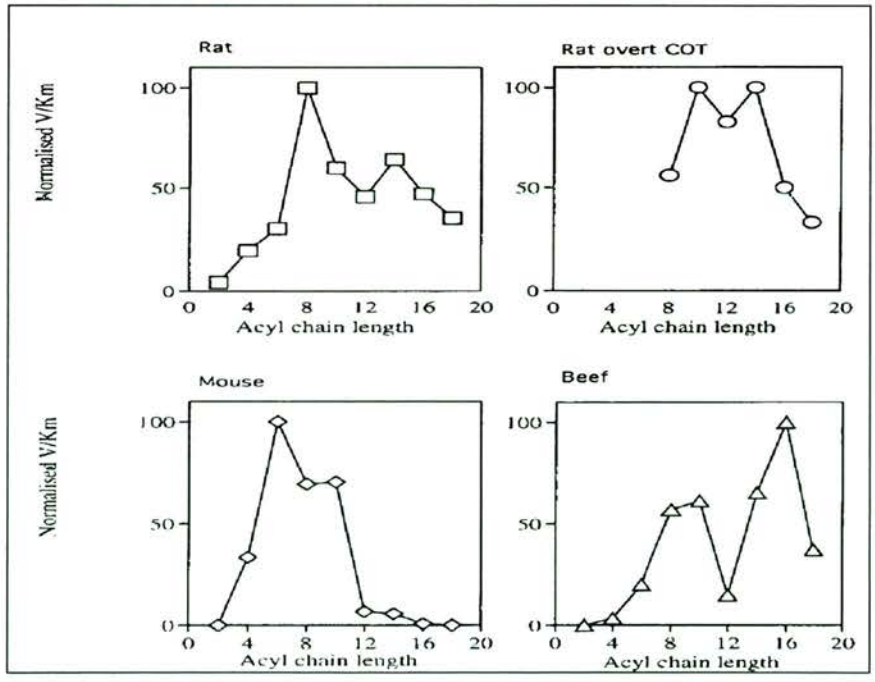

Figure 1.10: Substrate specificity of COT from rat, mouse and beef. The values are expressed as $Vmax/K_M$. (Ramsay, 1999)

Bovine COT has the longest chain-length preference, since it has good activity at C_{10} and an optimum at C_{16} (Ramsay 1988). The physiological importance of the differences between the specificity of peroxisomal COT from different species is not yet known. However, theoretically, the ability to transfer longer chain-lengths could be advantageous, because the carnitine system has been shown to be the main route for transfer of chain-shortened products from the peroxisomes to the mitochondria, where their further oxidation is accompanied by more efficient energy conservation (Ramsay, 1999).

1.6.7 Structure of COT

The crystal structure of mouse CrAT, published in 2003 (Jogl and Tong, 2003) superceded the initial model but allowed the Hegardt group to construct a much better model of COT because of its close sequence homology of the carnitine acetyltransferases. Although small crystals of COT have been grown in our laboratory (shown in chapter 3), no diffraction pattern has yet been obtained. The crystal structure of CrAT clearly defined the carnitine and CoA binding sites and a putative acyl-binding region. This putative binding region was then given functional support by the mutation of M564 to glycine in CrAT that resulted in activity with longer chain substrates (Hsiao et al., 2004; Morillas et al., 2004), and by the mutation in COT of G553 to the larger methionine which resulted in the loss of activity with any substrate longer than acetyl-CoA (Morillas et al.,2004). The crystal structure of mouse COT has now been published. The overall structure of COT is similar to carnitine actyltransferase (CrAT). The active site of COT is located at the interface of the two domains (Figure1.11).

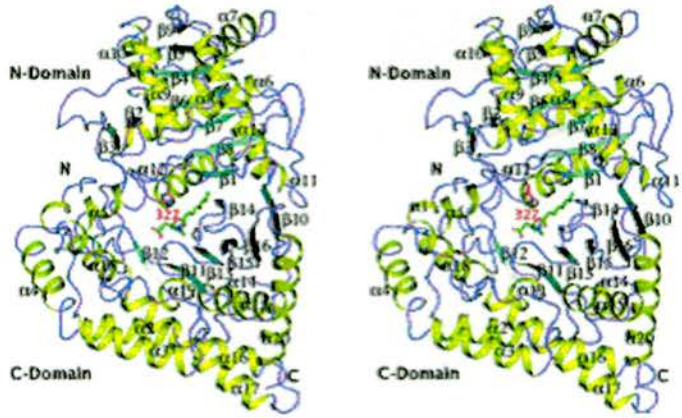

Figure 1.11: Structure of mouse COT. A stero diagram of the structure of CrOT and the catalytic histidine is shown in *red*. The octanoylcarnitine substrate is shown in *green*. (Jogl and Tong, 2005).

1.6.7.1 Substrate binding

The catalytic residue histidine 327 is positioned in the center of the enzyme. It is accessible from opposite surfaces of the enzyme through two tunnels that meet at the active site. One of these tunnels is for binding the carnitine the other is for CoA and a third tunnel extends from the active site toward the core of the N domain. This tunnel is for binding the medium-chain acyl chain of the substrate is shown in the figure 1.12 (Jogl et al., 2005).

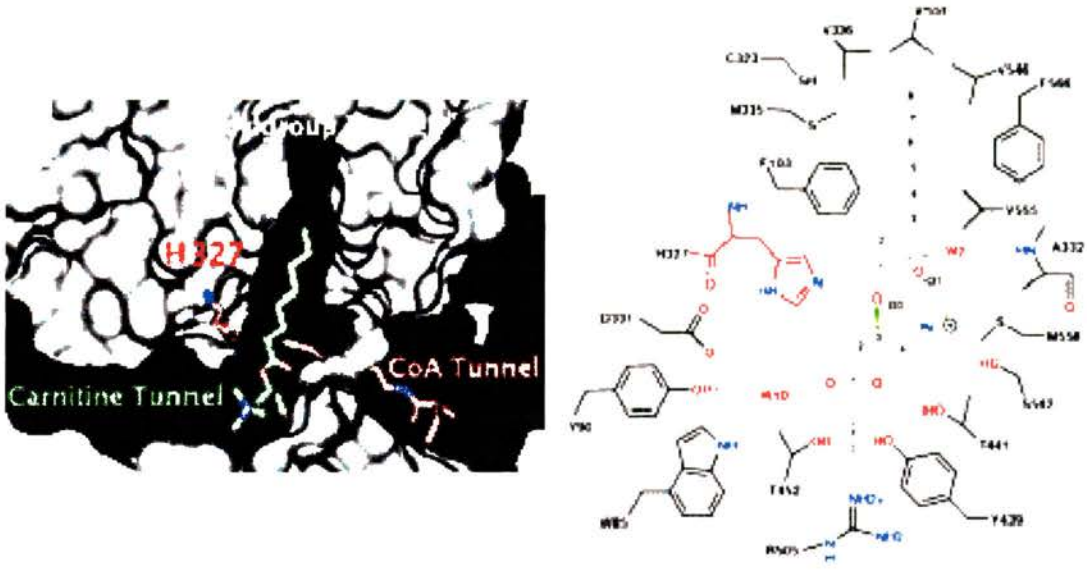

Figure 1.12: Active site of mouse COT showing the subtrates carnitine (green), CoA (red) and acyl (white) group bound in the active site histidine 327 (Jogl g and Tong L.,2003)

1.6.8 Is peroxisomal COT is sensitive to malonyl-CoA?

The malonyl-CoA sensitivity of peroxisomal COT, like that of mitochondrial CPT1, is reportedly lost on solubilization of the enzyme (Derrick and Ramsay, 1989; Farrell and Bieber, 1983; Miyazawa et al., 1983). The inhibition of COT by malonyl-CoA and related compounds and compared the characteristics of the inhibition of the purified enzyme with the inhibition of the enzyme in intact peroxisomes. In contrast to intact peroxisomes, the purified COT was inhibited by malonyl-CoA only as a substrate analogue, with a Ki of 106 μM. Intact peroxisomes were 50% inhibited by 1μM malonyl-CoA, similar to CPT1 and well within the physiological range (Derrick and Ramsay, 1989).

The malonyl-CoA inhibition of CPT1 and COT is strongly influenced by the particular assay conditions used, such as buffer composition, pH, acyl-CoA substrate and the presence or absence of serum albumin (Nic a'Bhaird and Ramsay, 1992). This

factor is particularly important in the kinetics of the inhibition, since IC_{50} values are critically dependent on the substrate concentration used (Nic a'Bhaird and Ramsay, 1992). It was also shown by Nic a'Bhaird & Ramsay, in 1992, that the pH dependent increase in sensitivity of CPT1 by malonyl-CoA is also observed for the purified COT, which can be explained by the presence of a histidine residue in the active site. Both COT in isolated peroxisomes and the purified COT show similar K_m values for fatty acyl-CoA esters, but the Ki value for the inhibition of COT in intact peroxisomes was dramatically lower (Nic a'Bhaird and Ramsay, 1992). Two possibilities were proposed to explain this fact. The existence of a regulatory subunit with a malonyl-CoA-binding site could be lost on solubilization of the enzyme, with a subsequent decrease in sensitivity to inhibition but this is not thought to happen now, Alternatively, the catalytic polypeptide could contain a separate binding site for malonyl-CoA, but on solubilization of the enzyme a conformation change can occur, which results in a lowered affinity for malonyl-CoA at this regulatory site (Nic a'Bhaird and Ramsay, 1992). . From these observations of the inhibition of *in situ* peroxisomal COT by malonyl-CoA, which resemble those of CPT1, Nic a'Bhaird & Ramsay suggested that parallel regulation of the overt COT in peroxisomes and of CPT1 in mitochondria might be necessary for the control of cellular fatty acid metabolism.

Further work on the malonyl-CoA sensitivity of COT in rat suggested that two non-catalytic site histidines were essential for the malonyl-CoA binding at high affinity and inhibition in peroxisomal membranes (Morillas et al., 2000). Cloned mutants of rat COT in yeast peroxisomal membranes were 57% inhibited by 200μM malonyl-CoA only if the conserved residues His131 and His340 were present. This

was similar to the competitive inhibition observed in purified bovine COT, where a Ki value of 106 μM for malonyl-CoA was determined (Ramsay and Bhaird, 1992).

Alignment of the known sequences of COT showed that human and bovine COT both lacks His340 in contrast to rat and mouse (Figure 1.13). Bovine, rat and human COT proteins heterologously expressed in either *E. coli* or *P. pastoris* were purified and characterised (Chapter 3). In all cases, the inhibition by malonyl-CoA was poor and competitive with substrate. The rat COT gave a Ki for malonyl-CoA of 147 μM and the activity of the human and rat COT dropped in parallel at a fixed substrate concentration. Thus H340 does not participate in the binding of malonyl-CoA to COT (shown in this thesis-Chapter 4).

```
Rat-COT. . . 320 IFGCSCDHAPYDAMLMVNIAHYVDEKLLETEG 351
Mouse-COT. . 320 IFGCCCDHAPYDAMVMVNIAHYVDERVLETEG 351
Human-COT. . 320 VFGCNCDHAPFDAMIMVNISYYVDEKIFQNEG 351
Bovine-COT.. 320 VFGSNCDHAPFDAMVLVKVCYYVDENILENEG 351
Fugu-COT. .. 285 TFGSNCDHAPYDAMVLVTMCWYVDQRIQSTGG 326
```

Figure 1.13: Sequence comparison of rat, mouse, human, bovine and fugu COT. Rat ans mouse COT has 340H and huaman and bovine has Y340. Mutation of Y340H shows no inhibition with malonyl-CoA

1.6.9 Selective inhibition of specific carnitine acyltransferases

The carnitine acyltransferases are potential targets for intervention of therapetic drugs in cases of abnormal lipid metabolism (Anderson, 1998), It is important to establish similarities and differences between the enzymes in this family in order to design of selective inhibitors. In 1998, before any structural information was available, Nic a' Bhaird *et al.*, demonstrated some differences between the active sites of beef liver COT and CPT2, using chemical reactivity of active site groups. Both enzymes

were treated with diethyl pyrocarbonate (DEPC), a histidine selective reagent. The pattern of inhibition of CPT2 was simple linear pseudo-first-order, whereas the inhibition of COT was biphasic with an initial rapid loss of activity followed by a slower loss of activity. The results of these experiments provide strong evidence for the presence of a single reactive and catalytically essential histidine at the active site of CPT2 (Nic a'Bhaird et al., 1998). This conclusion is consistent with site-directed mutagenesis results showing that H372 of rat liver CPT2 is essential for activity (Brown et al., 1994). Likewise, site directed mutagenesis of the histidine residue H327A in COT abolished the enzyme activity (Morillas et al., 2000). This conserved histidine is the catalytic residue first noted as the residue modified by the inactivator, bromo-acetylcarnitine (Chase and Tubbs, 1969). In the structure of CAT, the equivalent His 343 is clearly seen in a position to activate either CoA or carnitine by removal of a proton (Jogl and Tong, 2003).

The biphasic plots resulted from the treatment of COT with DEPC suggest that more than one residue is modified by DEPC and that the modification of the residue reacting in the faster phase does not lead to complete inactivation of COT (Nic a'Bhaird et al., 1998). In order to identify the residues reacting with DEPC, Nic a' Bhaird *et al*, accompanied the inactivation of COT by DEPC with the changes in the absorbance spectrum of COT and did substrate protection studies. The results provide strong evidence that the residue reacting in the faster phase of inhibition by DEPC is not a histidine but possible a serine. When this residue is modified there is only partial loss of activity, which suggests that it might not play a direct role in catalysis (Nic a'Bhaird et al., 1998).

One of the residues that might be modified by DEPC in the slow phase of inhibition of COT was a lysine. The effect of fluorodinitrobenzene (FDNB), a lysine selective reagent analysed on the activity of COT. The resulted linear pseudo-order kinetics indicates that the loss of activity observed on treatment of COT with FDNB is the result of one residue present at or near the active site of the enzyme, probably a lysine (Nic a'Bhaird et al., 1998). From sequence alignments and the structure of CrAT it is probable that the lysine modified was Lys354 in bovine COT. The equivalent Lys325 in mouse CrAT lies close to the active site histidine (as seen in the structure deposited as 1NDF in the Protein Data Bank).

The other catalytic site difference between COT and CPT2 is the presence of a thiol group (cysteine), which was thought to play a role in substrate binding of CAT (Colucci and Gandour, 1988). COT but not CPT2, slowly inactivated by thiol reagent (Ramsay 1988). Although no cysteine was apparent amongst the groups required for carnitine or CoA binding in the crystal structures (Jogl and Tong, 2003), there is a cysteine residue (Cys 325) in all COT sequences that is absent from CrAT. The reactivity of a lysine, cysteine and serine residues possibly present in the active site of COT but not of CPT2 provides the first indication of structural differences that could be very important in the design of selective inhibitors (Nic a'Bhaird et al., 1998). COT and CPT2 differ kinetically and they differ in their sensitivity to conformationally constrained inhibitors, which permits development of inhibitors that inhibit mitochondrial β-oxidation with minimal effects on peroxisomal β-oxidation and other acyl-CoA dependent reactions (Ramsay and Gandour, 1999).

1.6.9.1 COT inhibition and disease

Diabetes mellitus is the only non-infectious disease recognized as epidemic by the World Health Organisation (WHO), because of its worldwide occurrence, especially in western life-style countries. Diabetes can be divided into two major categories: Type I or insulin dependent diabetes mellitus (IDDM), and more common type II, or non-insulin dependent diabetes mellitus (NIDDM), the later accounting for more than 90% of all diabetic patients (Fabio et al., 2003).

In type II diabetes, characterised by insulin resistant and inadequate β-cell activity, increased fatty acid oxidation contributes greatly to ketone body by formation of high levels of acetyl-coenzyme A, which increases ketogenesis and thus ketone body production (acetone, acetoacetate and D-3-hydroxybutyrate). The mitochondrial oxidation of long chain fatty acids requires the intervention of CPT1 and CPT2. CPT1, the outer mitochondrial membrane enzyme, catalyses the formation of long-chain acylcarnitine. Its rate controls β-oxidation and formation of acetyl-CoA. CPT inhibitors indirectly reduce liver ketogenesis by decreasing the level of acetyl-CoA and hence helpful in the treatment of type II diabetes. Antiketotic agents such as acyl aminocarnitine particularly ST 1326 are under clinical trial.

Inhibitors of carnitine acyltransferases are shown in table 1.2. Etomoxir is a 2[6(4-chlorophenoxy)hexyl]oxirane-2-carboxylate compound once developed for the treatment of diabetes mellitus. It is an inhibitor of CPT-1, the mitochondrial enzyme that plays a key role in the transport of long-chain acyl-CoA into the mitochondria. Etomoxir inhibits fatty-acid metabolism but promotes that of glucose. It was a good candidate for an antiketonaemic and antidiabetic drug. However, etomoxir in the acute

dose given had only moderate effects on glucose turnover although chronic administration caused increased glucose turnover and glucose recycling in the rat (Kruszynska and Sherratt, 1987).

In 1992 Lilly *et al.*, reported that the etomoxiryl-CoA inhibited purified carnitine acyltransferases at nanomolar concentrations and also inhibited the carnitine acyl-transferases of rat heart mitochondria and rat liver microsomes. It was proposed by many investigators that the etomoxiryl-CoA must bind to a high affinity site with specific inhibition of mitochondrial CPT1. The concentrations of etomoxiryl-CoA required for 50% inhibition of the different carnitine acetyltransferases, microsomal and peroxisomal carnitine octanoyltransferase are in the low micromolar range.

Obesity and its attendant disorders, such as type 2 diabetes, are global health problems. C75, an inhibitor of fatty acid synthase (FAS) and stimulator of CPT I (Hu et al., 2003; Thupari et al., 2002), caused anorexia and profound weight loss in lean and genetically obese mice. In mice a single dose causes a rapid (>90%) decrease of food intake. These effects are associated with inhibition of fasting-induced up-regulation and down-regulation, respectively, of the expression of orexigenic and anorexigenic neuropeptide messages in the hypothalamus. This biological effect of C75 has driven efforts to understand the mechanism of action of this compound *in vivo*, and has led to renewed interest in the modulation of the fatty acid synthesis and fatty acid oxidation pathways for obesity therapy (Kumar et al., 2002; Thupari et al., 2004).

INHIBITOR	STRUCTURE					REFERENCE
		CPT1	CPT2	COT	CAT	
Deoxycarnitine	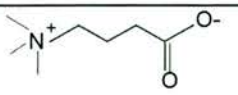	20,000	7000	5000		Nic A. Bhaird et al., 1993
Palmitoylcholine	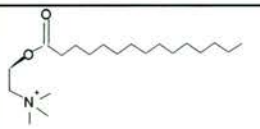	-	28	454		Ramsay and Gandour, 1999.
Acetyl-L-carnitine	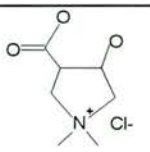	60%	100%	87%	4	Giannessi et al., 2001.
Acyl-aminocarnitine	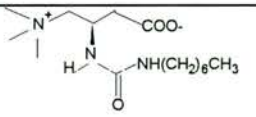			0.024		This thesis
Etomoxiryl-CoA	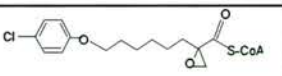	0.009	2.5	105		Morillas, et al., 2000.
Malonyl-CoA	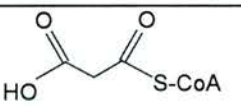	1		105		Morillas, et al., 2000.
C75 C75+Mal-CoA	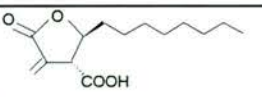			96.4		This thesis
HUC	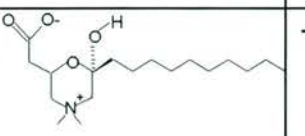	-	8.0	113		Ramsay and Gandour, 1999.
HPC	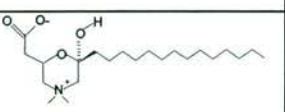	5	0.16	13		Ramsay and Gandour, 1999.

Table 4: A comparitive table shows the inhibitor and its structural difference. The range of different inhibitors was used in this study with purified COT are deoxycarnitine, aminocarnitine, acyl-aminocarnitine, etomoxiryl-CoA and malonyl-CoA. Literature values are given for all other inhibitors. (HUC-Hemi-undecanoylcarnitinium, HPC-Hemipalmitoylcarnitinium)

1.6.10 Peroxisomal Disorders

Current understanding of the vital functions of peroxisomes in animal cells has developed from the study of the striking effects of their total or partial dysfunction in human disease. Inherited disorders of peroxisomal structure or metabolism present a heterogenous array of clinical symptoms and overlapping phenotypes. They range from severe and progressive neurological degeneration to mild adrenal insufficiency. The most severe of these heterogenous disorders, Zellweger syndrome, presents with general abnormalities and malformation and degeneration of the brain (Poll *et al.*, 1998).

X-linked adrenoleukodystrophy(XALD) has a highly variable phenotype expression and mostly affects boys under 10 with behavioural disturbances, dimishing school performance, loss of vision and auditory discrimination. The diagnostic hallmark of XALD is the accumulation of very long chain fatty acids (VLCFA) notably C26-CoA in plasma which is due to lack of transport to oxidise VLCFA's from the cytosol to peroxisome. Patients have also been identified with defects in acyl-CoA oxidase, the bifunctional protein deficicency, and peroxisomal thiolase deficiency have all been described in only very few patients. These patients display similar phenotypes to that of the Zellweger spectrum (Ramsay, 2000).

1.7 Carnitine therapy

1.7.1 Angina

Carnitine might be a good addition to standard therapy for angina. In one controlled study, 200 individuals with angina (the exercise-induced variety) took either 2-gm daily of L-carnitine or were left untreated. All the study participants continued to take their usual medication for angina. Those taking carnitine showed improvement in several measures of heart function, including a significantly greater ability to exercise without chest pain. They were also able to reduce the dosage of some of their heart medications as their symptoms decreased. Similarly positive results were seen in a double-blind trial of 52 individuals with angina (Cherchi et al., 1985). Other studies using propionyl-L-carnitine have also found benefits (Bartles *et al.*,1996).

1.7.2 Intermittent claudication

People with advanced hardening of the arteries, or atherosclerosis, often have difficulty walking due to lack of blood flow to the legs. Pain may develop after walking less than half a block. Although carnitine does not increase blood flow, it appears to improve the muscle's ability to function (Sabba *et al.*, 1994). A 12-month double-blind placebo-controlled trial of 485 patients with intermittent claudication evaluated the potential benefits of propionyl-L-carnitine (Brevetti et al., 1999). Participants with relatively severe disease showed a 44% improvement in walking distance as compared to placebo. However, no improvement was seen in those with mild disease. Another double-blind study followed 245 people and also found benefit (Brevetti *et al.*, 1995). Similar results have been seen in most but not all other studies of L-carnitine or propionyl-L-carnitine. Propionyl-L-carnitine

may be more effective for intermittent claudication than plain carnitine (Bolognesi *et al.*, 1995).

1.7.3 Congestive heart failure

Several small studies have found that carnitine, often in the form of propionyl-L-carnitine, can improve symptoms of congestive heart failure (Caponnetto *et al.*, 1994). In one trial, benefits were maintained for 60 days after treatment with carnitine was stopped (Loster *et al.*, 1999). After a heart attack carnitine may help reduce death rate. In a 12-month placebo-controlled study, 160 individuals who had experienced a heart attack received 4 g of L-carnitine daily or placebo, in addition to other conventional medication. The mortality rate in the treated group was significantly lower than in the placebo group, 1.2% versus 12.5%, respectively. There were also improvements in heart rate, blood pressure, angina (chest pain), and blood lipids (Davini *et al.*, 1992). A larger double-blind study of 472 people found that carnitine may improve the chances of survival if given within 24 hours after a heart attack (Iliceto *et al.*, 1995).

1.7.4 Diabetes and neurological symptoms

Peripheral neuropathy associated with diabetes mellitus (DM) is extremely common, approaching over 28% of some populations. Various mechanisms of neuronal damage have been postulated, including polyol pathway generation of sorbitol and free radical damage. Reduced nerve conduction velocities occur in DM and have led to experimental models assessing this function in rats. Animals given ALC after experimental diabetes induction have improved nerve conduction velocities.

Correction of abnormal enteric peptides associated with autonomic neuropathies was also observed in animal models (Young *et al.*, 1993).

Human studies also show beneficial effects of ALC in neuropathies. Intramuscular administration of the compound given to 63 patients with painful neuropathy for 15 days showed significant improvement in motility and subjective measures. A small double-blind study in humans again using the I.M. route of administration, showed highly significant improvement in painful neuropathies. Again the anti-oxidant function of ALC was believed to be a likely mechanism of action (Quatraro *et al.*, 1996)

1.7.5 Chronic Obstructive Pulmonary Disease (COPD)

Evidence from three double-blind placebo-controlled studies enrolling a total of 49 individuals suggests that L-carnitine can improve exercise tolerance in COPD, presumably by improving muscular efficiency in the lungs and other muscles (Dal Negro *et al.*,1986).

1.7.6 Alzheimer's Disease

Numerous double or single blind studies involving a total of more than 1,400 people have evaluated the potential benefits of acetyl-L-carnitine in the treatment of Alzheimer's disease and other forms of dementia (Calvani et al.,1992, Thal *et al.*, 2000). Early studies found some evidence of benefit, although it was generally quite modest.

However, the two most recent and best-designed studies found no benefit. A double-blind placebo-controlled trial that enrolled 431 participants for 1 year found no significant improvement at all in the group treated with acetyl-L-carnitine. A close look at the results appeared to suggest some benefit in individuals who developed Alzheimer's disease at a particularly young age. However, when this possibility was tested in a 1-year double-blind placebo-controlled trial of 229 patients with early-onset Alzheimer's, shows no benefits (Thal *et al.*, 2000).

1.7.7 Mild depression

A double-blind study of 60 seniors with mild depression found that treatment with 3gm of carnitine daily over a 2 months period significantly improved symptoms as compared to placebo (Bella et al., 1990). Positive results were shown in another study as well (Garzya et al., 1990).

1.7.8 Hyperthyroidism

Enlargement of the thyroid (goiter) can be due to many causes, including cancer and iodine deficiency. In some cases, thyroid enlargement occurs without any known cause, so-called benign goiter. Treatment of benign goiter generally consists of taking thyroid hormone pills. This causes the thyroid gland to become less active, and the goiter shrinks. However, there may be undesirable effects as well. Symptoms of hyperthyroidism (too much thyroid hormone) can develop, including heart palpitations, nervousness, weight loss, and bone breakdown. A recent study found that use of L-carnitine could alleviate many of these symptoms. A 6-month double-blind placebo-controlled trial evaluated the effects of L-carnitine in 50 women who were taking thyroid hormone for

benign goiter. The results showed that a dose of 2 or 4 g of carnitine daily protected participants' bones and reduced other symptoms of hyperthyroidism (Benvenga et al.,2001).

1.7.9 Performance Enhancement

A 1996 review of clinical studies concluded that no scientific basis exists for the belief that carnitine supplements enhance athletic performance. A few studies have found some benefit, but most have not (Heinonen, 1996).

1.8 Aims of the Project

The aim of the project is to characterise COT cloned from several species to investigate its inhibition and to crystallise the protein for structural determination.

2. MATERIAL AND METHODS

2.1 Cloning of COT from different species

The cloning of COT was performed in Hannah Research Institute, Ayr, under the supervision of Dr. Nigel T. Price. The cDNA's for the wild type bovine, human, rat, bovine mutant G553M and human mutant Y340H COT were cloned into different vectors (pET-11, pET-21b and pGAPZB) for subsequent expression. All these clones were also subcloned into N-terminal $(His)_6$ tag vector pET-28a for the ease of purification. The cDNA sequences were downloaded from the GeneBank™ database.

2.1.1 PCR Primer design

Location of the restriction enzyme cleavage sites and development of cloning strategies were performed with the aid of Lasergen MapDraw Software (DNA star). PCR primers to amplify the target genomic DNA for bovine mutant G553M, wild type human COT and mutant Y340H were also designed using Lasergene Primer Select Software (DNA Star). All the primers (Table 2.1) were obtained from MWG-Biotech AG (UK) and were supplied after HPLC purification. The primers, shown in Table 2.1, were diluted with sterile water and used at 5μM final concentration for amplification of genomic DNA.

Primer Name	Nucleotide sequence
Human wt forward	5'-CCCCCTACATATGGAGAATCAACTGGCTAAATCAAC-3'
Human wt reverse	5'-ATGCCCTCGAGTCACAGGTGAGTAGAGTTCATC-3'
hY340H – A	GAGGCCGAGCTTTTGTCTTT
hY340H – B	CCACATAATGACTGATGTTCACCATAA
hY340H – C	GGTGAACATCAGTCATTATGTGGATGAGAAAA
hY340H – D	ATACTGGGCTTTAGCTTGGTTGAT
bG553M – forward	5'-TGGCAAAAAGCTAAGGAGAA-3'
bG553M – reverse	TACCATGGGAACCATCACCATCTGGACTCTTAAATAA-3'

Table 2.1: Primers used in the amplification of human wild type, mutant Y340H and bovine COT mutant G553M. The anticodon, and the restriction sites are underlined.

2.1.2 Plasmid DNA purification

2.1.2.1 Plasmid DNA from the bacterial cells

Wizard™ Plus SV Miniprep DNA purification system was used to extract plasmid DNA from bacterial cell suspensions. The procedure takes advantage of the fact that plasmids are relatively small supercoiled DNA molecules and bacterial chromosomal DNA is much larger and less supercoiled. This difference in topology allows for selective precipitation of the chromosomal DNA and cellular proteins from plasmids and RNA molecules. The cells are lysed under alkaline conditions, which

denature both nucleic acids and proteins, and when the solution is neutralized by the addition of potassium acetate, chromosomal DNA and proteins precipitate because it is impossible for them to renature correctly. Plasmids renature correctly and stay in solution, effectively separating them from chromosomal DNA and proteins.

A single colony was picked from a freshly streaked plate and inoculated into 5ml of LB medium containing appropriate antibiotics and incubated overnight at 37°C in the shaker incubator. Plasmid DNA was purified using Wizard™ Plus SV Miniprep DNA purification system (Promega). The overnight culture (5mL) was centrifuged at 5000rpm and pellets are collected, resuspended with 250ul of cell suspension solution and vortexed. Then 250µl of lysis solution was added and mixed immediately by inverting the eppendorff tube 4 times. 10µl of alkaline protease solution was added and mixed thouroughly then incubated 5mins at room temperature. After incubation 350µl of neutralization solution was added and mixed, then centrifuged at 14000rpm for 10minutes at room temperature.

The supernatant was transferred into the spin column to bind the plasmid DNA by centrifuging at 14000rpm for 1 minute. The flow through was discarded and the spin column was placed on the collection tube. Then the column was washed by adding 750µl of wash solution (Ethanol was added) and centrifuged at 14000rpm, the flow through was discarded and the column was transferred into sterile collection tube. Plasmid DNA was eluted by 100µl of nuclease free water was added and centrifuged at 14000rpm for 1min at room temperature and stored at-20°C.

2.1.2.2 DNA purification from the gel

Wizard® SV Gel and PCR clean up system was used to purify the DNA from the gel slices. This system is designed to extract and purify DNA fragments of 100bp-10kb from standard or low melting agarose gel. It is based on the ability of DNA bind to a silica membrane in the presence of chaotropic salts.

Following agarose gel electrophoresis the required DNA bands were excised from the gel and placed into eppendorff tube and weighed. Equal volume of binding buffer was added, mixed and incubated at 55-65°C until the gel slices dissolved. The dissolved gel was transferred into mini-SV column and incubated for 1minute at room temperature and centrifuged at 10000rpm for 1minute to bind the DNA. The column was washed twice with 100 & 50µl of membrane wash buffer by centrifuging at 10000rpm for 5minutes. The flow through was discarded and the column was transferred into a sterile eppendroff tube. The DNA was eluted by adding 50µl of nuclease free water and centrifuged at 10000rpm for 1minute and the DNA was stored at –20°C.

DNA for sequence analysis (15µg) was sent to MWG-Biotech as a dried pellet following ethanol precipitation. The DNA was ethanol precipitated by adding TE buffer to 400µl followed by 40µl of (1/10 volume) of 4M NaCl and 800µl (2x volume) of ethanol. After mixing, the solution was incubated at –20°C for 1hour (30minutes at –70°C) and spun at 14000rpm at 4°C for 10minutes. The supernatant was discarded and the pellet was washed in 600µl of 70% (v/v) ethanol. The precipitate was then dried.

2.1.3 Polymerase chain reaction (PCR)

The PCR reactions were performed using a Hybaid-PX2 (MWG-Biotech, UK) thermocycler. The reaction mixture (50µl total volume) consisted of 25ng of DNA, 5µl of 10x PCR buffer (Bioline), 1µl of dNTP, 1µl of sense primer, 1µl of antisense primer, with 2.5µl of DMSO and without, 0.5µl of *Pfu* TURBO DNA polymerase (Stratagene). The PCR reaction mixture is given in Table 2.2. The reaction mixture was then subjected to 30 cycles of specific amplification in a DNA thermocycler. Each cycle consisted denaturation at 95°C for 5minutes, annealing at 56.5°C for 20 seconds and extension at 72°C for 45 seconds. Following amplification, PCR products were checked by electrophoresis on 1% agarose gel stained with ethidium bromide.

Contents	**0% DMSO (µl)**	**5%DMSO (µl)**
DNA	41.5	39.5
10x PCR buffer	5	5
dNTP	1	1
Sense primer	1	1
Antisense primer	1	1
DMSO	0	2.5
Pfu TURBO polymerase	0.5	0.5

Table 2.2: PCR reaction mixture conditions were used for the amplification of the DNA

2.1.4 TA cloning

TA cloning is one of the most popular methods of cloning the amplified PCR product using *Taq* and other polymerases. These polymerases lack 5'-3' proof reading activity and are capable of adding adenosine triphosphate residue to the 3' ends of the double stranded PCR product. The PCR-amplified product can be cloned in a linearized vector with complementary 3' T overhangs. TA cloning is brought about by the terminal transferase activity of a DNA polymerase such as the *Taq* polymerase. This enzyme adds a single, 3'-A overhang to each end of the PCR product.

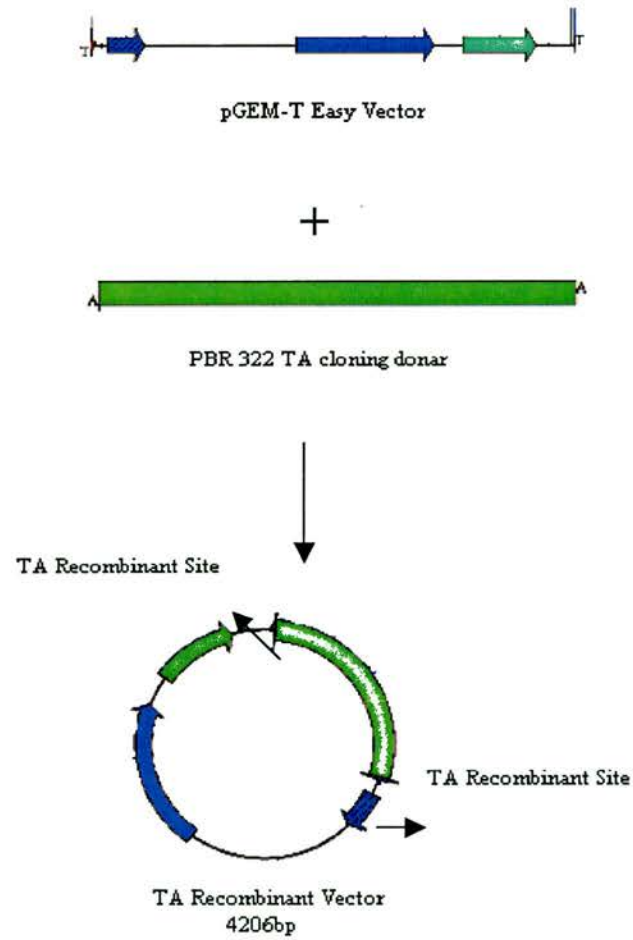

Figure 2.1: Schematic representation of TA cloning. The linearised pGEM-T vector and the TA cloning donor DNA are ligated together by a ligase. (note: restriction sites are not indicated).

As a result, the PCR product can be directly cloned into a linearized cloning vector that have single base 3'-T overhangs on each end. Such vectors are called T-vectors. The PCR product with A overhang, is mixed with this vector in high proportion. The complementary overhangs of a "T" vector and the PCR product hybridize. The result is a recombinant DNA, the recombination being brought about by DNA ligase. A schematic view of the TA ligation is shown in figure 2.1.

2.1.5 Agarose gel electrophoresis

PCR products were checked on a 1% (w/v) agarose gel to confirm successful amplification. To prepare the gel, 1gram of agarose was added in 1xTAE buffer (40mM Tris base, 0.1%(v/v) glacial acetic acid, 1mM EDTA, pH-7.2) in a conical flask and heated until the agarose was dissolved. The molten agarose solution was allowed to cool for 5minutes before 2µl of ethidium bromide were added. The solution was then poured into gel casting tray into which well forming combs has been placed. Once set, the gel was placed in an electrophoresis tank and submerged in 1xTAE buffer removing the well forming combs.

PCR products were mixed with 5µl of sample buffer (10mM Tris-HCL, pH 7.5, 50mM EDTA, 10% Ficoll, 0.25% bromophenol blue, 0.4 % Orange G) and 15µl of this mixture was loaded into the wells, alongside 1kb DNA ladder were loaded as a reference in a horizontal gel electrophoresis apparatus (Bio-Rad). Then the gel was run at 120V for 25 minutes and then the amplified fragments were visualised under ultraviolet trans illuminator and gel imaging system.

Enzyme	Restriction Buffer	Restriction site
NdeI	Buffer 4	CA↓TATG
XhoI	Buffer 4	C↓TCGAG
BamHI	BamHI buffer	G↓GATCC
SacI	Buffer 4	GAGCT↓C
BamHI	BamHI buffer	G↓GATCC

Table 2.3: Restriction enzymes and the buffers used in digestion of the vector and plasmid DNA.

2.1.6 Digestion DNA with restriction enzymes

The strategies to excise the COT genes from the plasmid DNA and to clone them into the vector pET-28a, pET-21b, pET-11, pGEM-T and pGAPZB were based on the information available about these vectors and on the map sequences of the cDNA and respective amino acids including the cleavage site of the restriction enzymes that cut once or twice in the genes not the vectors. The restriction sites of the genes were shown in the appendix. The restriction enzymes were used and its respective buffers were as well as the restriction sites are listed in Table 2.3.

The digestion recipe is given in Table 2.4. The mixture was incubated at 37°C for 1hour. Then another 0.5µl of restriction enzyme added and incubated for 1hour. When digestion with two enzymes requiring different restriction buffers was necessary, the digests were performed sequentially with an intermediate ethanol precipitation step. Following the digestion the vector arms are dephosphorylated and the samples were checked by 1% agarose gel electrophoresis.

Components	Volume used (µl)
DNA	30
Restriction buffer	5
BSA	0.5
Restriction enzyme	2
H_2O	12.5
Total Volume	50µl

Table 2.4: A standard table shows the components and the volume were used in the restriction digestion of the plasmid and the vector DNA

2.1.7 Dephosphorylation of plasmid vector

During ligation, DNA ligase will catalyze the formation of a phosphodiester bond between adjacent nucleotides only if one nucleotide contains a 5'-phosphate group and the other a 3'-hydroxyl group. Recircularization of plasmid DNA can therefore be minimized by removing the 5' phosphates from both ends of the linear DNA with calf intestinal phosphatase. As a result, neither strand of the duplex can form a phosphodiester bond.

For dephosphorylation, the vector digest was heat shocked at 70°C for 30 minutes then 38µl of nuclease free water, 10x alkaline phosphatase buffer (AP), 2µl Calf intestinal alkaline phosphatase (CIAP-Promega) were added to an end volume of 50µl. After incubation at 37°C for 30minutes, another 2µl of CIAP was added and further incubated for 30minutes to remove the phosphate group from the 5'-ends to

prevent the self-ligation of vector. After dephosphorylation the samples were checked on 1% agarose gel electrophoresis to isolate and purify the linearised vector and inserts for ligation.

2.1.8 Ligation of insert DNA with plasmid DNA

The next step is the ligation of the insert into the linearized vector. This involves the formation of phosphodiester bonds between adjacent 5'-phosphate and 3'-hydroxyl residues. The amounts of vector and the insert DNA used were estimated from the intensity of the ethidium bromide stained DNA band on the gel used. A molar ratio of vector:insert in the range 1:1 - 1:3 was used, with approximately 100ng of vector DNA. An example ligation protocol is shown in table. A control was always performed to check on the religation of the vector. After the ligation incubation, the ligase was heat-inactivated at 65°C for 15minutes and the DNA was transformed into bacterial cells.

2.1.9 Transformation of COT genes into electrocompetent cells

Transformation is the process of getting the recombinant vector from a reaction mixture or vector solution into *E. coli* cells. To enable the cells to take up circular vector DNA they have to be made competent. The method for the preparation of competent cells depends on the transformation method used and transformation efficiency required. For high efficiency we used electroporation and electroporation-competent cells. *E. coli* XL1 Blue was used to transform the plasmid DNA by electroporation (BioRad *E. coli* Pulser or Equibio Easyject Plus 0.2 cm gap cuvettes). 100µl of *E. coli* XL1 blue competent cells were transferred into the cuvettes

30minutes before electroporation. All the necessary materials were kept on ice. Approximately 10ng of plasmid DNA was mixed with 50ul of XL1 blue and 2.5 V applied. As a control, 1μL of plasmid DNA (145ng) of known concentration was also used. The mixtures were incubated for 1min at 42°C in a water-bath and placed on ice for 2minutes. 1mL of ice-cold LB was added and the culture shaken at 200rpm, 37°C for 1hour. The 1mL cultures with PCR products and 10μL of the control culture were plated out in LSLB-agar (LSLB plus 15gram/L agar) with 25μg/mL zeocin and incubated at 37°C overnight. The control was used to check the transformation efficiency. Single colonies of the transformants were chosen to incubate in 5mL of LSLB with 25μg/mL zeocin and the cultures were grown overnight in a 37°C shaker. The DNA was extracted and checked as described above

2.1.10 Cloning into pGAPZ

pGAPZ was available in three forms, a, b or c, the only difference being one restriction site on end of the polylinker, which was *Apa* I, *Xba* I or *Sna*B I, respectively. In case of later wanting to insert something on this site, the one choosen should not cut COT genes. Either pGAPZa and pGAPZb were suitable, the later being the one used.

The polylinkers in pGAPZb consist of the restriction sites of <u>*Bam*H I</u>/ *Sma* I/ *Kpn* I/ *Sac* I/ *Eco*R I and <u>*Sfu* I</u>/ *Eco*R I/ *Pml*I/ *Sfi* I/ *Bsm*B I/ *Asp*718 I/ *Kpn* I/ *Xho* I/ *Sac* II/ *Not* I/ *Apa* I (Invitrogen product manual), respectively, being the underlined one located immediately downstream of the promoter. Using this information, it was decided to *SacI* to cut the gene in theafter the 3'-end and to clone the gene in pGAPZb between *Sfu* I and *Eco*R I. All PCR products were checked for errors by sequencing

carries out by MWG-Biotech. The pGAPZb with the COT genes were then electroporated into *Pichia* and the respective expression levels were checked.

2.1.11 Transformation of the gene into yeast

To increase the efficiency of transformation and integration into the *Pichia pastoris* genome the DNA was linearized using Avr II. This enzyme cuts within the pGAPZ, but does not cut the COT cDNA inserts. The linearized plasmid integrates into *Pichia* genome by homologous recombination. Approximately 30μg of plasmid DNA was digested with 4 units of enzyme at 30°C in a volume of 100μL DNA solution. After several hours of digestion (ideally overnight), the DNA was purified (gel purification kit). After ethanol precipitation, the DNA was resuspended in 10.2μL of sterile, distilled water. This DNA solution (0.2μl) was analysed by gel electophoresis to confirm complete linearization.

Pichia pastoris cells were transformed by electroporation (Bio-Rad GenePulser II or Equibio EasyJect Plus, with 0.2cm path electroporation cuvettes) as described in the Invitrogen product manual. Briefly yeast cells (Pichia pastoris), were grown to an absorbance of 1.3-1.5, harvested by centrifugation (4°C) and washed several times with decreasing volumes of ice-cold water. After final resuspension using 1/250 of the original culture volume of 1M Sorbitol (Merck), 80μl aliquots were used for each transformation.

A modification of this method to improve competence of the cells was the incorporation of a DTT treatment before the washes. The cells were resuspended in 40mL sterile ice-cold water and after addition of 10mL 10X TE buffer (100mM Tris-HCl (Sigma) pH 7.5, 10mM EDTA (Sigma)) and 10mL of 1M lithium acetate, the solution was gently shaken for 45 minutes at 30°C. 2.5mL of 1M DTT (Sigma) was

added and the solution was gently shaken again for 15minutes at 30°C. The cells were pelleted again and washed as before.

The electroporation conditions used were 1.5kV of charging voltage, 25μF of capacitance and 400Ω of resistance for the Bio-Rad GenePulser II and 329Ω for the Equibio EasyJect Plus. Immediately after pulsing (time constant typically 8-10seconds), cells were mixed with 1mL of icecold 1M sorbitol, transferred to 15mL tubes and placed at 30°C. After 1h, 1mL of pre-warmed YPD (1% yeast extract, 2% peptone, 2% dextrose) was added and incubation was continued with shaking at 200rpm. After 4hour the transformed cells were plated out by spreading 250μL on YPDS agar plates (YPD containing 2% agar and 1M sorbitol) containing zeocin and grown at 30°C for 3-5 days until colonies appeared. The zeocin concentrations ranged from 0.1 to 8mg/mL.

2.1.12 Testing the insertions

To ensure the clones were zeocin resistant, they were streaked out for single colonies on YPD plates containing the appropriate concentration of zeocin and grown for 24 hours. The clones were grown in 5mL YPD (200rpm, 30°C) containing half the concentration of zeocin they were resistant to for two days and then transferred to 50mL YPD without antibiotic and incubated again for three days. The cultures were pelleted at 14000rpm for 5minutes at 4°C and washed twice with distilled water. The pellets were weighed and resuspended in 5mL of ice-cold breakage buffer (0.1mM Tris-HCl, pH 7.5, 1mM EDTA, 0.5mM PMSF (Sigma), 3mM DTT). 5mL of cold, acid-washed glass beads (425-600microns) from Sigma were added and allowed to stand for 2 minutes. The mixture was vortexed for 1minute and chilled on ice for at least 30seconds. This cycle was repeated 4 times. To separate the glass beads and the

cells debris from the enzyme suspension, the mixture was spun at 14000pm for 10minutes at 4°C. The COT assays were then performed on the final supernatant and the expression level in U/g_{yeast} calculated. The definition of activity unit (U) is μmol (product)/min using 50μm decanoyl CoA and 1mM L-carnitine (Sigma) as substrate. The clone found to have the highest expression level was used for further transformation and selection in higher zeocin concentrations in order to obtain higher expression levels. Glycerol stocks of the cells clones were made from overnight 5mL YPD culture. Culture aliquots (1mL) with 25% glycerol were snap frozen in liquid nitrogen and stored in -70°C.

2.1.13 Transformation of the recombinant genes into expression systems

The expression systems, *E.Coli*, Rosetta (DE3), Rosetta (DE3)pLySs, BL21 (DE3)pLySs, are purchased from Promega. The host strain is the BL21LacZY (TurnerTM strain) derivative to enhance the expression of eukaryotic proteins that contains codons rarely used in *E.Coli*. These strains supply tRNAs for the codons *AUG, AGG, CUA, CCC, GGA* on a compatible chloramphenicol resistant plasmid. Thus the Rosetta strains provide for universal translation, which is otherwise limited by the codon usage of *E.Coli*. The purified plasmid DNAs from bovine, bovine mutant G553M, human, human mutant Y340H, and rat COT were transformed into Rosetta (DE3)pLySs and in Rosetta (DE3) strains according to the manufacturer's instructions (Promega). The expression cells were thawed and 1μl of plasmid DNA was added to 100μl of expression cells. The cells were mixed gently and incubated on ice for 5 minutes. The tubes were then incubated at 42°C in water bath for 30 seconds without shaking. Then the tubes are placed on ice for 2minutes, 80μl of SOC medium was added into the cells and incubated at 37°C for 1hour in the shaker incubator.

After an hour 50µl of each transformation was spread on LB agar plates with the appropritate antibiotics and incubated overnight at 37°C.

2.1.14 Glycerol Stocks

The stocks of COT from different species expressed in *E.coli* and yeast are given in Table 2.5. Inoculum was prepared from a single isolated colony was picked from the plates and inoculated into 5mL LB with appropriate antibiotics and incubated overnight at 37°C. Then 1mL of this culture was inoculated into 10ml fresh LB broth with appropriate antibiotics and incubated in the shaker incubator at 37°C until the OD_{600}=0.5-0.8, 1mL of this culture was mixed with 25% glycerol, snap frozen with liquid nitrogen, and stored at –70°C for future used.

COT species	**Vector**	**Expression system**
Bovine	PET-28a, pET-11	Rosetta(DE3), Rosetta(DE3)pLysS, BL21(DE3)pLysS
Rat	PET-28a	Rosetta(DE3)pLysS
Human	PET-11PET-28a, pGAPZ	Rosetta(DE3), *Pichia pastoris*
HY340H	PET-11	Rosetta(DE3)
BG553M	PET-11, pET28a.	Rosetta(DE3)

Table 2.5: COT from different species with the vectors and expression systems used.

2.2 Optimisation of cell growth and expression

Growth of the bacterial expression systems (Rosetta(DE3), Rosetta(DE3)pLySs, BL21(DE3)pLySS) containing IPTG inducible COT from bovine, human, rat and mutants G553M and Y340H was optimised to yield large quantities of protein. The growth medium triptone phosphate buffer (TPB) was used. The conditions were designed for all species and mutants are IPTG concentration (0.1, 0.4, 1.0mM), induction temperature (37, 30, 25, 18°C) and induction time (3, 5 and 12hours). The expression levels were determined as specific activity as well as by SDS-PAGE (shown in Chapter 3).

2.2.1 Fermentation of COT and its mutants

Once the optimum expression condition was observed, all COT proteins from bovine, human, rat and mutants bovine-G553M and human-Y340H were grown on a large scale to obtain enough protein for crystallisation and functional studies. The fermentation conditions were growth at 37°C, agitation at 250rpm and air supply of 2L air/L media/min using a 12L microferm fermentor (New Burnswick Scientific). The fermentation stages were monitored by sampling and measuring the optical density at 600nm.

2.2.2 Cell growth and harvesting

2.2.2.1 Rosetta (DE3) pLySs and BL21 (DE3)pLySs

A loop full of glycerol stock was inoculated into 5mL of TPB medium containing 30μg/ml of chloremphenicol and kanamycin and incubated overnight at 37°C. In the morning the inoculum was transferred into 500mL of TPB medium with

appropriate antibiotics and incubated in the shaker incubator at 37°C until the OD_{600} reaches to 0.5. This was used as a starter culture for the fermentation. The fermentation medium TPB was prepared and the conditions were set at 37°C, 250rpm. The cell growth was monitored at 1hour time intervals until the OD_{600}=1.0. Once it reached the stationary phase the temperature was decreased to 18°C and the protein expression induced by adding IPTG and left at 18°C with agitation overnight. The cells were harvested by centrifugation at 6000xg for 10minutes and the pellets were stored at –70°C.

2.2.2.2 Pichia pastoris

Pichia cells expressing wild-type COT from rat, mouse and human were grown on a small scale to analyse the functional properties of COT in membrane and soluble forms. A single colony was picked from the streak plate and inoculated into 5mL YPD containing 1mg/mL zeocin and incubated in shaker incubator at 250rpm and 30°C until it reaches the late exponential phase then used as a starter culture to grow 1L culture. The fermentation medium 1L YPD was prepared and the starter culture was inoculated and left overnight in the shaker incubator at 30°C and 250rpm. The cells were harvested by centrifugation at 2000xg, for 5min at 4°C then the pellet were resuspended in a 4x volume/4x the dry cell mass of ice cold washing buffer (150mM KCL, 5mMTris-HCl, pH 7.2), then the suspension were centrifuged again at 2000rpm for 5minutes. The pellets and the supernatant were stored at-70°C.

2.3 Enzyme Assays

Carnitine acyltransferases catalyse the reversible transfer of acyl group from CoA to L-carnitine and their activity can be measured spectrophotometrically. The rate of CoASH release was measured by its reaction with thiol reagent, 4-dithiobispyridine (4-PDS), with which it undergoes disulphide exchange releasing thiopyridone (Figure 2.2). The thiopyridone absorbance at 324nm has an extinction coefficient of 19800 mM^{-1} cm^{-1}. The method used was based on Ramsay (1975).

Acyl- CoA + L-Carnitine ↔ acyl-L-Carnitne + CoASH

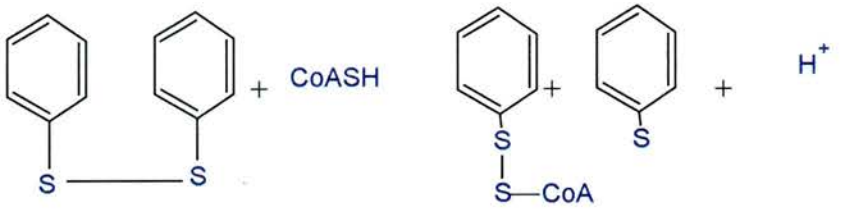

Dithiobis pyridine **Thiopyridone**

Figure 2.2: Conversion of dithiobispyridine to thiopyridone by CoASH

The UV-2401PC spectrophotometer (Shimadzu, UK) was used for this assay. The assay mixture contains 20mM potassium phosphate (KPi), pH 7.4, 125μM 4-PDS, 50μM acyl-CoA, 1mM L-carnitine and COT in a final volume of 1mL. The assay was performed at 324nm at a temperature of 30°C. The absorbance is measured over 300seconds. The order in which the reagents are added is important. The decanoyl-CoA is added first, then the enzyme and then the carnitine. The rate of

change in absorbance in the presence of decanoyl-CoA and enzyme was measured to determine the activity of hydrolases that are present, especially in crude samples. This background value is subtracted from the rate of change in absorbance when the reaction is started by the addition of L-carnitine. The background rate was measured just before the addition of L-carnitine, after the system has had an opportunity to equilibrate. However, for the measurement of COT activity the initial rate is measured, usually up to the point 10-15% of the substrate is used. Once the rate has been measured, the activity is calculated using the following equation.

$$\text{Activity} = \frac{\Delta\text{Abs/min}}{\text{extinction coefficient}} \times \frac{\text{total volume}}{\text{enzyme volume}} \times \text{dilution factor} = \mu\text{mol.min}^{-1}\ \text{ml}^{-1}$$

All acyl-CoA solutions were made in 5mM potassium phosphate, pH 6.5, to minimise hydrolysis. L-Carnitine hydrochloride was dissolved in 20mM potassium phosphate, pH 7.5, and neutralised by the addition of one equivalent of 6M KOH. The stock solutions of these substrates were standardised using the commercial pigeon breast CAT and limiting concentration of one substrate in the presence of excess of the other. For long chain acyl-CoA stocks, pure beef liver COT was used in the standardisation assay.

2.4 Purification of non-his tagged COT

2.4.1 Starter culture preparation

Glycerol stocks of Bovine COT BL21(DE3)pLysS are maintained at -70°C. The pure culture of this strain was achieved by streak plate method. The starter culture was prepared by selecting a single colony from the streak plate and adding this into a 6mL of TB+ carbenicillin (carb) + chloramphenicol (cam) (final concentration of 50μg/ml and 34μg/ml respectively) and incubated overnight at 37°C without shaking. The BL21 (DE3) pLySs strain is resistant to both antibiotics.

In the morning 3mL of one of the set up cultures was transferred into 500mL of terrific broth containing 34μg/mL chloremphenicol and 50μg/mL carbenicillin. The induction culture was incubated at 37°C with shaking until the OD_{600} reaches 0.6. After 3-4 hours the gene expression was induced by IPTG at a final concentration of 1mM. The temperature was decreased to 18°C and incubated overnight in the shaker incubator. The bacterial suspension was centrifuged at 5000g for 10 minutes at 4°C to pellet the cells. The supernatant was discarded and the pellet re-suspended in 0.1 culture volume of ice cold buffer which contains 50mM TRIS/HCl, pH 7.5, + 2mM EDTA + 1mM Phenyl Methane Sulphonylfluoride (PMSF) and frozen overnight. The components of the buffer preserve the activity of the protein by blocking oxidizing agents and proteolysis. As the cells carry pLySs they will lyse on thawing.

2.4.2 Cell disruption

A sonicator is a device used to break down cells using ultrasonic waves. Ultrasonic waves are transmitted through a metal rod, which is placed in a suspension

of the cells. The vibrations cause the cell membranes to rupture and the cellular contents are released into the surrounding medium. The cells were thawed and sonicated, 6x30 seconds with large probes, to lyse the cells thoroughly. The sample was then spun in an ultracentrifuge at 22000xg for 20 minutes at 4°C to bring the cellular debris down into pellets. The pellets containing insoluble bovine COT and cellular debris were discarded and the supernatant was used for ammonium sulphate precipitation.

2.4.3 Ammonium sulphate precipitation

Precipitation is widely used for product recovery of biomolecules especially proteins. The most common type of precipitation for proteins is ammonium sulphate precipitation. Protein solubility depends on several factors. It is observed that at low concentration of the salt, solubility of the proteins usually increases slightly. This is termed *Salting in*. But at high concentrations of salt, the solubility of the proteins drops sharply. This is termed *Salting out* and the proteins precipitate out. It was established that 40-55% ammonium sulphate cut would precipitate COT in the 55% pellet.

2.4.3.1 40% ammonium sulphate precipitation

The supernatant was transferred into clean beaker and 22.9g ammonium sulphate/100mL was added slowly and mixed thoroughly using a magnetic stirrer on ice. After 30 minutes of incubation the sample was centrifuged at 22,000xg in JA14 bottles at 4°C for 20 minutes. COT activity remained in the supernatant. The pellets were re-suspended in 5mL ice-cold 50mM TRIS/HCl, pH 7.5 + 2mM EDTA + 1mM

PMSF and the activity measured to verify that there was no loss of enzyme in the pellets.

2.4.3.2 55% ammonium sulphate precipitation

In addition to 22.9g/100mL ammonium sulphate already present in the supernatant, another 9g/100mL was added to increase the ammonium sulphate concentration to 55%. This was mixed thoroughly and incubated on ice for 30 minutes with stirring. Then the sample was centrifuged at 22,000xg in JA14 bottles at 4°C for 20 minutes and the pellets were re-suspended in ice-cold buffer and the supernatant was discarded.

2.4.3.3 Dialysis

The 55% ammonium sulphate pellet in 5mL ice-cold buffer was loaded into dialysis tube and dialysed against 20mM TRIS/HCl, pH 7.5 at 4°C with three changes of buffer. The minimum dialysis time was 2hours in between the buffer change. The volume of the sample was increased to about 150% of the original sample due to the water movement into the concentrated protein solution. The sample was then centrifuged at 22000xg and ready for further purification.

2.4.4 Purification by column chromatography

The dialysed COT was centrifuged and filtered through 0.22μm filter using syringe. The sample was further purified using column chromatography. In this method two different column materials and three different sizes of columns were used, the larger columns for salt elution and the small one for affinity elution.

1. DiEthylAminoEthyl (DEAE) Cellulose DE53
2. Blue Sepharose CL-6B with two different size of columns

Both the materials are processed and packed into the appropriate column as per the Sigma Chemical Company instructions.

2.4.4.1 Column 1: DEAE cellulose

DiEthylAminoEthyl-groups are covalently bound to the cellulose hydroxyl groups. This anion exchanger can be used for the purification of proteins with neutral isoelectric points (pI). Prior to loading the sample the column (20cm x 6.5 cm) was equilibrated with 10mM potassium phosphate (KPi), pH 7.5. Sample was loaded carefully with a pipette and the column washed with 2column volume (CV) of 10mM KPi at pH 7.5 to remove the bulk impurities from the crude sample. The enzyme was eluted with 20mM KPi at pH 7.5 and the fractions, checked for activity, pooled, volume measured and loaded into the big blue Sepharose CL-6B.

2.4.4.2 Column 2: Big blue sepharose CL-6B fast flow (Linear gradient)

All the pooled fractions from DEAE cellulose column were loaded into the big blue sepharose CL-6B column. In this column washing is a crucial factor to remove most of the impurities from the sample. The column was initially washed with 5CV of 20mM KPi, 2mM EDTA, 1mM PMSF, pH 7.5 and then with addition of 30mM KCl. The enzyme was eluted with a linear gradient of salt concentration from 30-300mM KCl in 20mM KPi, pH 7.5. Enzyme activity and protein (by the absorbance at 280nm) were determined in all the fractions and plotted on the graph. The active fractions were pooled and mixed together and the activity and protein were checked. The sample volume was very high and therefore concentrated by Amicon (Pmax, 60Psi, 5.3 kg/cm2) concentrator to bring to a small volume. The sample was dialysed against 20mM KPi to remove all the salt from the sample prior to affinity elution.

2.4.4.3 Small blue sepharose CL-6B fast flow (affinity elution)

Dialysed enzyme sample was centrifuged, filtered, and loaded onto the small blue column. The column was washed with 3CV of 20mM KPi alone and then with 2 column volumes of 20mM KPi + 30mM KCL to remove the protein impurities. Then the enzyme was eluted with 6CV of 20mM KPi + 30mM KCL containing 10mg of n-Octanoyl-CoA. This elution is slightly different, depending on the amount of hydroxy methylglutaryl-CoA synthase carried through from earlier stages. Only proteins that bind with octanoyl-CoA should be eluted (Ramsay *et al.*, 1987). The active fractions were plotted, pooled together and concentrated into small volume. The sample was mixed with 20% glycerol and 0.5mM dithithretol (DTT) and stored at –20°C.

2.4.5 Determination of protein concentrations

The quantity of protein in samples was measured using the Peterson-Lowry micro-assay, a modified Lowry assay which detects small quantities of protein (Petersen, 1977). A series of BSA standards (0-150μg) were used. To 100μL of each standard solution was added 0.4mL of H_2O and 50μL of 0.5% deoxycholate. After 5 min on ice, 75μL of TCA 55% w/v were added and mixed well.

The samples were incubated on ice for 15 minutes, centrifuged at 10,000g for 10 minutes at 4°C. The supernatant was removed and 0.5mL of 1M NaOH was added to redissolve the pellet. 0.5mL of Lowry reagent A (copper tartrate carbonate (CTC): 10% SDS: 0.8M NaOH: H_2O) was added, the samples were mixed and left at room temperature for 10 minutes. 0.25mL of Lowry reagent B (1mL of Folin-ciocalteau and

5mL H_2O) was added; the samples were mixed and developed in the dark for 30 minutes. The absorbance was read at 750nm.

The protein concentration of highly purified samples was determined by using the BCA method with and appropriate range of BSA concentrations as standards.

2.4.6 SDS-Polyacrylamide gel electrophoresis (SDS-PAGE)

SDS–PAGE was used to analyse the purity of the COT enzyme sample. The samples from different stages of purification were prepared at several concentrations (5, 10, 20 & 50μg/mL) to determine the success of each purification step. A 10% gel was prepared and the COT samples and prestained marker (invitrogen LC 9525) loaded carefully using clean syringes to avoid cross contamination. Electrophoresis (Bio-Rad mini-protean II electrophoresis cell) was performed at constant voltage of 200V(constant voltage) until the dye band had migrated towards the bottom of the gel (approx. 40-50 minutes). The gels are stained with Coomassie blue for 5 minutes and complete destaining was achieved after 12 hours with agitation. In some cases the gel was silver stained to detect minor impurities

Figure 2.3 SUMMARY OF PURIFICATION

Recombinant Bovine COT in *E. coli,* BE21(DE3) pLysS

Thawed, sonicated, centrifuged

↓

Supernatant Ammonium Sulphate precipitation

40-55% pellet

homogenized with 50mM TRIS/HCl pH 7.5+ 2mM EDTA+1mM PMSF

↓

Dialysis (with 3 changes of buffer 20mM TRIS/HCl, pH 7.4)

↓

Column Chromatography

DEAE Cellulose

10mM KPi wash and elution with 20mM KPi pH 7.5

↓

Large Blue Sepharose CL-6B fast flow

Initial wash with 20mM KPi, II wash with 20mM KPi+30mM KCl, pH 7.5

Eluted with 30-300mM KCl in 20mM KPi buffer.

↓

Concentrated by Amicon pressure filtration by PM 30 filter

Dialysed against 20mM KPi, pH 7.5

↓

Small Blue Sepharose CL-6B fast flow

Wash with 20mM KPi, and wash with 20mM KPi + 30mM KCl, pH 7.5

Enzyme eluted with 35 ml of 20mM KPi + 30mM KCl + 3.5mg n-Octanoyl CoA

↓

Concentrated, dialysed

Stored in 20% glycerol and 0.5mM Dithiothretol (DTT)

↓

Purity was checked by SDS-PAGE.
Activity and protein concentration determined.

2.5 His-tagged COT purification

The purification is based on Amersham Bioscience catalogue. The three basic steps involved in His-tagged protein purification from Rosetta(DE3)pLySs are shown in Figure 2.4. The steps were optimized for efficient recovery of the His-tagged proteins. The elution of His-tagged proteins from Ni^{2}+ high performance Sepahrose column is dependent on the nature of the protein: different proteins elute from the particles at varying concentrations of imidazole. Our experiments showed that COT from all the different species was eluted by 250mM imidazole.

2.5.1 Cell disruption

The Rosetta(DE3) cells from the freezer were resuspended in 50mL PBS, 0.5M NaCl, 10mM imidazole and 1 tablet of EDTA free protease inhibitor cocktail and the cell suspension was sonicated on ice using a large tip connected to Soniprep-150 at an amplitude of 10 microns for 3x30s. The suspension was centrifuged at 22000xg for 20min and the pellets were discarded. The supernatant was ultracentrifuged at 40000 rpm for 1hour and the pellets are discarded.

2.5.2 Selection of His-tagged protein by Ni^{2+} column

Ni-Sepharose (High Performance) consists of highly cross-linked 6% agarose beads to which a chelating group has been immobilized. This chelating group has then been charged with Ni^{2}+ ions. The resulting column selectively retains His-tagged recombinant proteins, allowing them to be purified from cellular contaminants or cell-free systems.

The supernatant was filtered through 0.22μm filter and loaded into high performance N^{2+} sepharose column (25mL) equilibrated with binding buffer (1xPBS,

0.5M NaCl, 10mM imidazole) at flow rate of 1mL/minute. The column was washed with 5CV of washing buffer (1xPBS, 0.5M NaCl, 30mM imidazole). The his-tag proteins were eluted with 5CV of elution buffer (1xPBS, 0.5M NaCl, 300mM imidazole) by linear gradient (Econo Gradient pump-BioRad-UK). The active fractions were pooled and dialysed extensively against 20mM Tris/HCl, pH 7.5 to remove imidazole.

2.5.3 Ion exchange chromatography

The dialysed protein sample was loaded into 5mL HiTrap Q Sepahrose column and washed with 5CV of 20mM Tris/HCl, pH 7.5 flow rate at 5mL/minute. The protein was eluted with 5CV high salt linear gradient (20mM Tris/HCl, 1M NaCl, pH-7.5). The active fractions were collected and dialysed against 1L 20mM Tris/HCl for 3 times, ready for the removal of the His-tag from the N-terminal by thrombin digestion.

2.5.4 Optimisation of thrombin digestion

The removal of N-terminal His-tag is essential for the structural studies. The enzyme thrombin was purchased from Novagen, Merk-Biosciences and the concentration of the enzyme required to cleave 1mg protein was optimised following Novagen procedure. The cleavage was analysed by 4-10% gradient gel and by Mass spectrometry. The conditions tested are reported in Chapter 3 and the best was routinely used thereafter. Once the His-tag was removed the protein sample was loaded onto the 5ml Ni^{2+} column and COT directly eluted by washing buffer (1xPBS, 0.5M NaCl, 10mM imidazole). The active COT samples were pooled and concentrated to 5mg/mL.

Figure 2.4 SUMMARYOF HIS-TAG COT PURIFICATION

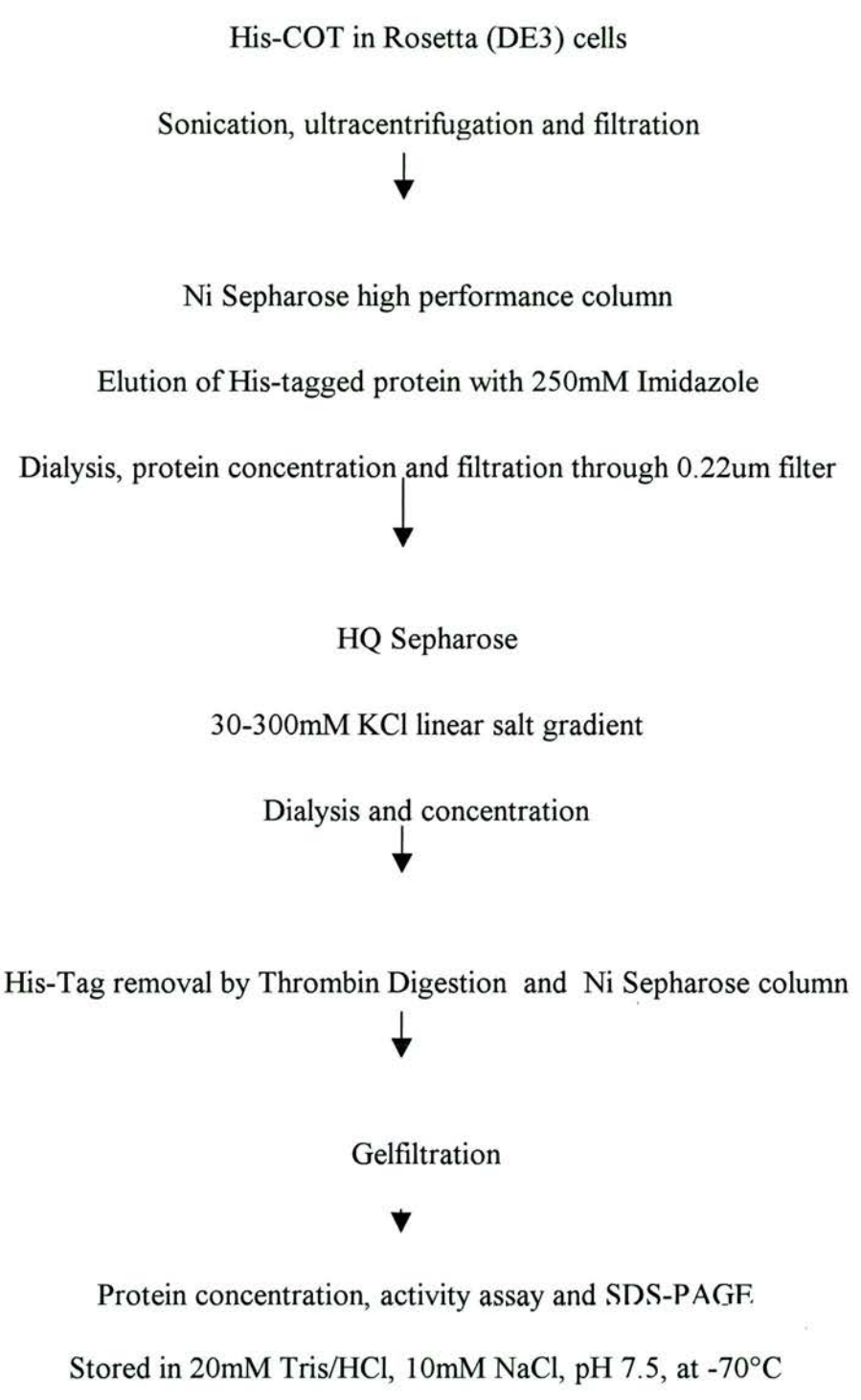

2.5.5 Gel filtration

His-tag cleaved COT was loaded into a gel filtration column (Sephacryl S-200, Size-16/16). The column was attached to the AKTA Prime purification system and equilibrated with 20mM Tris/HCl, 10mM NaCl, pH 7.5. The column flow rate was 1mL/min and 5mL sample was injected and eluted with same buffer. The molecular weight was determined by mass-spectral analysis. The purity of the protein was analysed by SDS-PAGE gel electrophoresis. The protein was concentrated to 20mg/mL in 20mM Tris/HCl, 10mM NaCl, pH 7.5, snap frozen with liquid nitrogen and stored at -70°C.

2.6 Extraction of COT from yeast

Pichia pastoris cells expressing COT were thawed and washed with ice cold buffer A (150mM KCl, 5mM Tris-HCl, pH 7.2) and centrifuged at 2000xg for 5minutes at 4°C. The pellets were resuspended in 1mL of buffer B (buffer B is buffer A in addition with 1mM PMSF, 0.5 benzamidine, 10ng/mL leupeptin), 3mL of cold, acid-washed small glass beads was added and the cells were disrupted by vigourous vortexing (4 pulses of 1minute and 2minutes intervals on ice). The homogenate were centrifuged at 800xg for 3minute at 4°C to remove the beads and cell debris. This crude extract was further centrifuged at 15000Xg for 10 minutes at 4°C. Pellets and supernatant were stored in small aliquots at –20°C.

Carnitine acyltransferase activity from the membrane (pellet) and the supernatant was measured by the production of thiopyridone detected at 324 nm in a Shimadzu 2101PC spectrophotometer after adding enzyme to 20 mM KPi, pH 7.4,

containing 125μM dithiobispyridine at saturating concentrations of acyl-CoA and L-carnitine.

2.7 Crystallisation of COT and CPT2

One aim of this work was to determine the structure of COT. This work was done in collaboration with Prof. James H. Naismith, Centre for Biomolecular Sciences, University of St Andrews. Purified COT from bovine, human, rat and CPT2 were used for crystal trials without freezing after the final step of purification. The protein was ultracentrifuged at 40000xg for 1 hour and concentrated to 15mg/mL in 20mM Tris/HCl, 10mM NaCl, pH 7.5. Initially 15mg/mL protein was given to the robotic system to lay on the plates. Proteins were also laid manually in different conditions. Table 2.6 shows the range of different conditions and the protein samples used in crystal trials.

In a 96 well plate 150μL of buffer was transferred into the buffer reservoir. In a well 2μl of 15mg/mL protein and 2μL of buffer was mixed gently and sealed with clean film. The plates were incubated at 2 different temperatures 4 and 20°C. All the plates were examined under the microscope every 3 days. Bovine COT was plated in the presence of substrate L-carnitine at 10mM concentration and with the bridge compound formed between 2-bromoacetyl L-carnitine and CoA (Sigma Tau, s.P.A, Italy). Rat CPT2 was also purified and used with the same conditions as for COT.

Crystal Screen	Protein sample
Wizard 1&II	Bovine, rat and human COT
Index I&II	Bovine,rat, human and CPT2
The PEG's	Bovine and CPT2
PEG Ion & Natrix	Bovine and CPT2
Ammonium Sulphate screen	Bovine COT

Table 2.6: Crystal screen and the protein samples were used in the crystal trials.

2.8 Kinetics analysis of COT

Initial rates for carnitine acyltransferase activity were analysed using the steady-state Michaelis–Menten equation. Both substrates were varied and the data plotted according to Hanes (S/v vs S) or Lineweaver-Burk (1/v vs 1/S). Initial velocities were measured by choosing enzyme concentrations that ensured a strictly linear relationship between incubation time and rate of reaction. Kinetic constants were determined in the 6cell spectrophotometer at 30°C. The reaction time was 5minutes and the 1mL reaction mixture contains 20mM potassium phosphate, pH 7.4, 125μM PDS and 6 different concentrations of acyl-CoA at a fixed concentration of L-carnitine (1mM), When L-carnitine was varied, acyl-CoA was kept at a fixed saturating concentration.

The apparent kinetic constants were calculated by fitting the data to the Michaelis-Menten equation using the Schimadzu kinetic software. Linear secondary plots constructed in Microsoft Excel yielded the true kinetic constants. The full

kinetic data were analysed by constructing double reciprocal plots of velocity and substrate concentrations, followed by re-plots of slopes and intercepts against reciprocal concentrations of changing fixed substrates in the initial velocity studies or against the inhibitor concentrations. Single points that deviated widely from the general pattern of double reciprocal plots were discarded. The re-plots were fitted to a straight line by least squares regression.

2.8.1 Substrate specificity

The substrate specificity of wild type and mutant COT were determined using different chain lengths of acyl-CoA and L-carnitine (discussed in detail in Chapter 3). The apparent Km and Vmax for each acyl-CoA was determined at 1mM L-carnitine.

2.8.2 Measurement of enzyme hydrolysis

The rate of hydrolysis was measured in the absence of L-carnitine. The assay mixture contains 1mL of 20mM potassium phosphate, pH 7.4, 125μM PDS and different concentrations of acyl-CoA and 1μg of pure COT. The Km for hydrolysis was determined using S/v vs S plot.

2.8.3 Reverse reaction

The activity in the reverse direction was measured as the increase in the thioester at 232nm (extinction coefficient, 4500 M^{-1} cm^{-1}) from acetyl-L-carnitine or decanoyl-L-carnitine, and CoA. The assay mixture (1mL) contained, 20mM

potassium phosphate, pH 7.4, acetyl-L-carnitine and decanoyl-L-carnitine (30-200 μM) and CoA (200μM).

2.9 Inhibition studies of COT

All inhibitors used were water soluble except C75 (in DMSO) and Stock solutions (10mM) were made in water the pH was neutralised with 1M KOH. Initial IC50 values were obtained from a series of different concentrations inhibitors were assayed with subsaturating concentrations of acyl-CoA and L-carnitine. Also saturating concentrations of both substrates were used to see wheather substrates could compete the inhibitors. The 1 mL assay contains 20mM KPi, 125μM PDS, 6 different concentrations of the inhibitor and sub-saturating concentrations of acyl-CoA(5μM decanoyl-CoA, or 2μM butyryl-CoA, and 400μM L-carnitine).The IC_{50} obtained from the inhibited rate divided by the control without any inhibitor added.

2.9.1 True Ki and the type of inhibition

The type of inhibition was determined from Hanes plots of velocity and substrate concentrations (S/v vs S), followed by re-plots of slopes and intercepts against inhibitor concentrations. The Ki value for each inhibitor was obtained from the replot of Km(app) against inhibitor concentration for both substrates but not for all the inhibitors.

2.9.2 Synthesis of etomoxiryl-CoA

Etomoxir is a 2[6(4-chlorophenoxy)hexyl]oxirane-2-carboxylate compound once developed for the treatment of diabetes mellitus. It is an inhibitor of carnitine palmitoyltransferase-I (CPT-1), the mitochondrial enzyme that plays a key role in the transport of long-chain acyl-CoA compounds into the mitochondria. In 1992 Lilly *et al.*, reported that the etomoxiryl-CoA inhibited purified carnitine acyltransferases at nanomolar concentrations and also inhibited the carnitine acyl-transferases of rat heart mitochondria and rat liver microsomes. It was proposed by many investigators that the etomoxiryl-CoA must bind to a high affinity site with specific inhibition of mitochondrial CPT1. The concentrations of etomoxiryl-CoA required for 50% inhibition of the different carnitine acetyltransferases, microsomal and peroxisomal carnitine octanoyltransferase are in the low micromolar range.

2.9.2.1 Etomoxir

Etomoxir was purchased from Sigma Chemical Co. and etomoxiryl-CoA was synthesised by *Mr.Gildas Deniau*, School of Chemistry. The synthesis of etomoxir to etomoxiryl-CoA was based on the method of Chase and Tubbs, 1992.

2.9.2.2 Etomoxir to etomoxir chloride

To a solution of etomoxir (4 mg) in toluene (1 mL) was added an excess of oxalyl chloride and 20 µl of catalyst dimethylformamide. The reaction was stirred for 6 hours at room temperature. The solvent was then evaporated under vaccum given etomoxir chloride as an oil (3.5 mg).

2.9.2.3 Etomoxir chloride to etomoxiryl-CoA

Etomoxir chloride was weighed (3.5mg) and 12mg of CoA were mixed in 2-methylpropan-2-ol adjusted to pH 8.0. The residual CoA was detected by nitroprosside test (1 drop of CoA mix + 1 drop of nitroprosside reagent on the filter paper). The reaction was confirmed by color change. If pink appeared reaction was not complete; if colorless, 1 drop NaOH in ethanol was added. The spot then turned purple-pink if all CoA was utilised to form etomoxiryl-CoA. The product was analysed spectrally (see Chapter 5).

2.9.2.4 Time-dependant inhibition

Purified human COT was assayed with etomoxiryl-CoA to see its inhibition pattern and IC_{50} obtained with saturating concentrations of decanoyl-CoA and sub-saturating concentrations of L-carnitine (400μM). Enzyme inactivation was studied by incubating equal amounts of enzyme and etomoxiryl-CoA at 30°C. This mixture was assayed at a series of different time intervals compared to enzyme alone incubated as a control. The assay was carried out by adding 20μl of mixture to a cuvette containing both substrates (50μM decanoyl-CoA and 1mM L-carniitne) and assayed for 300seconds. The data was plotted as time vs activity (mAbs/min) as discussed in Chapter 5.

2.9.3 COT inhibition by Malonyl-CoA

Malonyl-CoA is an intermediate in the synthesis of fatty acids and inhibits long chain carnitine acyltransferase at physiological levels. The aim of this assay was to determine the peroxisomal COT sensitivity to malonyl-CoA. The assay was

performed using various acyl-CoA derivatives at saturating and substurating concentrations of both acyl-CoA and L-carnitine. The IC_{50} values were obtained from a series of different concentrations of malonyl-CoA (5-300μM) at sub-saturating concentration of both substrates.

2.9.4 COT inhibition by C75

C75 (*trans*-4-carboxy-5-octyl-3-methylenebutyrolactone) is inhibitor of fatty acid synthase that acts centrally to reduce food intake and body weight. C75 was purchased from Sigma Chemical Co. and 20mM stock was made in DMSO. The assay was performed with a series of different concentrations of C75 (5,10,50,100, &200μM) at saturating concentrations of both decanoyl-CoA (50μM) and L-carnitine(1mM). Purified human COT was used without pre-incubation with inhibitor.

3. Cloning, expression, purification and crystallisation

3.1 Cloning

Carnitine octanoyltransferase (COT) catalyse the reversible transfer acyl groups from CoA to L-carnitine and facilitates the transport of medium chain fatty acids through the peroxisome membrane to the mitochondria for further oxidation. Understanding of the role of specific amino acid residues involved in substrate specificity, catalytic activity and malonyl-CoA sensitivity is hampered by the high sequence conservation observed in mammalian COT. The aim in this section was to clone COT from bovine, rat, human to species in sequences and conserved effects of mutations on substrate specificity and malonyl-CoA sensitivity. The amino acid sequence of mammalian carnitine acyltransferase from different species are obtained from the SwissProt data bank and all the sequences are given to ClustalW for the identification of conserved residues. The output results are given in appendix. From the sequence analysis we proposed two hypotheses, outlined below, for the acyl binding site and for the malonyl-CoA sensitivity of COT.

3.1.1 Substrate specificity

CAT is the only member of the family for which the structure has been solved. In the structure, a putative site for the binding of long chain acyl groups was identified, but access to the pocket was blocked by Met564 and the equivalent residue in COT is Gly553. If it is mutated to the larger Met, the acyl binding cavity should be blocked. The sequence alignment and the conserved residues are indicated in figure 3.1.

A

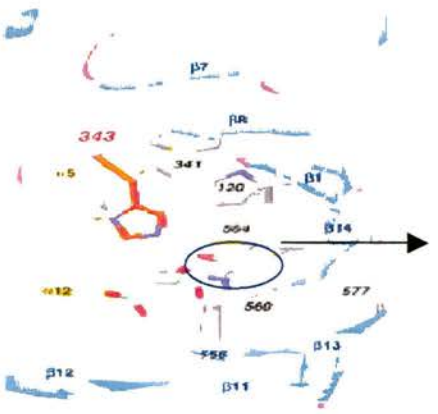

B

```
CAT-RAT   SYAIAMHFN--LSTSQVPAKTDCVMFFGPVVPDGYGICYNPMEAHIN  587
CAT-Mouse SYAIAMHFN--LSTSQVPAKTDCVMFFGPVVPDGYGICYNPMEAHIN  587
COT-HS    FSKSGGGGNFVLSTSLVGYLRVQGVVVPMVHNGYGFFYHIRDDRFV 575
COT-Rat   FSRSGGGGNFVLSTSLVGYLRIQGVVVPMVHNGYGFFYHIRDDRFV 575
COT-Bovine FSRSGGGGNFVLSTSLVGYLRVQGVMVPMVHNGYGFFYHIRDDRFV575
```

Figure 3.1: A. Mouse CAT structure shows larger methionine at 564. **B, Amino acid sequence alignment of mammalian CAT, COT and CPT.** Sequences from SwissProt data bank were aligned using Clustalw. The mouse CAT shows methionine at 564 in pink and the corresponding conserved residue in COT is glycine553 indicated green in colour.

From this result we constructed a mutant G553M to see its effects on acyl-CoA. The wild type bovine COT was used as a template to amplify the mutant sequence.

3.1.2 Malonyl-CoA sensitivity

It has been proposed that COT might be regulated by malonyl-CoA in rat, which has His at 131 and 340 but not in cow, which does not (Figure 3.2). Human COT has His at 131 but Y at 340. If we mutate the Y340 to H in human COT it should be more sensitive to malonyl-CoA. From the sequence comparison, we decided to construct wild type human and mutant Y340H mutant to see its sensitivity to malonyl-CoA. This is first time human COT is been constructed.

```
Rat-COT. . . 320 IFGCSCDHAPYDAMLMVNIAHYVDEKLLETEG 351
Mouse-COT. . 320 IFGCCCDHAPYDAMVMVNIAHYVDERVLETEG 351
Human-COT. . 320 VFGCNCDHAPFDAMIMVNISYYVDEKIFQNEG 351
Bovine-COT.. 320 VFGSNCDHAPFDAMVLVKVCYYVDENILENEG 351
Fugu-COT. .. 285 TFGSNCDHAPYDAMVLVTMCWYVDQRIQSTGG 326
```

Figure 3.2: The amino acid sequence alignment of the mammalian COT obtained from SwissProt data bank and aligned using ClustalW. The conserved catalytic H327 is highlighted. Also highlighted is H340 in rat and mouse COT but in human and bovine COT the corresponding residue is Y.

3.1.3 Polymerase Chain Reaction

The wild type bovine COT in a pET11-vector was expressed in *E. Coli* strain BL21(DE3)pLysS and the plasmid DNA was purified prior to PCR. The purified plasmid DNA was digested with Ndei-BamH1. The PCR product was analysed by 1% agarose gel electrophoresis (Figure 3.3).

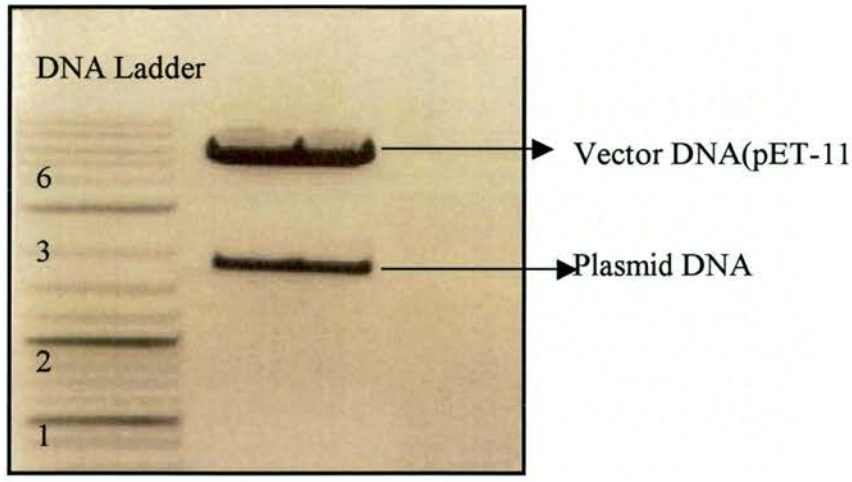

Figure 3.3: The gel shows that the vector and the plasmid DNA was successfully cleaved and shows on the correct DNA size. The plasmid DNA from the wild type bovine COT which was expressed in BL21(DE3)pLySs was purified and digested with NdeI-BamH1 restriction enzyme.

The plasmid DNA of bCOT from the gel was excised and purified from the gel for the PCR amplification of the mutant G553M. The Gly553Met mutation was introduced by PCR using the primers 5'-TGGCAAAAAGCTAAGGAGAA-3' (forward) and 5' TACCATGGGAACCATCACCATCTGGACTCTTAAATAA-3' (reverse: Gly antcodon and *Nco*I site underlined) with pET-bCOT^{wt} as template.The product was digested with *Bsr*GI-*Nco*I and used to replace the corresponding fragment in pET-bCOT^{wt}. The PCR product was analysed by 1% agarose gel electrophoresis.(Figure 2) The sequence was confirmed by DNA sequence analysis.

3.1.4 Identification of the cDNA encoding human COT

The human COT open reading frame was amplified from HepG2 cell cDNA using the primers 5'-CCCCCTACATATGGAGAATCAACTGGCTAAATCAAC-3' (forward, *Nde*I site) and 5'-ATGCCCTCGAGTCACAGGTGAGTAGAGTTCATC-3' (reverse, *Xho*I site). The PCR product was cloned into pGEM-T (Promega) and the sequence verified.

3.1.5 Site-directed mutagenesis of human COT mutant Y340H:

The coding sequence of human COT cDNA was subcloned into pET-21b as an NdeI-XhoI fragment and was expressed in *E. coli* strain BL21(DE3). It was also subcloned into the Eco72I-XhoI sites of the *Pichia pastoris* expression vector pGAPZB as a (blunted NdeI)-XhoI fragment.

The Y340H mutation was introduced by overlap extension PCR. Separate PCR reactions were performed with primers A (GAGGCCGAGCTTTTGTCTTT) and B (CCACATAATGACTGATGTTCACCATAA), and C (GGTGAACATCAGTCATTATGTGGATGAGAAAA) and D

(ATACTGGGCTTTAGCTTGGTTGAT), with the wild-type cDNA as template. The purified products were annealed, extended, and amplified for 5 cycles using primers A and D. The PCR product was cloned into pGEM-T (Promega) and its sequence verified. The SpeI-SacI fragment containing the mutation was used to replace the corresponding region of the wild type COT in pGAPZB. A *Spe*I-*Bam*HI fragment was subsequently transferred to COT in pET-21b.

Both the complete wild-type and Y340H hCOT coding sequences were also subcloned separately from pET-21b into pET-28c(+) vector as *Nde*I-*Bam*HI fragments, thus adding an N-terminal $(His)_6$ tag for ease of purification. Expression was performed in *E. coli* strain Rosetta(DE3) according to the Novagen catalogue. Once the vector and plasmid DNA was confirmed by the gel (Figure 3.4), the DNA bands are excised and the purified for the gel and they are ligated together with its appropriate vectors. Table 3.1 shows the plasmid DNA and the vectors used to ligate to get the desired clones.

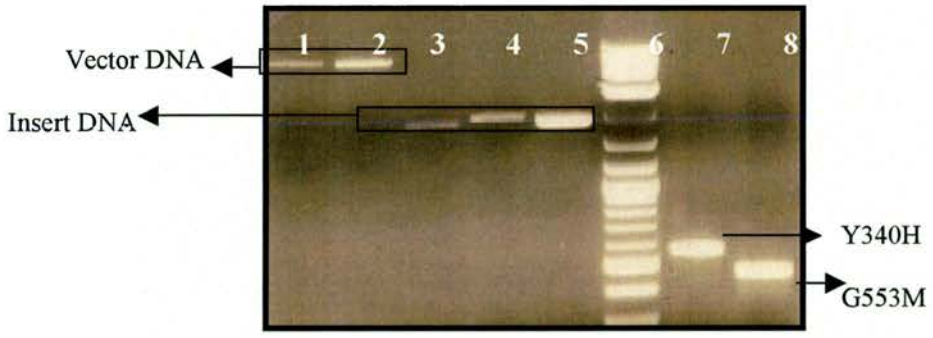

Figure 3.4: The band pattern of the purified vector and plasmid DNA used for the transformation. Lane 1: pET-11, 2. pET-28a, 3. bovine, 4. human, 5. rat COT. which was purified for the ligation and 6. DNA ladder, 7.Y340H, 8. G553M are PCR products. The gel shows that the vector and the plasmid DNA was successfully cleaved and shows on the correct DNA size.

COT Species	Vector
Bovine	PET-11& pET-28a
B-G553M	PET-11
Human	PET-11, & pET-28a
H-Y340H	PET-11
Rat	PET-28a

Table 3.1 Vectors used with each clone.

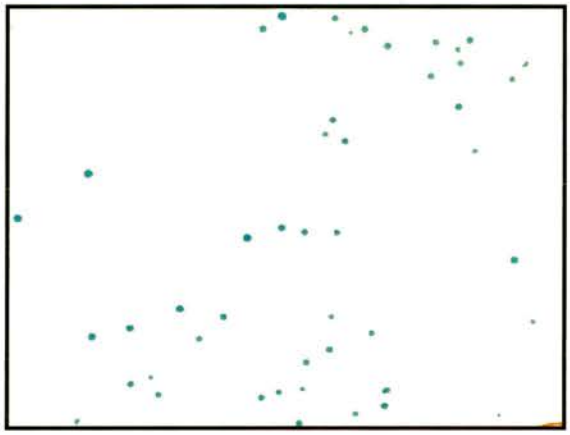

Figure 3.5: X-gal plate with white colonies of the bovine mutant confirms successful transformation of the bovine mutant.

Ligated bovine mutant was transformed into X-gal blue cells to verify the clones. The growth of white colonies confirms successful transformation as shown the Figure 3.5.

After the successful transformation, 2 colonies were picked from the plates and inoculated into LB+carbenicillin broth and grown overnight. The DNA was purified and digested with NdeI-BamH1 buffer and the product was analysed by agarose gel shows both the insert and vector (Figure 3.6).

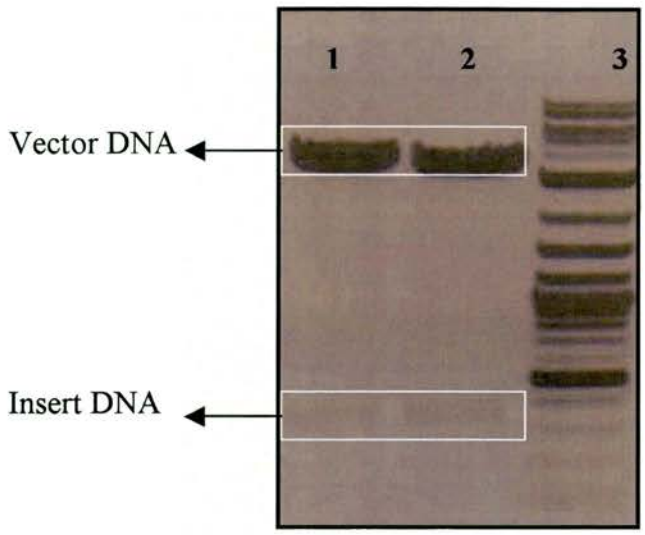

Figure 3.6: Bovine mutant was digested with NdeI-BamH1 restriction enzyme and run on the gel shows both the vector and insert DNA (faint band).

3.2 Optimisation of expression of COT

The gene encoding the COT was expressed in *E.coli, BL21(DE3) pLySs*. To achieve the highest expression of COT, the cells were treated in different conditions (Table 3.2). The cells were grown at 37°C for 4 hours until the optical density was OD_{600}=0.6-1.0. The expression was induced at the chosen temperature by IPTG with three different concentrations for either 3 hours or overnight. The harvested cell pellets were weighed, mixed with ice-cold buffer, and sonicated at 15amplitude for 3x30 second on the sonicator with 2 minutes intervals on the ice. The sample was centrifuged and the pellets re-suspended in 1ml buffer. The expression level was analysed by measuring the specific activity of COT and by SDS-PAGE gel (Table 3.2). There was only a minimal activity in the pellet and it was discarded. The level of expression of protein was checked by SDS-PAGE, stained with Coomassie blue stain. The gel in figure 3.7 shows a clear dominant band at the correct molecular weight (~70 kDa) in the sample induced by incubation with 0.5 mM IPTG at 18°C overnight. This

sample also gave the best specific activity, 10-fold better than the standard protocol of 1 mM IPTG at 30°C for 3 hours.

IPTG (mM)	**INDUCTION TEMPERATURE** 30°C		25°C		18°C	
	3hr	O//N	3hr	O/N	3hr	O/N
0.1mM Cell weight (g/10ml)	0.12	0.19	0.13	0.09	0.22	0.10
Specific Act ($\mu mol/min^{-1}/ml^{-1}$)	126.2	278.4	342.4	678.8	886.4	997.8
0.5mM Cell weight	0.11	0.15	0.08	0.13	0.09	0.05
Specific Act	776.0	1287.0	1675.7	2567.0	2768.0	7289.0
1.0mM Cell weight	0.22	0.30	0.16	0.13	0.12	0.24
Specific Act.	738.0	977.0	892.0	2803.0	988.0	3023.0

Table 3.2: Optimisation of over-expression of COT. The expression of COT at 3 different concentrations of IPTG (0.1, 0.5, 1.0mM), 3 different induction temperature (30, 25, and 18°C), and two different induction time (3hrs and overnight-O/N). The weight of cells obtained and the specific activity of COT in the supernatant of lysed cells is shown for b COT.

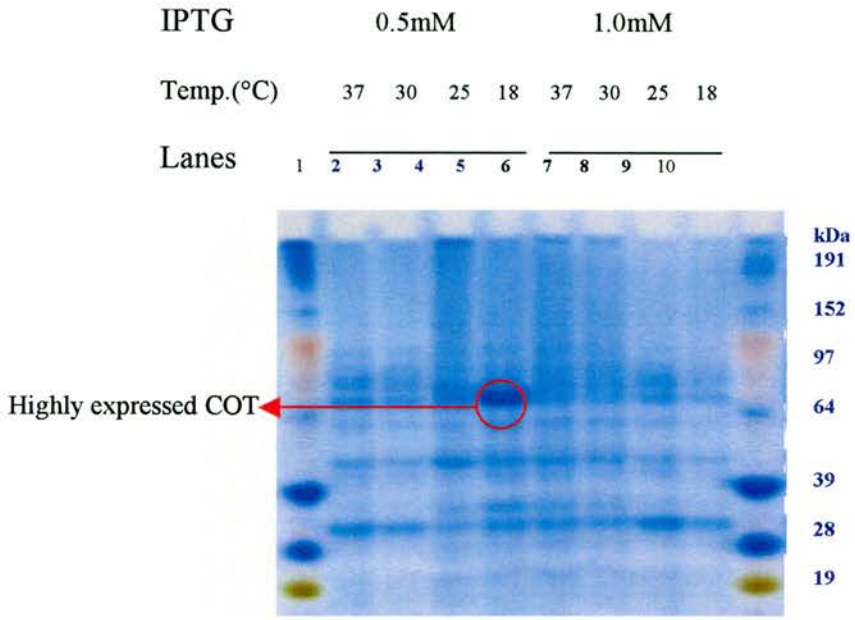

Figure 3.7: Protein expression pattern for optimisation of COT over-expression. 10μl of each sample was loaded into each well. The SDS-PAGE gel was stained with Coomassie blue. Lanes 1 & 10 are markers (250kDa), 2. 37°C, 3. 30°C, 4. 25°C, 5. 18°C (0.5mM IPTG) 6. 37°C, 7. 30°C, 8. 25°C, 9. 18°C (1.0mM IPTG).

3.3 Purification of COT

The purification of COT was optimised after many trials. Two purification strategies were used to obtain ultrapure COT for crystallisation. One is based on the original method used to purify COT from liver (Ramsay *et.al.*, 1987), the other on a standard protocol for the purification of histidine-tagged protein (Amersham Bioscience).

3.3.1 Purification of non-His tagged bovine COT

3.3.1.1 Initial extraction

The *E. coli* BL21 DE3 pLySs cells expressing COT were thawed and mixed with ice cold buffer and sonicated for 6x30 seconds with 2 minute intervals on ice to lyse the cells thoroughly. After the sonication, the sample was liquid in nature. The samples were then centrifuged at 22000xg for 20 minutes at 4°C to remove the cellular debris. There was no activity in the debris that was discarded. The supernatant was used for ammonium sulphate precipitation.

3.3.1.2 Native bovine COT from E.coli

The results of a typical purification are summarised in Table 3.2. After the cell disruption and centrifugation the supernatant containing soluble bovine COT activity had 15.6μmol.min^{-1}. ml^{-1}. The supernatant was subjected to 40-55% ammonium sulphate precipitation. The ammonium sulphate precipitation was performed carefully in the cold room with slow addition of the precipitant and foaming was avoided. At each step of the ammonium sulphate precipitation the COT activity was assayed and the total protein determined by the Biuret method using a standard curve based on known concentrations of BSA. The resuspended pellet from 40% ammonium sulphate precipitation and the supernatant from 55% ammonium sulphate cut had a minimal activity and so were discarded. The pellet from 55% ammonium sulphate precipitation was then homogenised with 5mL of ice-cold 50mM TRIS/HCl, pH 7.5 + 2mM EDTA and 1mM PMSF. The homogenized sample was viscous in nature and brown in colour and the activity was checked prior to desalting.

The sample was dialysed to remove the excess salt, first against cold water. After two hours the buffer was changed to 1L 20mM TRIS/HCl, pH 7.5. The total volume of the sample was increased from 25mL to 47mL after 3 changes of buffer and the sample was removed carefully and there was no precipitation. The sample was centrifuged at 22000xg for 10minutes at 4°C and concentrated to 25mL. The specific activity was 2.63units/mg protein.

3.3.1.3 Purification by column chromatography

3.3.1.3.1 Big Blue Sepharose CL-6B Fast Flow

The dialysed sample was filtered through 0.22μm filter and loaded into Big Blue Sepharose CL-6B fast flow column (3cmx15cm) and washed with 20mM KPi, pH 7.5. Fractions were collected and protein was measured at 280nm and COT activity with decanoyl-CoA at 324 nm. The flow through sample had some unbound active COT protein was eluted and the total activity was 150units. The second wash with 30mM KCl salt in 20mM KPi, pH 7.5 and the fractions from 12-37 that have high protein but low activity, meaning that some of the impurities were washing out of the sample. The enzyme was then eluted by a linear gradient of 30-300mM KCl in 20mM KPi, pH 7.5 (figure 3.8). The graph shows that the activity was high from fractions 45-68 with similar protein profile. The volume of the pooled fractions (45-68) volume was 115ml and the pooled sample was dialysed overnight. The dialysed sample was filtered through a 0.22μm filter and concentrated to 12.5mL. The specific activity had increased to 4.56units/mg.

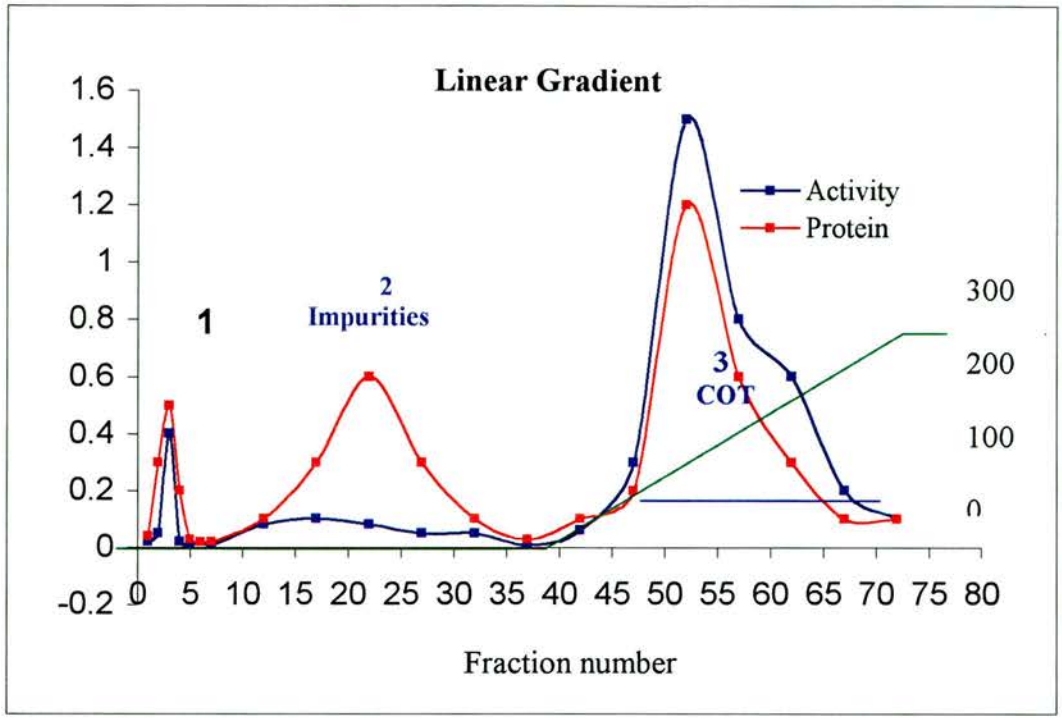

Figure 3.8: The COT elution from Blue Sepharose by linear gradient with high salt concentrations. Peak 1 is unbound COT with some impurities, peak 2 is impurities with high protein concentrations and peak 3 is active pure COT .

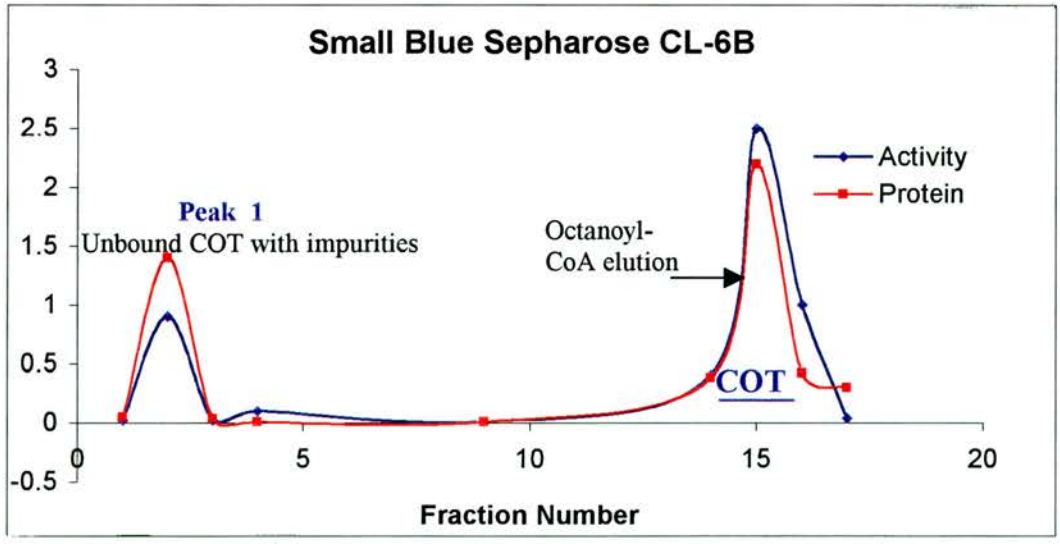

Figure 3.9: Purification by affinity elution from Blue Sepharose CL-6B. Peak 1 is unbound COT. The peak 2 is the bound COT that was eluted with octanoyl-CoA. Fractions were 5ml.

3.3.1.3.2 Small Blue Sepharose CL-6B column

After loading the dialysed sample, the column was washed with 2 column volumes of 20mM KPi and then with 3 column volumes of 30mM KCl in 20mM KPi, pH 7.5. The COT was eluted with 20mM KPi, 30mM KCl, 10mg of n-octanoyl-CoA in 100ml buffer as the final step of purification. The chromatogram of the affinity elution profile is shown in the figure 3.9. After loading, approximately 140 units a substantial amount of active protein was lost during the wash (about 140units total). Affinity eluted fractions were pooled and the volume of 15mL concentrated to 3mL. Purified COT was stored at -20°C with 20% glycerol and 0.5mM DTT. The recovery of the COT enzyme was 32.9% of the total sample with highest specific activity about 21units/mg protein. Table 3.3 shows that the greatest loss in the last column indicating that the affinity elution was not efficient even at high concentrations of octanoyl-CoA (15mg/10mL).

3.3.1.4 SDS-PAGE electrophoresis

The purity of the enzyme in selected samples during and after purification was assessed by SDS-PAGE electrophoresis and stained with Coomassie blue and silver stain to observe any minor impurities in the pure COT (Figure 3.10). The amount of protein loaded in each well was defined according to the protein concentration of each sample during the purification steps.

The SDS-PAGE gel stained with two different stains shows the improvement of the purification in stepwise. The protein band in lane 6 & 7 with 10 & 5 μg of protein loaded shows there were no impurities present. Another gel stained with silver stain confirms that no impurities could be detected in the purified COT. The purified

COT band molecular weight was calculated to be 70kDa and confirmed by mass spectrometry. Although purity was achieved, only 32.9% of the total COT activity was recovered.

Sample	**Vol. (ml)**	**Activity μmol/min^{-1}/ml^{-1}**	**Total Units**	**Protein mg/ml**	**Spec. Act. Units/mg**	**Yield (%)**
Sonicated	75	15.6	1170	22	0.709	100
Spn-40%	95	11.3	1073	18.8	1.66	91
Pellet	20	4.8	96			8.2
Spn-55%	108	2.375	263			22.4
Pellet	25	32.4	810	12	2.7	69.2
Dialysed +Concent.	25	30.6	765	11.5	2.63	65.3
Big Blue Sepharose	12.5	42	525	9.2	4.56	47.1
Small Sepharose	3	128.3	385	30.5	21	32.9

Table 3.3: The purification of bCOT. The table shows the protein and activity at different stages of purification.

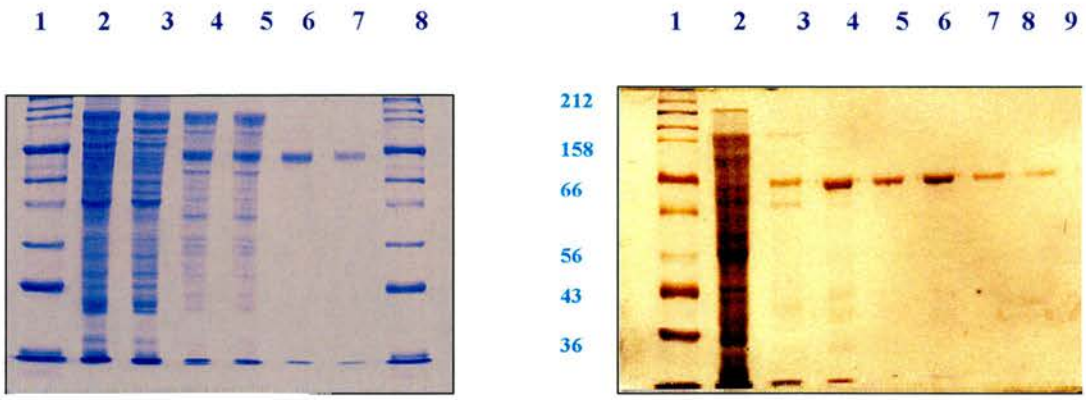

A. Coomassie Stain **B. Silver Stain**

Figure 3.10: SDS-PAGE analysis of samples of COT during and after purification. Two different gels are shown with different stains.

Gel A. Gel A shows the improvement of the purity at different stages. The lanes 1 and 8 are marker protein with 212kDa (BioLabs, UK, # P7702S), Lane 2 (10μg) and 3 (5μg) are dialysed of pellet 55% ammonium sulphate cut. Lane 4 (10μg) and 5 (5μg) are concentrated sample from big Blue Sepharose CL-6B. Lane 6(10μg) and 7(5μg) are concentrated sample after small Blue Sepharose.

Gel B. Lane 1 is marker; 2, crude homogenate; 3, big Blue Sepharose; 4, small Blue Sepharose; lanes 5-9, different concentrations of pure COT showing no other bands are visible.

3.3.2 His-tagged COT purification

3.3.2.1 Optimisation of over-expression of COT

The gene encoding the COT from different species was expressed in *E.Coli* (Rosetta (DE3) pLySs. To achieve the highest expression of COT, the cells were treated in different conditions (Table 3.4). The expression level was analysed by measuring the specific activity of COT and by SDS-PAGE gel.

IPTG (mM)	**INDUCTION TEMPERATURE** 37°C		30°C		25°C		18°C	
	3hr	O/N	3hr	O/N	3hr	O/N	3hr	O/N
0.1mM								
Cell weight (g/10ml)	0.11	0.10	0.09	0.12	0.16	0.19	0.22	0.09
Specific Act. ($\mu mol.min^{-1}.ml^{-1}$)	456.3	365	156.4	567.8	356.4	978.6	786.4	985
0.5mM								
Cell weight	0.14	0.22	0.04	0.15	0.25	0.17	0.13	0.09
Specific Act.	988.5	853.2	876.5	1287	1675.7	4567	645.9	6289
1.0								
Cell weight	0.23	0.17	0.13	0.35	0.16	0.11	0.14	0.24
Specific Act.	423	962	1738	677	1092	2803	978	1023

Table 3.4 : Optimisation of over expression of His-tagged COT. The expression of each species of COT at three different concentrations of IPTG (0.1, 0.5, 1.0mM), four different induction temperature (37, 30, 25, & 18°C) and two different induction time (3hrs and overnight-O/N). The weight of cells obtained and the specific activity of COT in the supernatant of lysed cells is shown for bovine COT.

The cells were grown at 37°C. After 4 hrs the optical density was OD_{600}=0.6-1.0. The expression was induced at the chosen temperature by IPTG with three different concentrations for either 3hours or overnight. The harvested cell pellets were weighed, mixed with ice-cold buffer, and sonicated at 15 amplitude for 3x30 seconds on the sonicator (Soniprep-150) at 2minute interval on ice. The sample was centrifuged, the pellets resuspended in 1mL buffer, and the activity measured in both the pellets and the supernatant. There was only a minimal activity in the pellet and it was discarded. The level of protein expression of protein was checked by activity (Table 3.4) and by SDS-PAGE electrophoresis, stained with coomassie blue (Fig 3.11).

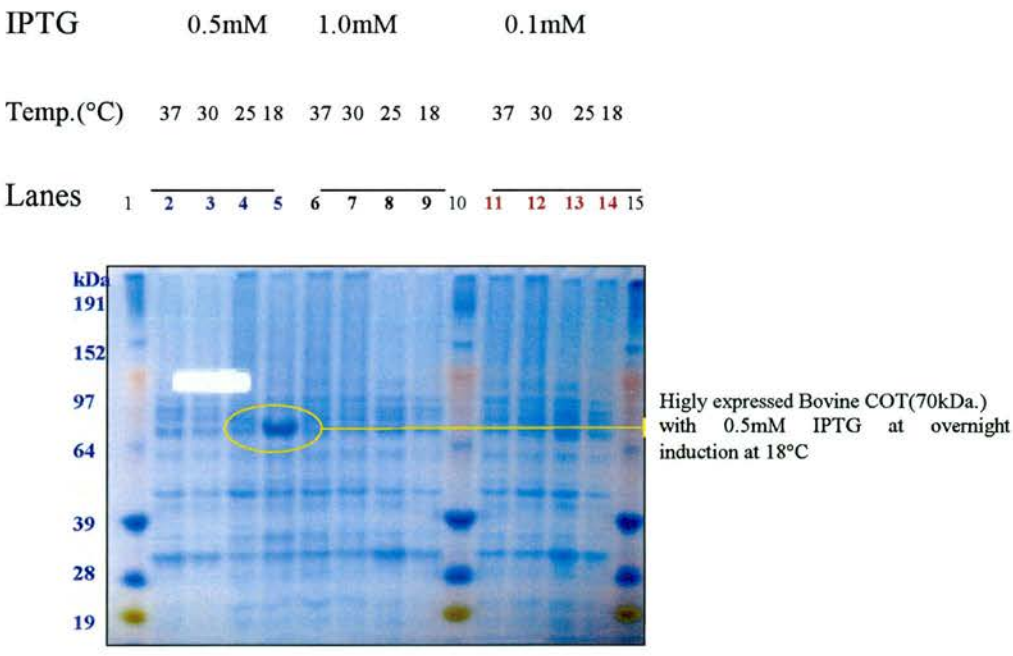

Figure 3.11: Optimisation of COT over-expression. 10µl of each sample was loaded into each well and the SDS-PAGE gel stained with coomassie blue. Lanes 1,10 &15 are Markers (250kDa), 2. 37°C, 3. 30°C, 4. 25°C, 5. 18°C (0.5mM IPTG) 6. 37°C, 7. 30°C, 8. 25°C, 9. 18°C (1.0mM IPTG) 11. 37°C, 12. 30°C, 13. 25°C, 14. 18°C (0.1mM IPTG)

The highest expression level was achieved with 0.5mM IPTG concentration after overnight induction. Compared to all other conditions, the amount of protein at 70kDa was also very high, seen as a very thick band in lane 5. None of the other conditions produced a band like lane 5, even at 0.1mM IPTG. The same optimum expression conditions (0.5mM IPTG with overnight incubation at 18°C) applied to all other species (data not shown).

3.3.2.2 Initial extraction

The cells from the freezer were resuspended in 50ml 1xPBS, 0.5M NaCl, 10mM imidazole, containing one tablet of EDTA-free protease inhibitor cocktail. The cell suspension was sonicated on ice using a large tip connected to Soniprep-150 at an amplitude of 10 microns for 3x30sec at 2minute intervals on ice. The suspension was centrifuged at 22000g for 20 min and the pellets were discarded. The supernatant was ultra centrifuged at 40000 rpm for 1 hour and the pellets were discarded.

3.3.2.3 His-tagged COT purification by Nickel column

The supernatant was filtered through 0.22μm filter and loaded into high performance Ni^{2+} Sepharose column (25mL) equilibrated with binding buffer (1xPBS, 0.5M NaCl, 10mM imidazole) at flow rate of 5mL/min. The column was washed with 5column volumes of washing buffer (1xPBS, 0.5M NaCl, 30mM imidazole). The flow-through and the washed sample activity were checked; this revealed minimal activity with substantial protein loss producing a brown colour. The His-tagged protein was eluted with 5 column volumes of elution buffer (1xPBS, 0.5M NaCl, 300mM imidazole) by linear gradient (figure 3.12) (AKTA-PRIME-FPLC-Amersham Biosciences). Some of the bound impurities were eluted during the void volume of the

column. The active fractions were pooled and dialysed extensively against 20mM Tris/HCl, pH 7.5 to remove imidazole. The protein purity was analysed by SDS-PAGE showing high and low molecular weight impurities were present in the sample (figure 3.12) although most impurities were washed through the Nickel column.

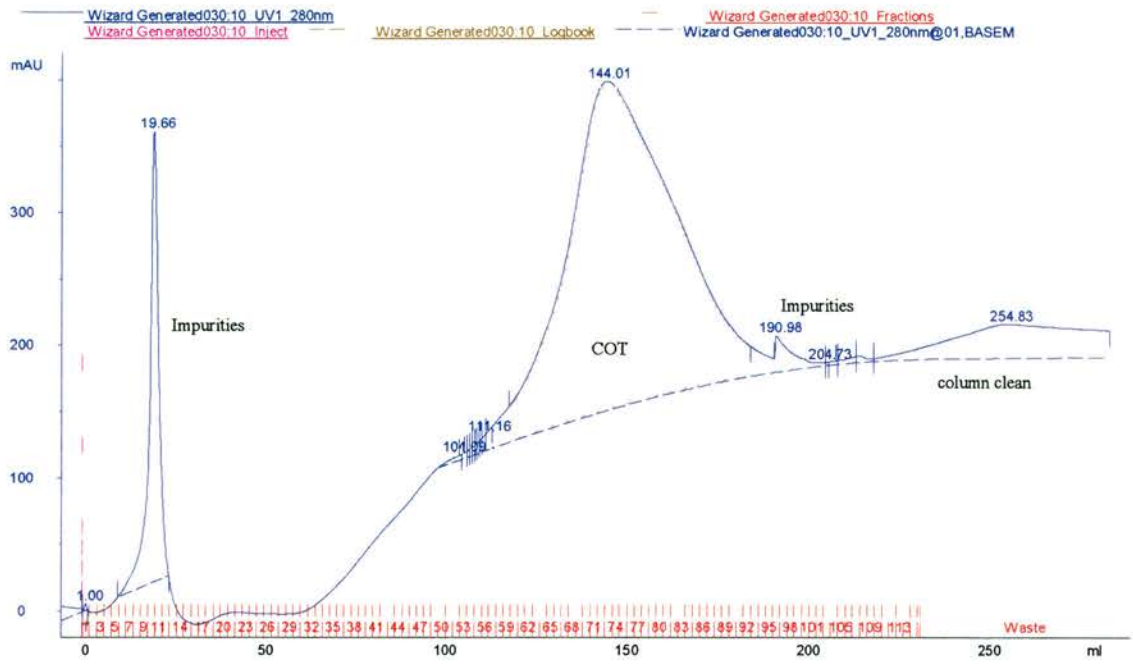

Figure 3.12: His-tagged protein from elution nickel-Sepharose by a linear imidazole gradient (50-300mM). Peak 1 is bound impurities and peak 2 is COT. Some other bound impurities were washed off during the column cleaning phase but those fractions possessed no activity.

3.3.2.4 Purification by Hi-TrapQ High Performance Sepharose

The dialysed protein sample was loaded into 5 ml HiTrap Q Sepharose column and washed with 5 column volume of 20mM Tris/HCl, pH 7.5 at flow rate 5mL/min. The protein was eluted with 5 column volumes of a high salt linear gradient (20mM Tris/HCl, 0-1M NaCl, pH 7.5). The active fractions were collected and the purity was checked by SDS-PAGE which shows only a few bands corresponding to 30kDa (Figure 3.13). All the active fractions were pooled together and dialysed against 1 L

20mM Tris/HCl 3 times, ready for removal of the his-tag from the N-terminus by thrombin digestion.

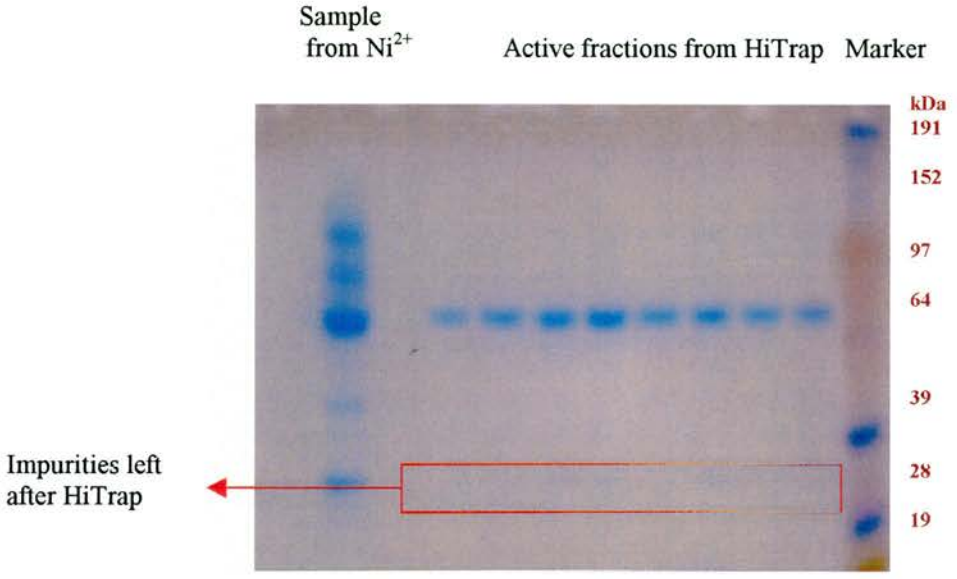

Figure 3.13: Purification of COT by HiTrap Q Sepharose column by FPLC. 10μl sample from the active fraction were loaded and stained with coomassie blue. The gel shows that most of the impurities were cleaned from the sample. Only few bands corresponding to 30kDa were clearly observed on the gel.

3.3.2.5 Optimisation of Thrombin Digestion

The removal of N-terminal His-tag was essential for the structural studies. The enzyme thrombin was purchased from Novagen, Merk-Biosciences and the concentration of the enzyme required to cleave 1mg protein was optimised. The conditions were given in Table 3.5. The procedure was as per the Novagen catalogue. The concentrated His-COT was diluted with thrombin digestion buffer to final concentration of COT was 1mg/mL. The different concentrations of thrombin were

Temperature	Thrombin Con. (dilution factor) (Units/mL)				
22°C	1:50	1:100	1:125	1:150	1:200
Result	+	+	-	-	-
4°C	1:50	1:100	1:125	1:150	1:200
Result	-	-	-	-	-

Table 3.5: Optimisation of thrombin digestion. Thrombin was diluted in the thrombin digestion buffer at different concentrations and incubated at two different temperatures. The results are indicated as positive (+) or negative (-). At 22°C the cleavage was successful with 1:50 and 1:100 but there was no cleavage at 4°C for any of the dilutions.

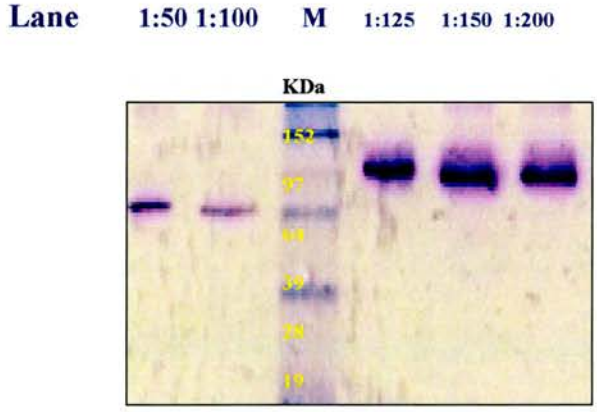

Figure 3.14: SDS-PAGE of thrombin digestion products. His-COT was digested with different concentrations of thrombin and efficient cleavage was found at room temperature. Pure non-tagged COT was loaded as reference (far left). The COT band at 1:100 dilution (far right) corresponds to the reference at molecular weight of 70kDa, the same as the non-tagged COT.

added and incubated at 2 different temperatures for 1 hour. The successful cleavage was analysed by 4-10% gradient gel (Figure 3:14) and by Mass Spectrometry.

All the samples with different concentrations of digestion were also sent for mass spectrometric analysis. The data showed that the 1:50 and 1:100 dilutions gave complete cleavage of the tag from the N-terminal of COT. Both of these dilutions gave the same result. Since thrombin is expensive, 1:100 dilution was chosen to cleave the tag. Figure 3.16 shows the mass spectrum of successful cleavage by indicating the peak with 70.580kDa after and 72.33kDa before thrombin digest.

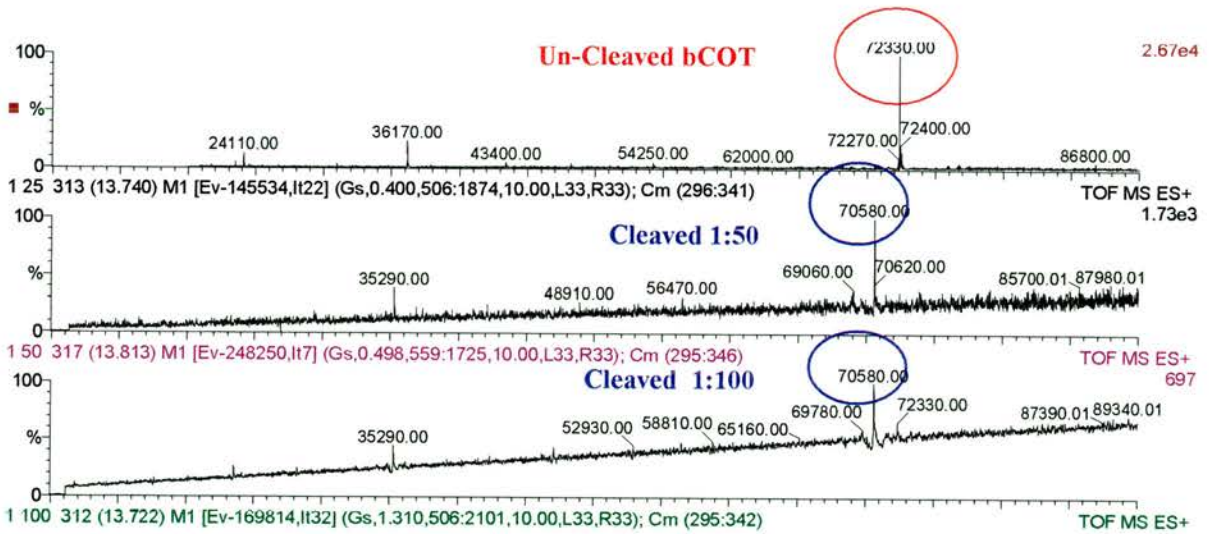

Figure 3.16. Mass spectrum after thrombin digestion of bovine COT. The cleaved COT peaks are circled in blue at 70.580kDa, the red circled is un-cleaved bovine COT at 72.330kDa.

The molecular masses found before and after cleavage of the His-tag from COT by thrombin correlated well with the expected masses from sequence analysis with Protparam, a bioinformatic tool used to analyse the sequence to get accurate molecular weight. The analysis was done for each of the COT species. Bovine, human

and rat COT were all very similar by this analysis, with human COT being marginally smaller (Table 3.6).

Species	No of AA	Molecular weight With (His)6-Tag(kDa)	Molecular weight without (His)6-Tag (kDa)	pI
Bovine	612	72.35	70.563	6.28
Human	612	72.27	70.484	6.63
Rat	612	72.33	70.580	6.26

Table 3.6 Sequence analysis of COT from different species. All the species had equal number of amino acids (AA) and the molecular weight varies with and without the 6-histidine tag. The isoelectric point (pI) values are also very similar between each species.

Once the his-tag was removed, the protein sample was loaded onto the 5ml Ni^{2+} column and washed by binding buffer (1xPBS, 0.5M NaCl, 10mM imidazole). Since the his-tag was removed, COT was washed through the column using the binding buffer. All the active fractions are pooled together and concentrated to 10ml. Activity and protein were measured. The sample was filtered through 0.22μm filter and ready for a final polishing step using gel filtration.

The amino acid analysis of the preparation was checked also (Table 3.7). This differs slightly from that found for the COT isolated from bovine liver (Ramsay *et al.*, 1987) but is in agreement with the deduced sequence based on cDNA.

Amino acid		Total number	Percentage
Ala	(A)	30	4.9%
Arg	(R)	30	4.9%
Asn	(N)	28	4.6%
Asp	(D)	27	4.4%
Cys	(C)	14	2.3%
Gln	(Q)	29	4.7%
Glu	(E)	48	7.8%
Gly	(G)	36	5.9%
His	(H)	19	3.1%
Ile	(I)	22	3.6%
Leu	(L)	64	10.5%
Lys	(K)	38	6.2%
Met	(M)	18	2.9%
Phe	(F)	29	4.7%
Pro	(P)	31	5.1%
Ser	(S)	40	6.5%
Thr	(T)	30	4.9%
Trp	(W)	12	2.0%
Tyr	(Y)	23	3.8%
Val	(V)	44	7.2%
Asx	(B)	0	0.0%
Glx	(Z)	0	0.0%
Xaa	(X)	0	0.0%

Table 3.7: The amino acid composition of the bovine COT. The total number of amino acid and its amount are expressed in percentage.

3.3.2.6 Gel Filtration

The cleaved COT was polished through a gel filtration column (Sephacryl S-100). COT was eluted with 2 column volumes of 20mM Tris/HCl, 20mM NaCl, pH 7.5. The chromatogram (figure 3.17) shows that a single pure COT peak eluted out after the void volume and few lower molecular weight impurities were eluted during the cleaning of the column. The purity of the protein was checked by SDS-PAGE. The protein was concentrated to 20mg/ml and stored in 20mM Tris/20mM NaCl, pH 7.5, 0.5mM DTT and 20% glycerol.

The SDS-PAGE stained with Coomassie blue showed a single band (figure. 3.19). The COT purified by this his-tag protocol had excellent specific activity of 54.2 units/mg with 50% recovery (Table 3.8). This proved more successful than the traditional method and similar to that from bovine liver (Ramsay *et al.*, 1987).

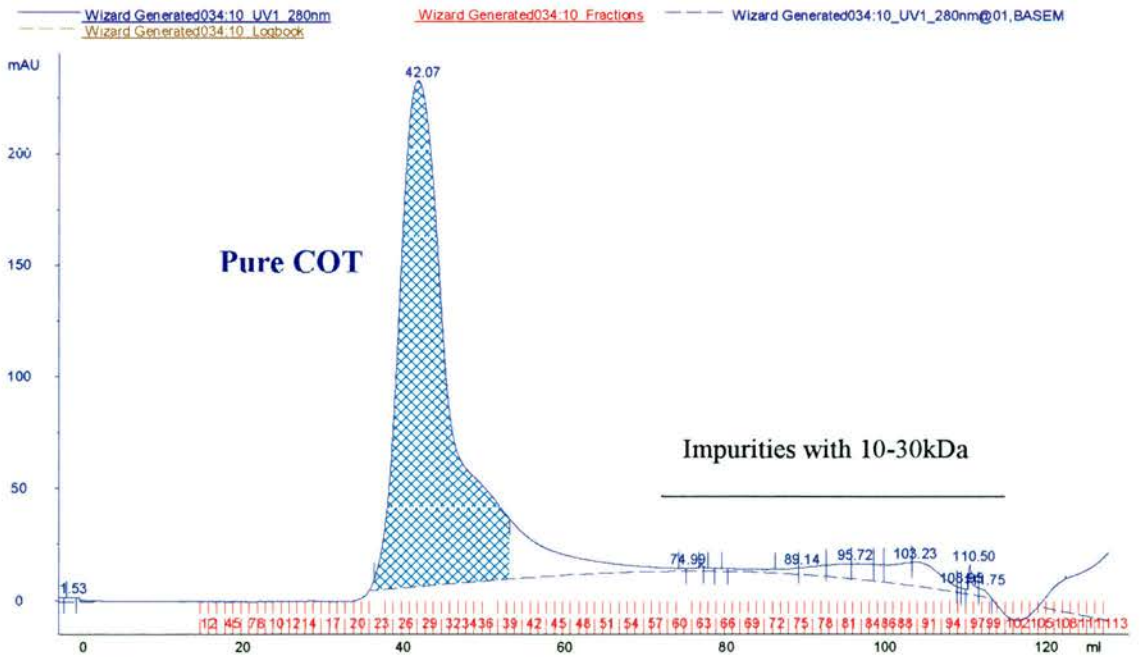

Figure 3.17: Size exclusion of COT by gel filtration (Sephacryl S-200). Peak 1 is pure COT and the small peaks are the impurities with low molecular weight. The Y-axis is the absorbance at 280 nm.

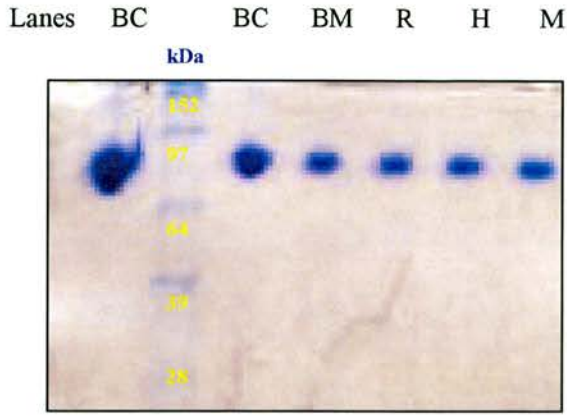

Figure 3.19: SDS-PAGE of purified COT from his-tag expression system with Coomassie stain. Purified protein from bovine (BC), rat(R), human (H), mouse(M) and bovine mutant G553M (BM) all show a single pure COT band at 70 kDa.

STEP	Vol. (ml)	ACTIVITY $\mu mol/min^{-1}/ml^{-1}$	Total Units	Protein mg/ml	Units/mg protein	Yield (%)
Sonicated	50	40	2000	19	2.105	100
Ni2+	45	38.5	1737	12.5	3.08	86.75
HiTrapQ	10	116	1116	9.6	12.08	55.8
GF	5	206	1030	3.8	54.2	51.5

Table 3.8: Purification of His-tagged COT. The table shows the purification at each stage. Ni2+ is high performance nickel Sepharose, used to elute only his-tagged COT from the crude sample. HiTrapQ is high performance Q Sepharose, an ion exchange column used to remove other impurities. Finally, GF is gel filtration used to polish the protein. The purity was achieved with 51.5% recovery and a specific activity 54.2 units/mg.

3.3.3 Discussion of purification

The expression of COT was optimised and the highest expression was shown at 18°C with 0.5mM IPTG induction overnight. This condition is applicable for all the *E. coli* based COT expression systems in our lab. The purification of COT was successful and reproducible in both his-tagged and non-his tagged COT. Recovery of the protein from his-tagged expression systems was about 50% with good specific activity, so this is the method of choice for preparation of samples for crystallography. The purity of COT was very high in terms of percentage protein present. The gel picture shows that only a single COT band was observed even at 50μg loading and the silver stain confirmed that there were no impurities present. The protein was used for the crystal trials at 10mg/mL and also used for functional studies.

3.4 CRYSTALLISATION OF COT

The aim of this experiment is to reveal the structure of COT. Purified COT from different species was characterised and analysed for its ability to crystallise. The purity of the enzyme was successful and reproducible. The protein sequence was analysed by Glob Plot to determine any potential disorientation within the sequence

3.4.1 Globplot analysis

To analyse the location of any disordered region within the bovine COT protein sequence, it was submitted to the GlobPlot server (http://globplot.embl.de) for analysis. Globplot is a bioinformatic tool that was designed to facilitate structural biology in the post genomic era. By rapid definition of the boundaries of intrinsically unstructured regions within the polypeptide chain, it is possible for crystallographers

to determine the suitability of a target for structural studies (Linding 2003). GlobPlot uses an algorithm that predicts the propensity for each amino acid within a protein sequence to be in an ordered or disordered state. The computer output is a graphical representation of disorder propensity versus residue number. The results for the bovine COT sequence (figure 3.20) indicate no areas of disorder, a favourable result for the potential to crystallise.

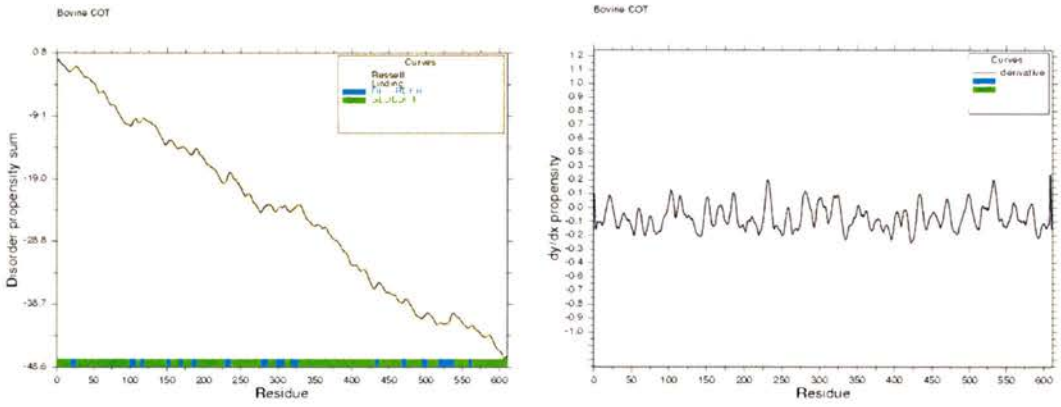

Figure 3.20: GlobPlot result for the bovine COT sequence . The protein sequence has no large disordered regions thus favouring crystallisation, so its crystallisation is not hindered.

3.4.2 Crystals from the sitting drop method

Purified protein was ultracentrifuged at 40000g for 1 hour and concentrated to 15mg/mL in 20mM Tris/HCl, 10mM NaCl, pH 7.5 using Amicon concentrator. Protein was diluted to 5, 10 &15mg/ml for crystal trials. In a 96 well plate, 2µl of each protein solution and 2µl of screen buffer were mixed well. The plates were stored at two different temperatures (20°C and 4°C). Plates were examined every 3 days under the microscope. It was observed that about 30% of the wells in a plate had precipitation. Most of the wells with salt crystals and protein crystal were found in PEG-3350 screens (Figure 3.21). Protein crystals were confirmed by izit dye staining (Figure 3.21B). The protein crystal size was 20µm, not big enough for diffraction. All

the conditions were optimised with different concentrations of buffer and pH to achieve bigger crystals.

Ligands can sometimes help crystallisation. The substrate L-carnitine at 10mM concentration was used in some crystal trials. The substrate analog, 2-bromoacetyl L-carnitine, which, in the presence of CoA, forms a bridge compound in the active site was obtained from Sigma Tau and used to inactivate the enzyme. Excess reactants were removed and the enzyme-bridge complex used for crystallisation trials. No crystals were obtained with either liganded form of COT.

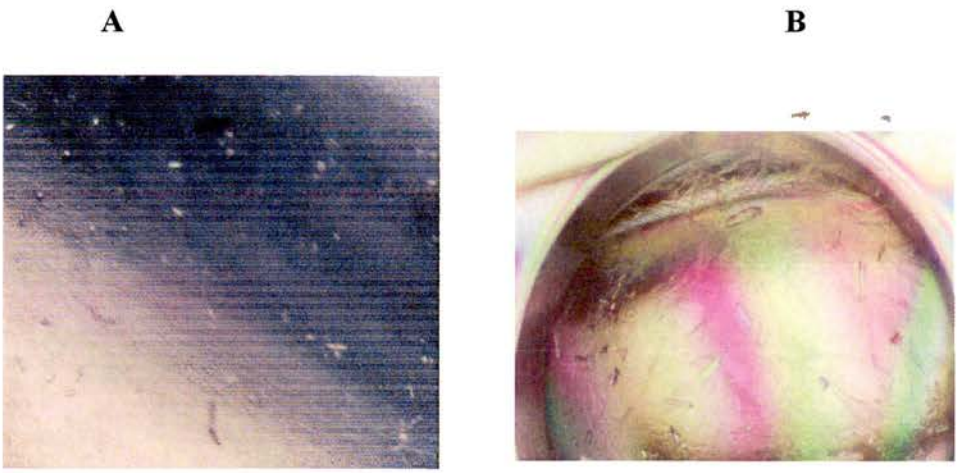

Figure 3.21: Crystals of bovine COT. A. His-tagged bovine COT with 3 dimensional square crystals that are not very clear in this picture.B. Non-his-tagged bovine COT formed small needle-like protein crystals under Wizard 1(10% ammonium acetate, 0.1M sodium chloride, pH 7.5) conditions with 15 mg/mL.

A **50μM** **B** **15μM**

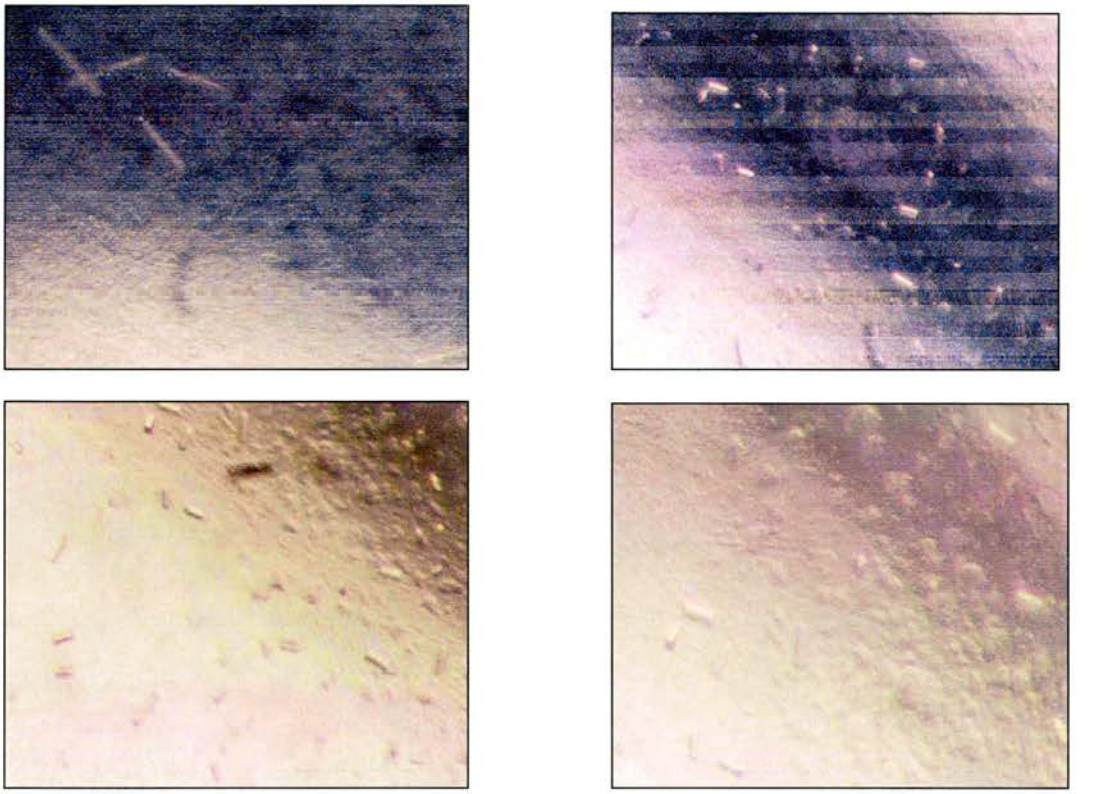

Figure 3.22: Crystals of CPT2. Purified protein crystals found in Index screen 2 with 10% ammonium acetate and PEG3350 show two different morphologies a needle form and square crystals.

Mitochondrial CPT 2 was also expressed in E. coli and purified for crystal trials. The protein crystals grew in 3 days, especially in the PEG screen with no salt at a low pH, which confirms that the protein grows well under acidic conditions. The morphology of the crystals varied in different conditions. A needle form, square and spherical crystals were seen (Fig. 3.22). All these crystals are confirmed by izit stain and will be diffracted very soon.

4 KINETIC PARAMETERS OF COT

Carnitine acyltransferases represent a group of enzymes that are important in the regulation of fatty acid oxidation and of fatty acyl-CoA pools throughout the cell. The role of COT is to transfer the chain shortened acyl-CoA product of peroxisomal fatty acid oxidation to carnitine for export to mitochondria. The aim of this chapter is to characterise the purified COT cloned from several species, including human COT, to understand the kinetic properties that dictate what leaves the peroxisomes.

4.1 Variation of COT kinetic properties in various species.

4.1.1 The cloned bCOT is identical to that purified from bovine liver

Since the heterologous expression of COT was intended to facilitate the crystallographic and kinetic study of inhibitors for future drug development, it was important to establish that the COT expressed in *E. coli* retained the same kinetic properties as that isolated from mammalian tissue. The properties of purified bCOT (Ramsay et al., 1987) were compared with those of bCOT from *E. coli* and bCOT expressed with a His-tag that was removed after purification.

Table 4.1 lists the kinetic properties of the various bCOT preparations. The Vmax values are of the same order, with differences perhaps being due to the relative purities of the preparations. The Km values for palmitoyl-CoA or decanoyl-CoA and L-carnitine are as close to the values obtained in preparations purified from liver as these are to each other. It is concluded therefore that the expression of COT in *E. coli* does not change its catalytic properties.

Source of COT	K_M (μM)		V_{max}
	L-Carnitine	Acyl-CoA	mmol.min^{-1}-mg^{-1}
Bovine liver Nic a'Bhaird (1993) Ramsay (1987)	 108 182	 *C16* 0.6 *C16* 0.8	 36 58
E.coli BL21(DE3)pLysS COT	94 168	*C10* 0.34 *C16* 0.50	15.8 10.0
E. coli Rosetta(DE3) 6HIS-COT	99	C10 0.39	13.6

Table 4.1 Kinetic parameters for COT from bovine liver or cloned sources.

4.1.2 Rat COT

Rat COT was expressed and purified for comparative studies on malonyl-CoA sensitivity. Only partial data for other kinetic parameters were obtained from one experiment each. The apparent Km values for butyryl-CoA (3.2 mM) and palmitoyl-CoA (0.5 μM), both obtained at 1 mM L-carnitine, and for l-carnitine (80 μM) obtained at 50 μM butyryl-CoA, are all similar to those for the bovine enzyme. The apparent Vmax values do differ, at 28 μmol.min^{-1}mg^{-1} when butyryl-CoA is varied but only 6.7 μmol.min^{-1}mg^{-1} when palmitoyl-CoA is varied. This was expected from previous studies: both mouse and rat have specificity for shorter chain length substrates (Farrell et al., 1984; Miyazawa et al., 1983).

	Forward (C10)		Reverse
HUMAN			
C10-CoA Km (uM)	1.5	CoA Km (uM)	28.0
L-Carnitine Km (uM)	58.0	C10-L-carnitine	22.0
Vmax (umol.min-1.mg-1)	7.0	Vmax (umol.min-1.mg-1	19.0
BOVINE			
C10-CoA Km (uM)	0.30		
C16-CoA	0.50	CoA Km (uM)	16.0
L-Carnitine Km (uM)	108.0	C16-L-carnitine Km (uM)	7.4
Vmax (umol.min-1.mg-1)	36.0	Vmax (umol.min-1.mg-1)	37.0
RAT			
C10-CoA Km (uM)	0.46		
L-Carnitine Km (uM)	80 with C4		
AppVmax (umol.min-1.mg-1)	C4-CoA		
	28.0		
Vary acyl-CoA at 1mM Cn	C16-CoA		
	7.0		
Vary Cn at 50uM acyl-CoA	L-Cn, 9.0		
TROUT			
C10-CoA Km (uM)	1.1	CoA Km (uM)	20.0
C16-CoA Km (uM)	0.6		
L-Carnitine Km (uM)	50.0	C10-L-carnitine	14.0
Vmax (umol.min-1.mg-1)	8.5	Vmax (umol.min-1.mg-1	3.2

Table 4.2: Kinetic parameters of COT in forward and reverse reactions

		Acyl-CoA varied	L-Carnitine varied	
Acyl-CoA Chain length	**Acyl-CoA** Km (uM)	**Vmax** (umol.min-1.mg-1)	**L-Carnitine** Km(uM)	**Vmax** (umol.min-1.mg-1)
C4	3.0	19.0	128.0	12.0
C6	3.8	26.0	133.0	17.0
C8	4.1	32.0	115.0	10.0
C10	1.5	26.5	71.0	9.5
C12	1.0	11.5	nd	nd
C14	0.68	8.2	nd	nd
C16	0.85	12.9	nd	nd
C18	0.5	7.3	nd	nd

Table 4.3 : Kinetic Parameters for hCOT. The experiments were conducted in duplicate at 30°C for 200 seconds using 20mM KPi buffer (pH 7.5), 125□M PDS and 0.05% BRIJ detergent to give a final assay volume of 1ml. In the assessment of kinetic parameters for acyl-CoAs, the concentration of L-carnitine was saturating at 1mM, while varying concentrations of acyl-CoA were used. For determination of kinetic parameters for L-carnitine, an acyl-CoA concentration of the Km value was used with varying concentrations of L-carnitine

4.1.3 Human COT

(in collaboration with A.-M.M. Morrill, Nuffield Foundation Summer Student)

Human COT was first cloned and studied as part of the peroxisomal pristanoyl-CoA oxidation (Ferdinandusse et al., 1999). It had good activity with the branched chain product, 4,8-dimethylnonanoyl-CoA, with a Vmax close to that for octanoyl-CoA (Ferdinandusse et al., 1999), but data for the aliphatic acyl-CoA derivatives was not published. Human COT (hCOT) was expressed in *E.coli*, purified as described in Chapter 3, and its acyl-CoA specificity and kinetic parameters investigated.

The kinetic constants for the transfer of a C10 acyl group from CoA to carnitine (the 'forward reaction") are compared with those for COT from other species in Table 4.2. The values for the kinetic constants are of the same magnitude as for COT from other species in both the forward and reverse reactions. The Vmax values in the forward and reverse direction for hCOT are more disparate than for the bCOT but still indicate a freely reversible reaction.

The acyl chain length specificity for human COT was studied because it is this that determines what chain lengths will be transferred to carnitine. Table 4.3 gives the Km and Vmax values for the acyl transfer to carnitine. The optimum substrate for hCOT in terms of the specificity constant ($Vmax/K_M$) is C10 but there is good activity with C16 and C18 also. However, the rate of catalysis is greatest with C8 for which the Vmax is 2.5 times that with C16. The K_M values are several □M for C8 and below, but drop to 0.5 □M for C10 and above. This pattern of increased affinity above C10 is the same as for other species (see below) and is consistent with removal of acyl groups longer than C10 from the peroxisome.

The K_M for L-carnitine varies with the chain length of the acyl-CoA used as the other substrate. This has previously been observed with rat COT from rat liver (Miyazawa et al., 1983) although no obvious trend was seen for COT from mouse liver (Farrell et al., 1984) or bovine liver (Ramsay et al., 1987). COT from bovine liver gave and an interaction factor (α) close to 1, meaning that each substrate bound equally well to either free enzyme or the complex of enzyme with the other substrate. The variation with acyl-CoA substrate suggests that L-carnitine bind better to the COT-acyl-CoA substrate, especially with longer chain substrates. The extreme example of this effect is the ordered reaction of CPT2 where L-carnitine binds only to the acyl-CoA-CPT2 complex ((Nic a'Bhaird, N et al., 1993).

4.1.4 Bovine COT

The parameters for bCOT are given in Table 4.2 and the specificity constants for the different acyl-CoA are shown in Fig. 4.1. The bCOT purified after expression in *E. coli BL21(DE3)pLysS* is the form of the enzyme most used for the work in this thesis and forms the reference for comparison.

4.1.5 Trout COT

COT was prepared from trout liver provided by N. Fawcett and Dr V.J. Smith. The kinetic parameters are shown in Table 4.2. The specific activity is lower than for the other species in the table but this preparation was less pure, giving several bands on SDS-PAGE. The K_M for L-carnitine is lower than for bCOT but similar to hCOT. For the acyl chain length specificity, the data was combined with that from N.Fawcett (Ph.D. Thesis, University of St Andrews) to give the complete picture in Fig. 4.1.

4.1.6 Comparison of cloned human, rat, beef , and trout COT

Table 4.2 compares the kinetic parameters for all the species of COT studied after cloning into *E.coli*. The Km values for acyl-CoA and L-carnitine are of the same order in all species. However, there are small differences, so the chain length specificity was examined as the specificity constant (V/K_M) expressed as a percentage of the highest value for ease of comparison. Fig. 4.1 compares the relative specificity constants ($Vmax/K_M$) for rat, human, cow, and trout. The low chain length specificity of rCOT with its maximum at C8 is clearly similar to the mouse COT that gave the enzyme its name (Clarke and Bieber, 1981). However, the optimum substrate for hCOT is C10 and there is good activity with C16 and C18 also. The bCOT has an optimum at C16 (as previously reported, Ramsay, 1988), as has tCOT. The tCOT has good activity with C18 too, perhaps reflecting adaptation to the higher content of very long chain fatty acids in the marine diet.

Better activity of peroxisomal COT on longer acyl chain CoA derivatives will favour transfer to the mitochondria at an earlier stage of degradation, so longer chain specificity favours more energy efficient oxidation of the fats, since the mitochondrial oxidation pathway conserves energy at the first step, acyl-CoA dehydrogenase. Taking the ratio of the specificity constants for C16/C10 as the indicator, that species can be ranked in order: rat (0.5), human (0.85), trout (1.5), cow (1.6). However, the trout has a broader specificity for long chains and seen its high C18 activity compared to that for cow.

The kinetic parameters also reveal that the specificity comes from the catalytic process rather than from binding. Although Km is a kinetic parameter rather that a binding constant (see equations below), it is equal to Ks in rapid equilibrium enzymes such as COT where k_3 is small compared to k_1 and k_2.

$$E + S \underset{k_2}{\overset{k_1}{\div}} ES \overset{k_3}{'} E + P$$

$$K_M = (k_2 + k_3)/k_1$$

$$K_s = k_2 / k_1$$

Fig. 4.2 compares the K_M and V values for hCOT and tCOT. For both species the K_M is several □M until C10 when it drops to about 0.5 □M. The V values are much more variable, with the human enzyme showing highest V at C8 and very much lower rates from C12 – C18. In contrast, the tCOT V is relatively constant across the whole acyl chain range. These differences must arise from placement of the groups being acted upon relative to the catalytic histidine in the active site.

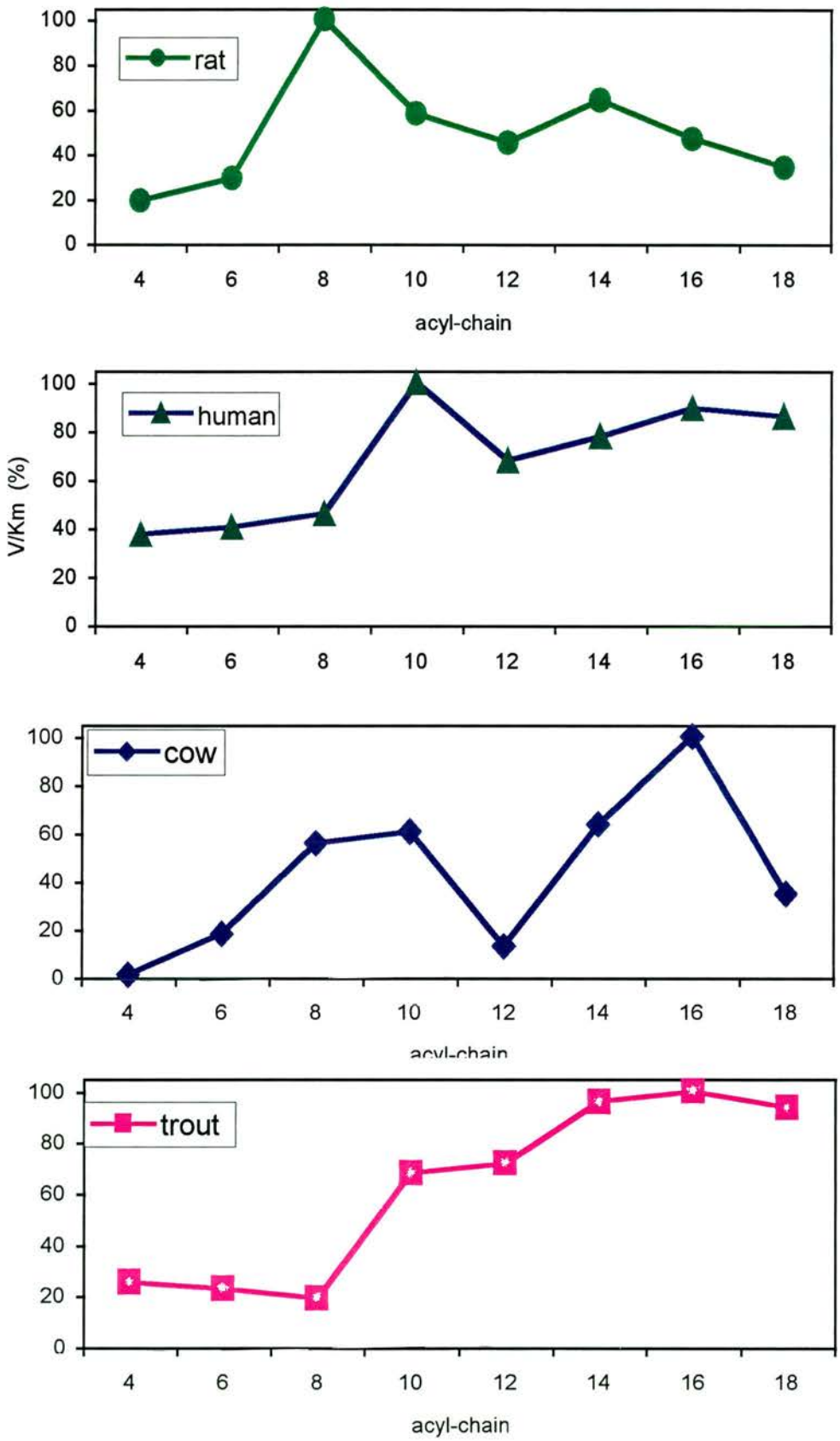

Fig. 4.1 Specificity constants for COT alter with the species

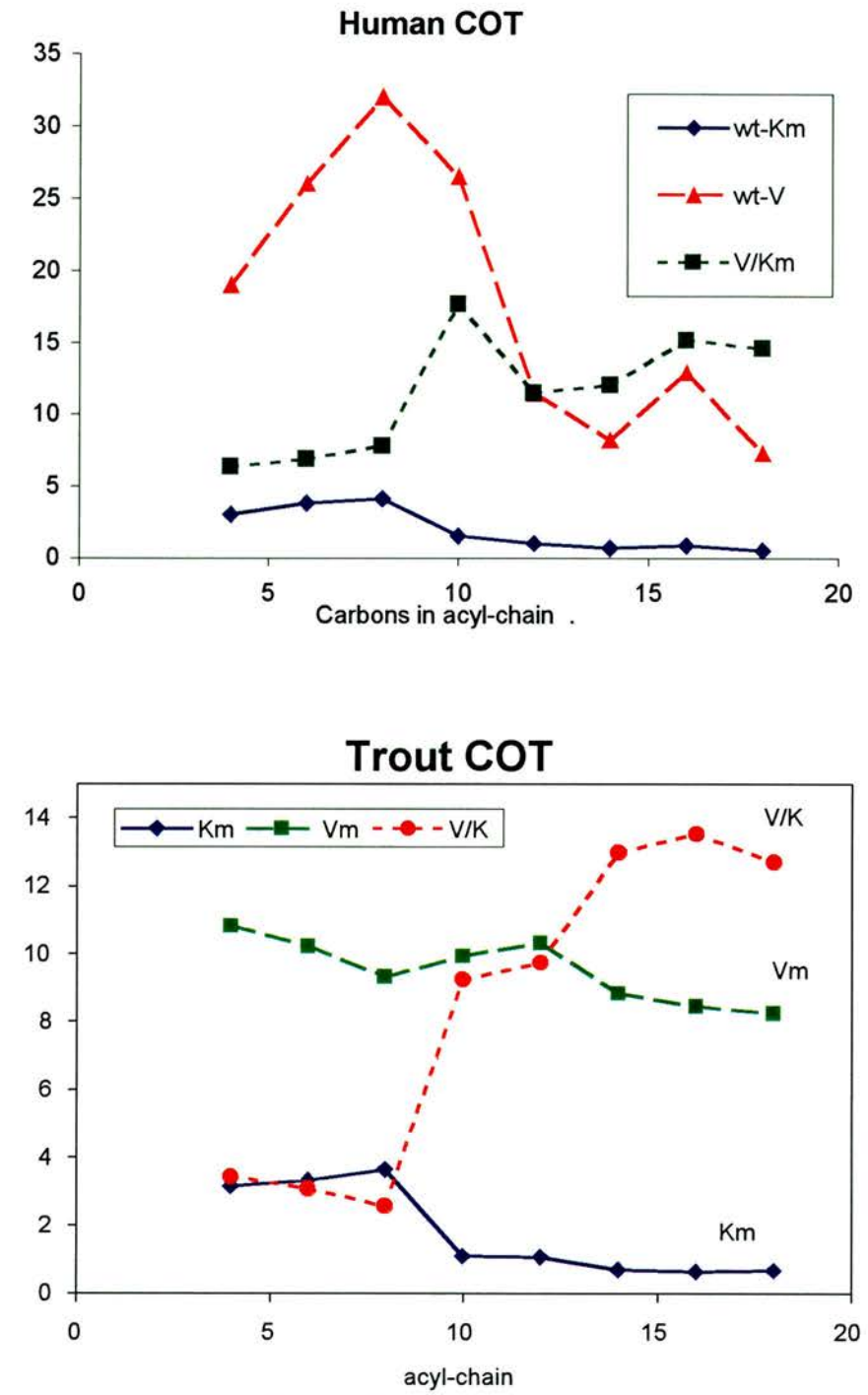

Fig. 4.2. Compaison of acyl-chain specificity in hCOT and tCOT: Specificity comes from catalysis, not binding.

4.2 Is COT malonyl-CoA sensitive?

COT is localised in the peroxisomes where presumably malonyl-CoA changes in the cytosol do not influence its activity because the peroxisomal membrane is impermeable to CoA derviatives (Van Roermund et al., 1995; van Roermund et al., 1999). As expected, COT purified from beef liver was inhibited only competitively by malonyl-CoA with a K_i of 106 μM (Nic a'Bhaird, N. and Ramsay, 1992). It was surprising, therefore, that rCOT, when heterologously expressed in the membrane fraction of yeast, was reported to be malonyl-CoA sensitive with up to 50% inhibition detected below 20 μM (Morillas et al., 2000). The H131/H340 double mutant to alanine was not inhibited, so these residues were implicated in the binding of malonyl-CoA (Morillas et al., 2000). H131 is common to all species of COT but in bCOT, the amino acid at position 340 is Y rather than H (Fig. 4.2.1). This led to the hypothesis that H340 could be responsible for the difference in sensitivity to malonyl-CoA inhibition between rat and cow. Since hCOT also has Y at the equivalent position (Fig. 4.2.1), it would be predicted that hCOT should be sensitve to malonyl-CoA. To test the hypothesis, hCOT and its Y340H mutant were expressed in *E.coli* with the help of Dr Nigel T. Price, Hannah Research Institute, and the inhibition by malonyl-CoA examined in comparison to rCOT.

```
Rat-COT. . . 320 IFGCSCDHAPYDAMLMVNIAHYVDEKLLETEG 351
Mouse-COT. . 320 IFGCCCDHAPYDAMVMVNIAHYVDERVLETEG 351
Human-COT. . 320 VFGCNCDHAPFDAMIMVNISYYVDEKIFQNEG 351
Bovine-COT.. 320 VFGSNCDHAPFDAMVLVKVCYYVDENILENEG 351
Fugu-COT. .. 285 TFGSNCDHAPYDAMVLVTMCWYVDQRIQSTGG 326
```

Fig. 4.3 Sequence alignment for COT

The alignment of database sequences for COT from rat (P11466), mouse(Q96C50), human (O9UK019), cow (O19094) and fugu (AA020903) shows the catalytic histidine at 327 and the histidine 340 proposed to influence malonyl-CoA inhibition.

	Acyl-CoA varied		L-Carnitine varied	
Acyl-CoA Chain length	**Acyl-CoA** Km (uM)	**Vmax** (umol.min-1.mg-1)	**L-Carnitine** Km(uM)	**Vmax** (umol.min-1.mg-1)
C2	26.55	12.12	nd	nd
C4	3.62	9.13	138.0	11.97
C6	1.21	13.78	133.2	17.11
C8	1.36	10.83	114.9	10.11
C10	0.73	9.45	58.0	8.44
C12	0.84	7.75	nd	nd
C14	nd	nd	nd	nd
C16	4.82	12.9	nd	nd
C18	1.19	7.3	nd	nd

Table 4.4 Kinetic Parameters of Y340H Human COT for L-Carnitine and Acyl-CoA.

The experiments were conducted in duplicate at 30°C for 200 seconds using 20mM KPi buffer (pH 7.5), 125μM PDS and 0.05% BRIJ detergent to give a final assay volume of 1ml. In the assessment of kinetic parameters for acyl-CoAs, the concentration of L-carnitine was saturating at 1mM, while varying concentrations of acyl-CoA were used. For determination of kinetic

parameters for L-carnitine, an acyl-CoA concentration of the Km value was used with varying concentrations of L-carnitine.

4.2.1 Kinetic parameters for the Y340H mutant of hCOT

The Y340H mutant was characterised to ensure that its catalytic properties remained the same as the wild-type. The Km values in Table 4.2.1 are not very different from the equivalent values for wt-hCOT in Table 4.2. The maximum velocities were slightly lower (approximately half those for the wild-type) but the preparation was less pure. The variations in Vmax with acyl chain length followed the same trend as the wild-type. Thus, the mutation of Y340H does not perturb the kinetic properties of the enzyme.

4.2.2 Inhibition of wt-hCOT and itsY340H by malonyl-CoA

The purified wild-type (wt) hCOT and the Y340H mutant were assayed with saturating decanoyl-CoA and L-carnitine to see if they showed malonyl-CoA sensitivity. Fig 4.4 shows that netither wt-hCOT nor its Y340H mutant are sensitive to malonyl-CoA. Even at 200 uM malonyl-CoA, no decrease in rate was seen. When the L-carnitine was made sub-saturating, still no inhibition was seen (Fig 4.2). Only when the acyl-CoA substrate was made subsaturating could any inhibiton by malonyl-CoA be detected. The Fig. 4.5 shows that with 6uM butyryl-CoA (2 x K_M) both the wt and the mutant were inhibited to the same extent.

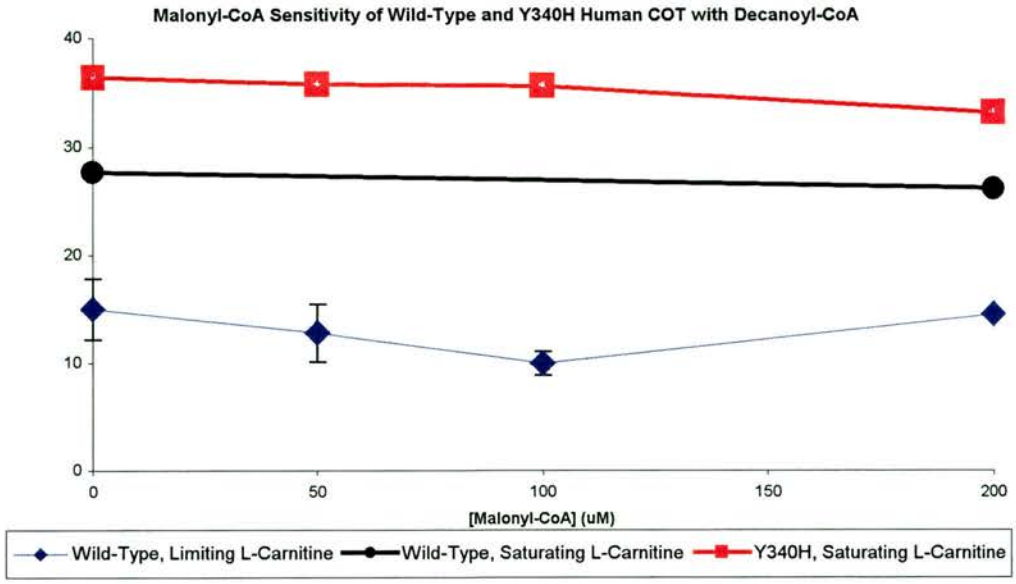

Fig. 4.4 Neither wt-hCOT not its Y340H mutant shows sensitivity to malonyl-CoA at saturating substrate concentrations. Assays contained the appropriate limiting (0.1mM) or saturating (1mM) concentration of L-carnitine. The concentration of decanoyl-CoA was 20uM.

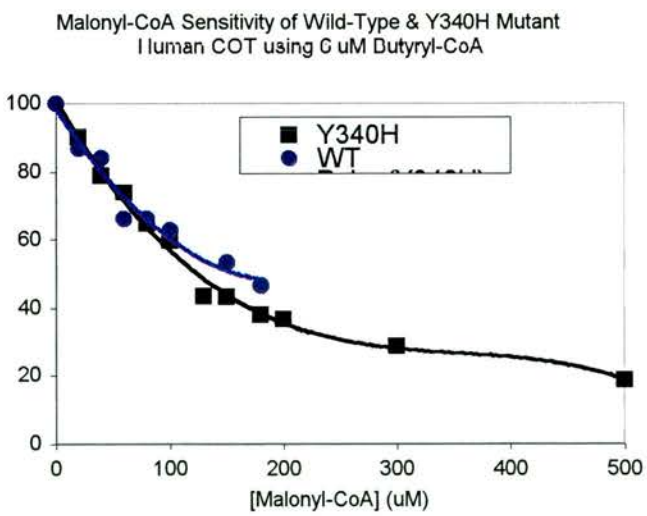

Fig. 4.5 Malonyl-CoA inhibition of hCOT and Y340H mutant at subsaturating acyl-CoA. The assays contained 6 uM butyryl-CoA and 1 mM L-carnitine.

The inhibition at subsaturating acyl-CoA substrate suggested that the malonyl-CoA might compete at the active site, so full kinetics were done to determine the type of inhibition. Butyryl-CoA was used as the substrate to avoid the problems of the very low K_M for decanoyl-CoA which limits the maximum possible absorbance change in an assay to <0.005. The Hanes plot in Fig. 4.6 (top) shows parallel lines with increasing malonyl-CoA concentration, indicating competitive inhibition.

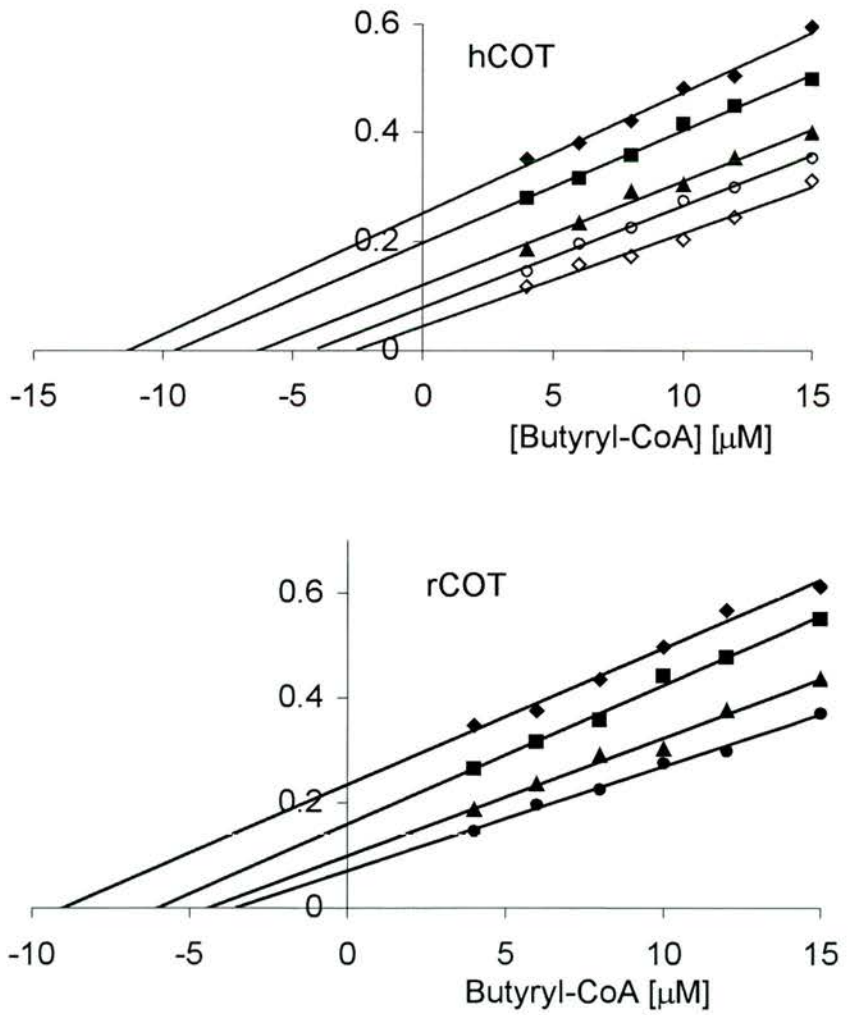

Fig.4.6 Competitive inhibiton of both COT and rCOT by malonyl-CoA.
The assays contained butyryl-CoA as indicated and 1 mM L-carnitine.

Enzyme	K_i for malonyl-CoA (μM)
hCOT	140
Y340H-hCOT	148
rCOT	175
bCOT	106

Table 4.5 Ki values for inhibition of COT by malonyl-CoA. The assay contained varied butryl-CoA and 1 mM L-carnitine.

4.2.3. Neither hCOT nor rCOT are sensitive to malonyl-CoA inhibition

The same result for both the wild-type and mutant (not shown) hCOT made it imperative to do the same experiment for purified rCOT. With purified rCOT, the same pattern was found (Fig.4.6, bottom). There was no sensitivity to malonyl-CoA at saturating concentrations of the acyl-CoA substrate (either decanoyl-CoA or butyryl-CoA) and the Hanes plot showed parallel line indicating competitive inhibition against butyryl-CoA.

Table 4.5 shows the Ki values for inhibition of COT by malonyl-CoA competing with butyryl-CoA. Clearly rCOT is inhibited no more that hCOT. Both rCOT and hCOT are not sensitive to malonyl-CoA in the way that is seen with CPT1 but rather they are inhibited by competition at the active site. That hCOT with Y at 340, its mutant with H at 340, and rCOT with H at 340 all show the same competitive inhibition means that the residue at 340 is not involved in malonyl-CoA binding.

4.2.4 Does the membrane confer malonyl-CoA sensitivity on COT?

The lack of inhibition of rCOT by malonyl-CoA using soluble rCOT contracts with the published data of Hegardt's group (Morillas et al., 2000). They observed about 50% inhibition using membrane bound COT after expression of the COT sequence in yeast. Dr. N.T. Price kindly provided rCOT constitutively expressed in P. pastoris. The yeast cells were grown, broken and the membrane and soluble fractions separated. Only 1% of the rCOT remained with the membranes. The soluble fraction was partially purified and found to have the same competitive malonyl-CoA inhibition as the rCOT after expression in *E. coli.* The membrane fraction was then tested under conditions as close as possible to those used by (Morillas et al., 2000).

The membrane associated rCOT was only 1 % of the total. It gave the same Km for L-carnitine (138 μM) as the purified rCOT. The Km for decanoyl-CoA was 2.8 μM similar to the value reported in Morillas et al., 2000, and slightly higher than that found for the purified rCOT (see above), as would be expected if there were some binding of acyl-CoA to membrane components.

The problem with assays involving long chain acyl derivatives is that these hydrophobic groups tend to form micelles, bind to membranes or bind to proteins such as serum albumin. Indeed, most assays of CPT1 routinely contain bovine serum albumin (BSA) to hinder the formation of palmitoyl-CoA micelles and to avoid lysis of mitochondrial membranes by the detergent action of this amphipathic compound. Binding of palmitoyl-CoA to BSA is well characterised, so we investigated its effect as well as that of yeast membranes on the malonyl-CoA inhibition of rCOT in yeast membranes.

No inhibition whatsoever was found when the enzyme was assayed with saturating concentrations of either decanoyl-CoA or palmitoyl-CoA (Fig. 4.7). However,

if serum albumin (BSA) were added to the assay mix, it would effectively decrease the concentration of free palmitoyl-CoA to below 1 μM. The free palmitoyl-CoA concentration in Fig.4.7, bottom right panel, can be estimated at less that 1 μM. This estimate is based on the experimental determination of palmitoyl-CoA binding to BSA that demonstrated the presence of two high affinity sites with dissociation constants around 0.7 μM and four low affinity sites with dissociation constants around 55 μM (Richards et al., 1990). In the experiment shown, the BSA is 20 μM, giving 40 μM high affinity sites. Under these conditions, inhibition with malonyl-CoA, was seen for all COT species tested whether the COT had H or Y at position 340 (Fig. 4.7, bottom right). The IC50, even in the presence of BSA, was greater than 200 μM. Yeast membranes have the same effect as BSA (not shown). Whether in the presence of yeast membranes or of BSA, no more than 50% inhibition of the activity by malonyl-CoA was observed.

The conclusion is that all soluble COT species are competitively inhibited by malonyl-CoA. In the membrane, the observation of inhibition and the observed sensitivity will depend on the specific conditions of the assay.

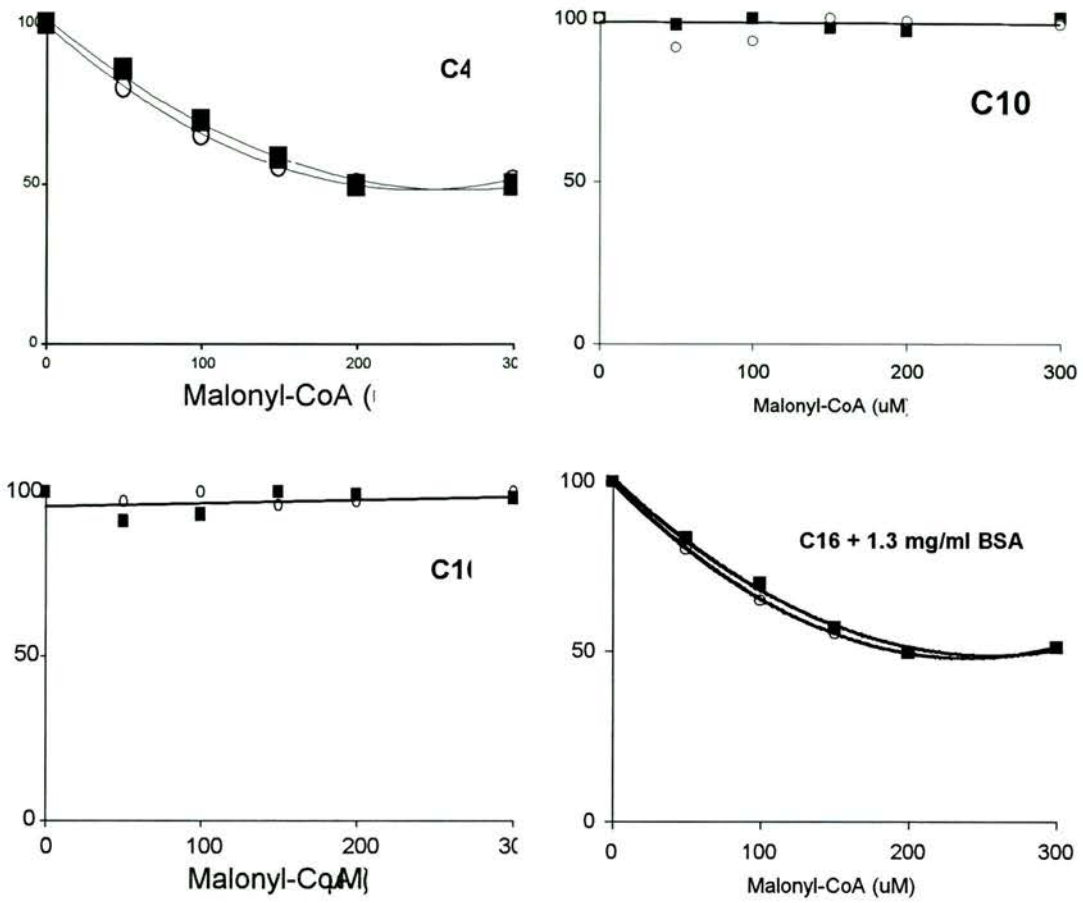

Fig. 4.7 Inhibition of COT by malonyl-CoA

Human COT (open circles) and rat COT (closed squares) are inhibited by malonyl-COA when assayed with subsaturating concentrations of C4-CoA (C4, 6mM) but no inhibition is seen at saturating concentrations of C10-CoA (C10, 50 mM) or C16-CoA (C16, 50 mM). If bovine serum albumin is added to reduce the concentration of free palmitoyl-CoA, inhibition is again seen (C16 + 1.3 mg/ml BSA). Yeast membranes have the same effect as BSA (not shown).

4.3 The acyl binding site of bovine COT

The structure of carnitine acetyltransferase revealed a putative binding site for longer acyl chains but access to the site was blocked by methionine 564 (Jogl, G. and Tong, 2003). The equivalent residue in all long chain carnitine acyltransferases is a conserved glycine. Mutation of glycine 553 to methionine in bovine COT would therefore be predicted to prevent binding of the acyl chain and change its specificity from a medium chain transferase to a short chain transferase. This mutation was prepared at the Hannah Institute, Ayr, under the supervision of Dr N.T. Price.

4.3.1 Changed chain length specificity

The kinetics of the purified G553M COT activity with respect to its substrates, L-carnitine and acyl-CoA were determined using purified enzyme. The acyl chain-length specificity for the wild type and mutant are given in Table 4.6. The wt-COT shows increased activity as the chain length of acyl-CoA is increased from 2 carbons to 10 carbons. Although wt-bCOT is active with substrates from C2-C18, the G553M mutant showed no activity whatsoever with any acyl chain length substrate apart from C2-CoA. It gave the same activity as the wild type with C2-CoA (Fig. 4.8 and Table 4.7) The change in the substrate specificity of COT induced by the G553M mutation from the native broad chain length range (C2–C18) to activity with only acetyl-CoA (C2) is a clear indication that acyl chain binding is prevented. Thus, the increase in the size of the residue at the position 553 has blocked binding of acyl chains greater than C2, as predicted from the structure of CrAT

Acyl-CoA Substrate	Activity ($\mu mol^{-1}.min^{-1}.mg^{-1}$)	
	WT-COT	G553M-COT
C2-CoA	1.23	1.21
C4-CoA	10.8	0
C6-CoA	17.3	0
C8-CoA	22.7	0
C10-CoA	38.2	0

Table 4.6 Acyl substrate specificities of wt-COT and G553M-COT assayed with 50μM acyl-CoA and 2mM L-carnitine.

Parameter	**Forward (C2)**		**Parameter**	**Reverse**
	wt	**G553M**		**G553M**
C2-CoA Km (μM)	30	32 ±5	CoA Km (μM)	
L-Carnitine Km (μM)	106	116 ±20	C2-L-carnitine Km (μM)	150
Vmax ($\mu mol.min^{-1}mg^{-1}$)	5	4 ±1	Vmax ($\mu mol.min^{-1}mg^{-1}$)	5

Table 4.7 Kinetic parameters for bCOT and its G553M mutant.

The assays used acetyl derivatives as substrates. For the reverse reaction the CoA concentration was fixed at 200 uM (>10xK_M).

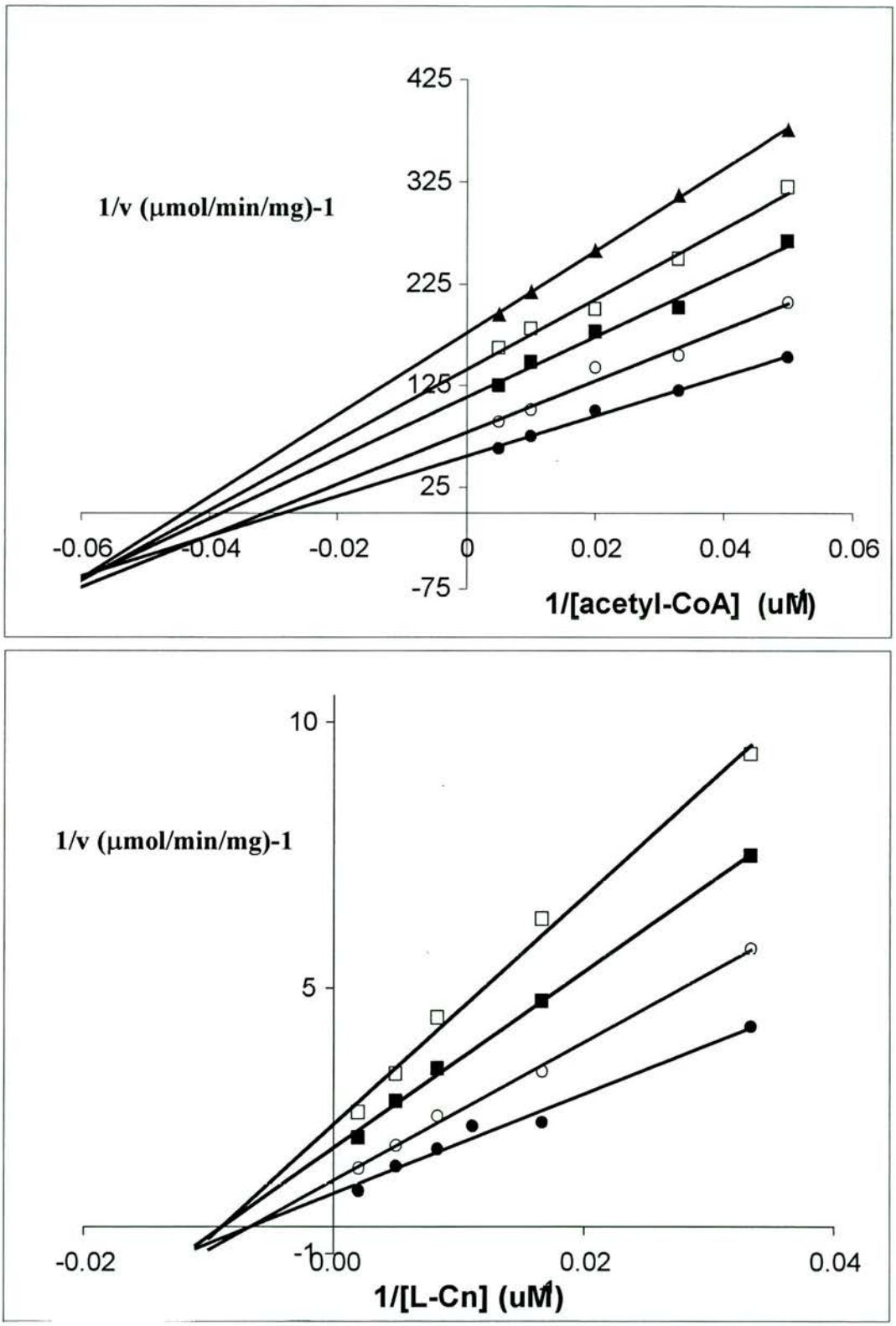

Fig. 4.8 Lineweaver-Burk plots for the acetyltransferase activity of G553M-COT (50 nM) assayed with series of increasing concentrations of L-carnitine (30-500 μM) and acetyl-CoA (20-200 μM).

The kinetic properties of wt-COT and G553M-COT were characterized using acetyl-CoA as the substrate. Fig. 4.8 shows a Lineweaver-Burk plot of the data for G553M-COT to illustrate that the pattern is consistent with the rapid-equilibrium random mechanism determined for the native enzyme. The kinetic constants using acetyl-CoA as a substrate are the same as for the wt-COT (Table 4.7). Thus, the mutation alters neither the catalysis of acetyl transfer by the enzyme nor the binding of either substrate.

The activity of G553M-COT was measured in the reverse direction by monitoring the CoA thioester formation directly at 232nm. In the reverse direction (acetyl-L-carnitine to CoA, using 200uM CoA), the V was 5 μmol^{-1}. $min^{-1}.mg^{-1}$ (Table 4.7), the same as the rate for the forward direction.

4.3.2 Inhibition of G553M-bCOT by long-chain acyl-CoA esters

When 100 μM decanoyl-CoA was added to an assay of G553M-COT with 100 μM acetyl-CoA and 2mM L-carnitine, the activity was inhibited by almost 70%. This indicated that decanoyl-CoA could bind to the enzyme and prevent the acetyl-CoA binding. The apparent Ki for decanoyl-CoA inhibition of the acetyltransferase activity at 100μM acetyl-CoA (3 x K_M) was 20μM and 22μM in two separate experiments (Fig. 4.9). The inhibition by decanoyl-CoA suggests that the longer chain substrates can still bind but not in a catalytically competent mode. The low affinity for decanoyl-CoA (indicated by the apparent Ki value of 21μM) suggests that the binding is due to the CoA moiety only. Similar inhibition of CrAT by palmitoyl-CoA has been reported (Chase and Tubbs, 1966).

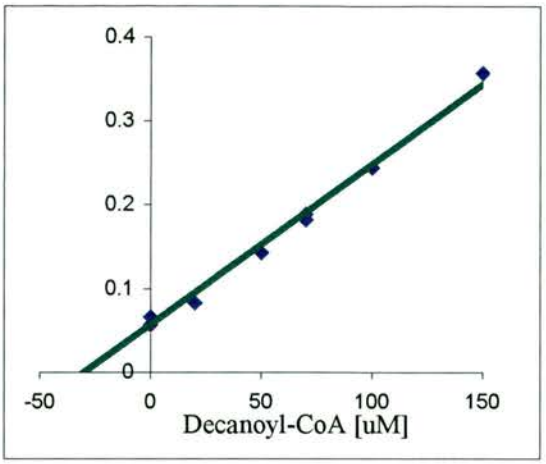

Fig. 4.9 Dixon plot for the inhibition of acetyl-CoA transferase by decanoyl-CoA. The assays contained 1 mM L-carnitine and 100μM acetyl-CoA. The inhibition constants were 20uM and 22uM (as shown) from the two different experiments.

4.3.3 A novel hydrolase activity in the G553M mutant of bCOT

In the absence of carnitine, a rapid hydrolysis of acetyl-CoA was observed with the G553M mutant whereas there was no hydrolysis by the wild-type enzyme. Previous kinetic studies revealed no hydrolase activity in COT isolated from bovine liver (Nic a'Bhaird, N. . et al., 1993), so this indicates a change in the catalytic site. The hydrolysis is saturable with acetyl-CoA (Fig. 4.10A, left) and analysis of the data gives a Vmax of 8.3 μmol^{-1}. $min^{-1}.mg^{-1}$ and a K_M for acetyl-CoA of 113 ± 15 μM (mean ± sd of four determinations). The hydrolase activity was also inhibited by decanoyl-CoA (Fig. 4.10B, right), with an apparent Ki value of 30 μM (against 100μM acetyl-CoA).

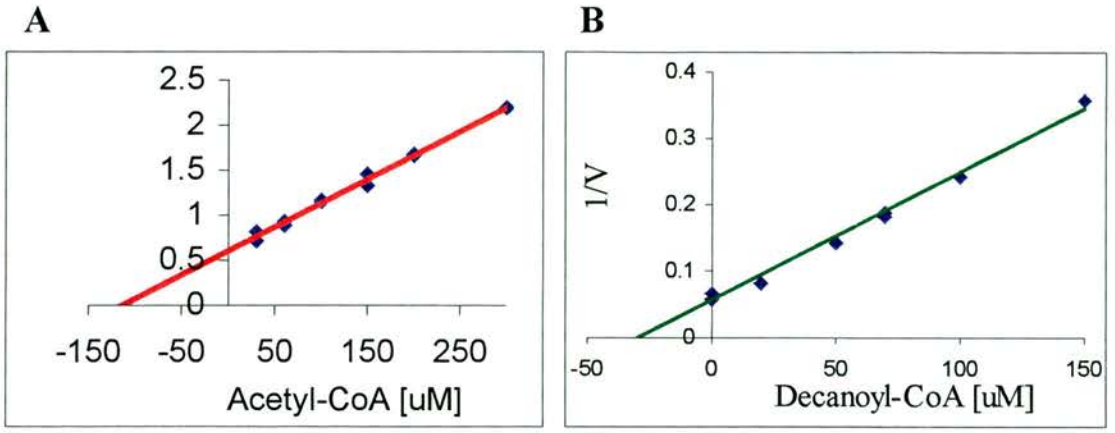

Fig. 4.10 Hydrolase activity of G553M-bCOT and its inhibition by decanoyl-CoA.

A. The Hanes plot for acetyl-CoA hydrolase activity in the absence of L-carnitine gives a K_M of 118 uM.

B. Dixon plot for the inhibition of the hydrolase activity by decanoyl-CoA shows an apparent Ki of 30 μM . The assay contained 100 μM acetyl-CoA.

The appearance of the hydrolase activity means that an active site group in G553M COT is able to activate water directly or to catalyse the hydrolysis via an active site group such as serine. Chemical modification experiments have provided evidence for a reactive group, possible serine, that prevented labelling of the catalytic histidine (Nic a'Bhaird, N. et al., 1998). At low protein concentrations, L-carnitine inhibits the rate of release of CoA, rather than stimulating it. This indicates that carnitine either competes with a putative water for activation or its binding prevents activation of the water or active site group responsible for the hydrolysis.

In the structure of COT just published, there is a water molecule hydrogen bonded to the main chain amide of Ala332 that may be responsible or the hydrolysis of the acyl esters (Jogl et al., 2005). Further evidence for steric alteration of the active site is seen in the decrease stability of the mutant protein. The G553M protein,

although stable during purification, becomes labile after freezing, its activity decreasing over the course of a few hours. The appearance of acetyl-CoA hydrolase activity in the absence of carnitine is consistent with observations of hydrolysis in CrAT during crystallisation. Only carnitine or CoA were found in the active site of the crystal whether the crystal was grown in acetyl-L-carnitine or soaked with acetyl-CoA respectively (Jogl and Tong, 2003).

5. INHIBITION OF COT

The design of inhibitors used in this study was based on the proposed active site as inferred from kinetic and binding studies. From kinetic and chemical studies, CAT was proposed to have tetrahedral intermediates containing CoA, carnitine and the acyl group (Gandour *et al.*, 1986). Figure 5.0 shows the schematic view of the accommodation of a tetrahedral intermediate in the active site of COT as presented by Ramsay and Gandour (Ramsay and Gandour, 1999). From this model, conformationally constrained analogues were designed and synthesised by Gandour *et al.*, and shown to inhibit differentially the CPT isoenzyme (Gandour *et al.*, 1992; Nic a'Bhaird *et al.*, 1993). The rational and strategy for the design of inhibitors for this family of enzymes was described in Chapter 1. Here conformationally constrained analogues that mimic the carnitine and acyl parts of the substrate or tetrahedral intermediate were obtained from Sigma Tau, Pharmaceutical Industries S.p.A, Italy to study the inhibition properties of COT.

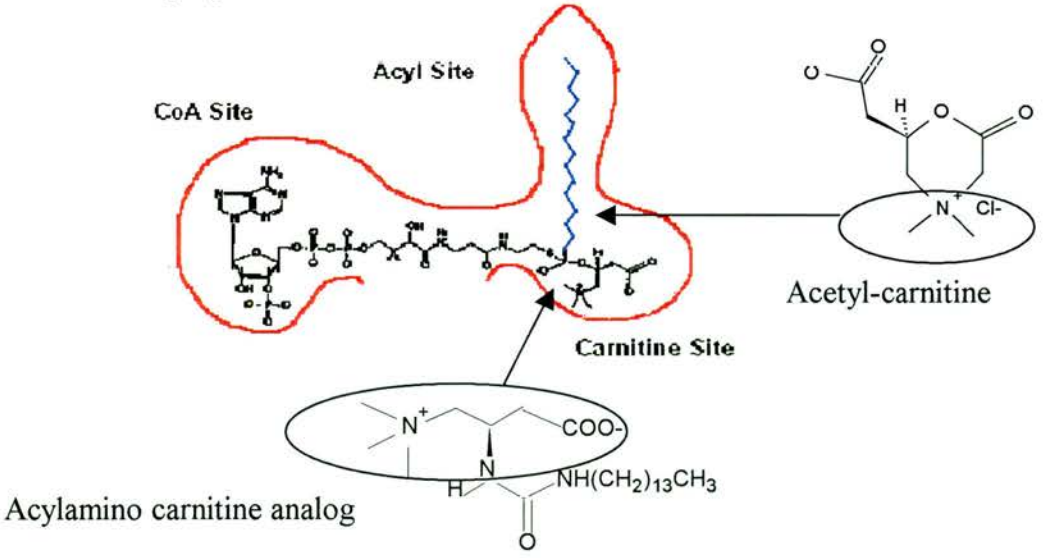

Figure 5.0: The schematic representation of the COT active site with a tetrahedral intermediate occupying the CoA, acyl and carnitine sites. Two of the carnitine analog inhibitors used in this study and their possible binding site are shown.

Purified bovine COT was used to analyse the inhibition constants and inhibition patterns given by the carnitine and acyl-carnitine analogs. Deoxycarnitine (competitive with carnitine) and etomoxiryl-CoA (an irreversible inhibitor) were also used in this study for comparison with the new compounds. The inhibition constant IC50 was first determined by assaying the enzyme with different concentrations of inhibitor at fixed concentrations of decanoyl-CoA (5 μM) and L-carnitine (200 μM). The true Ki values are obtained by varying either decanoyl-CoA or L-carnitine at fixed concentrations of the other substrate. The type of inhibition was determined from the family of lines at increasing inhibitor concentrations by varying either the decanoyl-CoA or the L-carnitine at saturating concentration of the other substrate. For either substrate varied, an increasing apparent Km without Vmax change was observed for all the Sigma Tau inhibitors used (see below), indicating competitive inhibition.

5.1 Inhibition of COT by deoxycarnitine

Purified bovine COT was used to study the inhibition pattern for the substrate analogue, deoxycarnitine. When L-carnitine was varied at fixed concentrations of palmitoyl-CoA (25 μM) clear competitive inhibition was observed (figure. 5.1, right). The Ki value of 5 mM was comparable with previous work (Nic a'Bhaird *et al.*, 1993). When palmitoyl-CoA was varied, a non-competitive inhibition pattern was obtained (figure 5.1 left). This study also confirmed that cloned COT followed the same kinetic mechanism as that isolated from bovine liver (Nic a'Bhaird *et al.*, 1993).

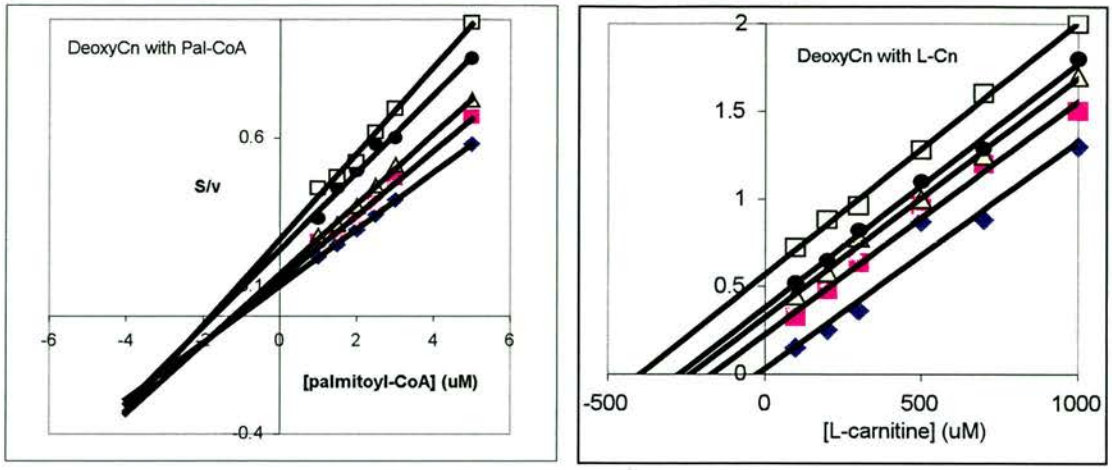

Fig. 5.1 Inhibition patterns for deoxycarnitine inhibition of cloned bovine COT. Left panel, L-carnitine was fixed at 1 mM and deoxycarnitine was 1, 3, 5, 8 and 10 mM. Right, palmitoyl-CoA was fixed at 25 μM and deoxycarnitine varied as before.

Inhibitor ID	Structure	IC_{50} (μM)	Ki (μM)	Type of Inhibition
ST-1163	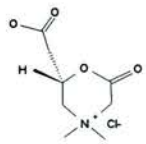	10.5	9.5	Competitive
ST-1164	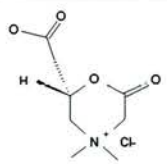	10	10.2	Competitive
ST-1175	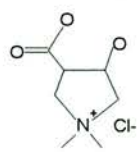	12	13.1	Competitive
ST-1177	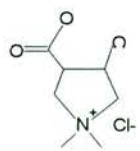	12.5	13.3	Competitive

Table 5.1: The IC_{50} and Ki values for the constrained acetyl-L-carnitine analogs. The IC_{50} values were determined at fixed concentrations of decanoyl-CoA (5 μM) and L-carnitine (0.1 mM). Plots of S/V vs S gave increasing Km(app) values for L-carnitine with increasing concentrations of inhibitor without change in V_{max}. The Ki values were calculated from secondary plots of 1/Km (app) against 1/I.

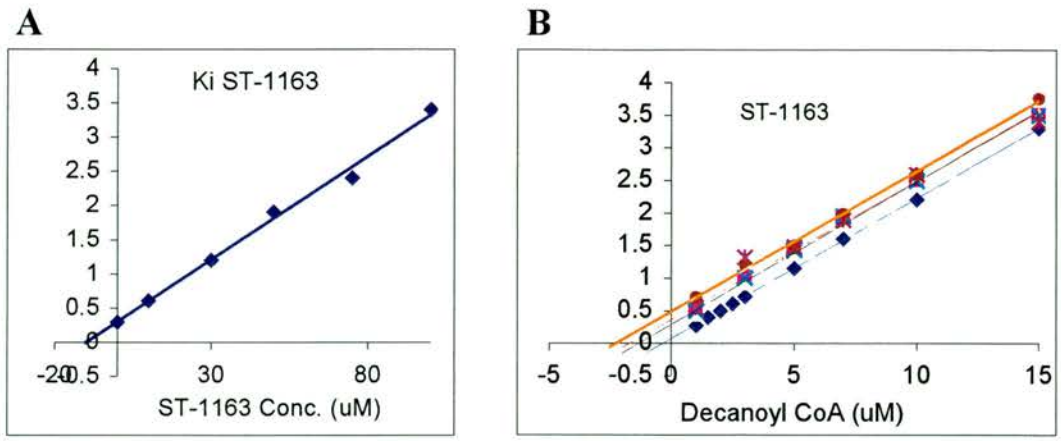

Figure 5.2: The Ki and the type of inhibition for ST-1163. A. The replot f Km (app) from (B) gives a Ki of 9.5μM. **B**. The Hanes plot at 50 μM L-carnitine shows increasing apparent Km as the inhibitor concentration is increased and the lines are parellel to each other.

5.2 Acetyl-carnitine analogues

Four analogues of carnitine locked into specific conformations by a ring structure (see Table 5.1) were tested for their inhibition of COT as a measure of their affinity for the enzyme active site. The experiment was designed to test the need for a specific conformation of the carboxyl group to obtain optimum binding. Previous work had established that the morpholino ring kept the N-C-C-O in the correct *gauche* conformation (Colucci and Gandour, 1988). Preliminary analysis (IC50 values in Table 5.1) with purified bovine COT at 5 μM decanoyl-CoA (10 x Km) and 200 μM L-carnitine (2 x Km) showed that the different relationship between the hydroxyl group and the carboxyl group in space made no difference to the inhibition constant. In all cases the Ki of around 10 μM is more than 10-fold lower than the Km or Ks for L-carnitine (108 μM). The five-membered ring compounds are constrained to slightly less than the favoured angle suggested by the putative transition-state analogue. The favoured angle was confirmed by the structure of the active site (Ramsay and Naismith, 2003). Each of these compounds (ST-1163/ST1164 and ST1175/ST1177)

are mixtures. One is a racemic mixture of the cis enantiomers, the other one is a mixture of the trans enantiomers. Since the data in Table 5.2 indicate identical results for both, then the cis or trans configuration must not matter.

All the acetyl-carnitine analogues were competitive inhibitors against decanoyl-CoA, with a Ki of around 10 μM, much lower than the Km for acetyl-L-carnitine of 150 μM (Sitheswaran *et al.*, 2005). This suggests that the compounds are indeed mimics of the form of the substrate that bind to the enzyme, constrained into the conformation of the transition state that binds better to the active site than the substrates.

The inhibition was competitive against both L-carnitine and decanoyl-CoA. At first glance this is a little surprising, but consideration of the structure of the inhibitors makes it clear. The inhibitors in Table 5.1 are analogues of acetyl-carnitine and its transition state and so could block not only the carnitine site but also the acyl binding site. In ST1175 and ST1177, the OH group is also in the position of the thiol group of CoA. The low Ki values of around 10 uM enable successful competition against the binding of the CoA moiety which is around 20 uM (Nic a'Bhaird *et al.*, 1993) if the acyl moiety binding site is blocked.

5.3 Acyl-L-carnitine analogues

A considerable number of researchers have investigated carnitine analogues as alternate substrates and inhibitors of the carnitine acyltransferases (See Chapter 1). Analogues of carnitine itself are best described in a review about CAT (Colucci and Gandour, 1988). Amino-carnitine was shown to have antiketotic and hypoglycaemic affects in rats (Jenkins and Griffith, 1986) and selectivity between the isoforms of the carnitine acyltransferases (Murthy *et al.*, 1990).

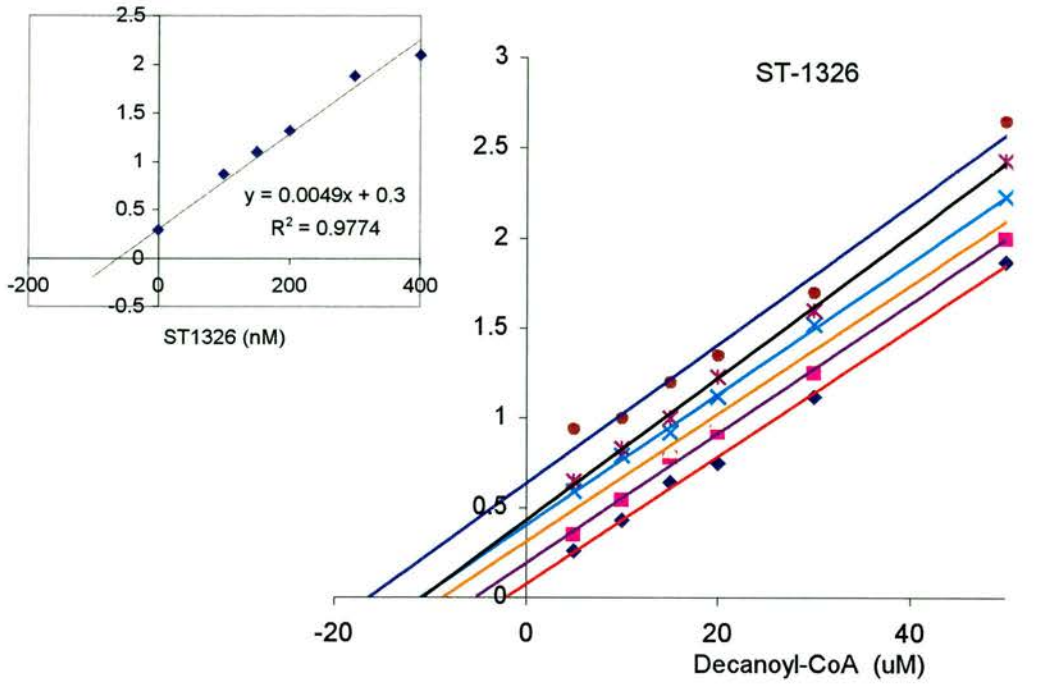

Figure 5.3: Inhibition of COT by ST-1326. The Ki was determined with series of different concentrations of inhibitor varying decanoyl-CoA (5-50μM) at a fixed saturating concentration of L-carnitine (1mM). *Inset:* secondary plot of the apparent Km values.

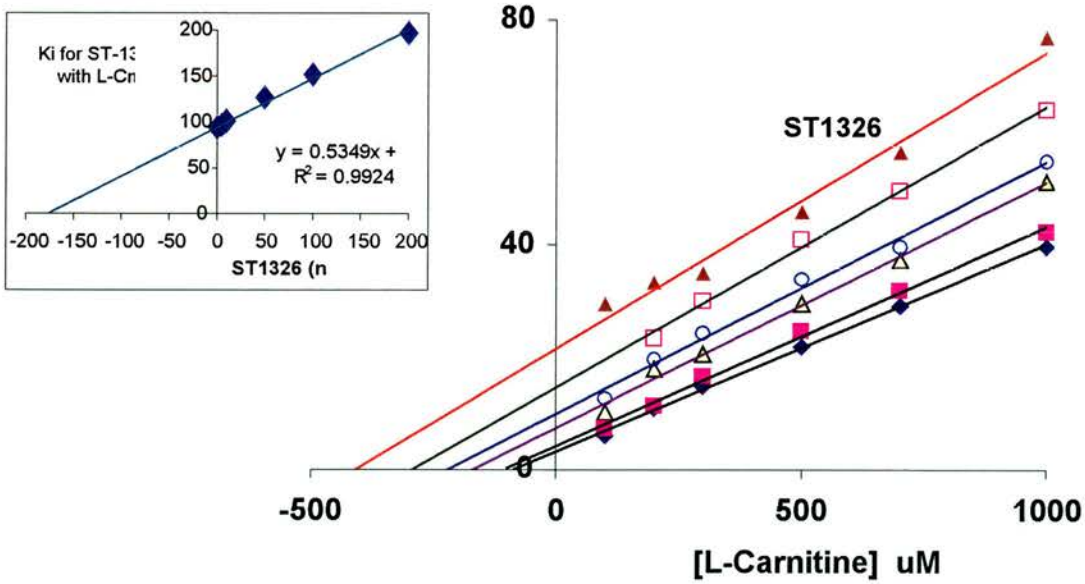

Figure 5.4: Inhibition of COT by ST-1326. The Ki was determined with series of different concentrations of inhibitor varying l-carnitine (5-200μM) at a fixed saturating concentration of decanoyl-CoA (50μM). *Inset:* secondary plot of the apparent Km values.

This made it a good basis for synthetic chemistry to seek new forms of antidiabetic drugs that would be competitive inhibitors of CPT1 and so free of the cardiotoxic effects of compounds such as etomoxir (Anderson *et al.*, 1995). Out of a study that measured CPT1 inhibition by analogs of carnitine where the OH group was altered (Giannessi *et al.*, 2001), compounds selectively active against liver CPT1 were chosen (Table 5.2). These were an acyl-suphonamide inhibitor (ST-1420) and three ureido derivatives of different chain lengths for comparison (ST1328, 1375, and 1326 in order of chain length). All these compounds were water-soluble. These acyl-carnitine analogs all inhibit COT competitively (Figures. 5.3 and 5.4). The Hanes plot showed parallel lines when increasing concentrations of inhibitors were used and decanoyl-CoA was varied, as expected for a competitive inhibitor that shares the same binding site. This was slightly surprising for a carnitine derivative, but clearly the acyl group must be able to bind to the acyl site and so compete with the acyl moiety of the decanoyl-CoA. These inhibitor compounds are, in effect, product analogues for the assay in the forward direction.

The Hanes plots when L-carnitine was varied were also almost parallel (Figure 5.4). Here, however, the Ki value was 175 μM, rather than the 10 μM seen when decanoyl-CoA was varied. This means that these values are not true Ki values but Ki (app) for binding to the COT-substrate complex, and indeed this is how the experiment was done. Thus, the Ki (app) of 10 μM obtained when decanoyl-CoA was varied was for competition with decanoyl-CoA binding to the COT-L-carnitine complex, showing that the acyl chain successfully competed with the decanoyl chain on the CoA, even without binding of the carnitine moiety of the inhibitor. In the other experiment (Figure. 5.4), the acyl binding site is blocked by the saturating acyl-CoA and the affinity of the inhibitor for the enzyme depends on the aminocarnitine moiety.

Inhibitor ID	Structure	IC_{50} (nM)	Ki (nM)	Type of inhibition
ST-1326	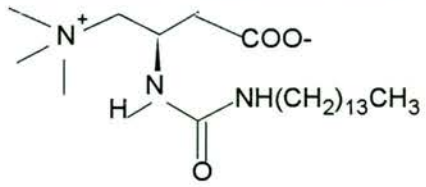	200	175	Competitive
ST-1328	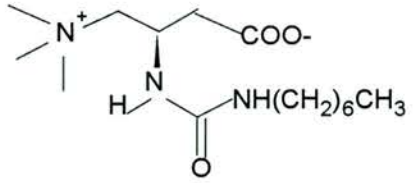	150	100	Competitive
ST-1375	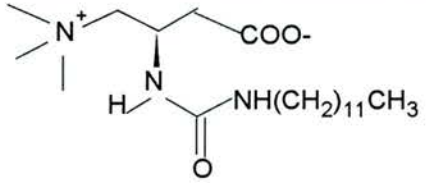	50	50	Competitive
ST-1420	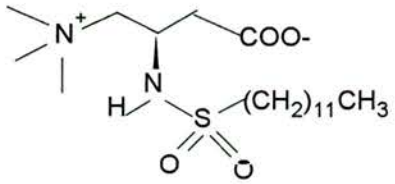	30	30	Competitive

Table 5.2: Inhibition constants for acyl-aminocarnitine derivatives. The IC_{50} values were determined using 5 μM decanoyl-CoA, 200 μM L-carnitine, and 50 nM bCOT. The type of inhibition and Ki values were obtained by varying L-carnitine (0.01-1mM) at fixed, saturating decanoyl-CoA (50 μM). Values below 100 nM are not valid (see text).

Compound	K_D (nM)
ST-1326	100
ST-1328	97.7
ST-1375	1.08
ST-1420	1.1

Table 5.3: **Dissociation constants for acyl-aminocarnitine derivatives.**

Thus, the apparent Ki of 175 nM reflects binding to the carnitine site. Table 5.2 gives the IC_{50} and Ki values for the four inhibitors tested: all are in the nM range. These values indicate clearly that the acyl moiety competes successfully against the decanoyl-CoA (Km 0.5 μM). The improved affinity comes from the acyl group (C12>C8, 50 nM and 100 nM, respectively) as seen for substrates, but the C14 compound is less effective with a Ki of 175 nM.

The nature of the link to aminocarnitine also makes a difference. ST-1420 with a sulphonamide linkage gives a Ki of 30 nM compare to the 50 nM obtained for ST1375 with the same acyl chain but an uriedo linkage. With such low Ki values these compound are clearly good lead compounds for inhibition of COT. However, inhibition of COT is not the aim: it is CPT1 that must be inhibited for good antiketotic effect. The C10 analog of ST-1420 gives an IC50 against L-CPT1 of 1.6 μM in membrane preparations. The IC50 against COT is 10-fold lower, but the assay used purified COT and had no agents capable of binding the acyl tail. When serum albumin was added to the COT assay to mimic the presence of membranes, the concentrations of decanoyl-CoA required for saturation increase.

5.3.1 **Dissociation constants (K_D) for acyl-amino-L-carnitines**

The dissociation constants for the acyl-aminocarnitine derivative are obtained by calculating the concentration of bound and unbound inhibitors with the enzyme from the fractional occupancy measured as v_i/v_0. Figure 5.5 shows the Scatchard plots for ST-1328 and 1420. The dissociation constants for all the acylaminocarnitine analogs are shown in Table 5.3. The values for ST-1326 and ST-1328 are both consistent with the Ki values. However, the two more effective inhibitors give much lower K_D values than Ki values. This difference arises because the concentration of

the enzyme in the kinetic experiments was 50 nM, so steady state analysis using the Michaelis-Menton assumption that the initial concentrations of ligands are not changed was not valid. Thus, ST-1375 and ST-1420 are tight binding inhibitors of COT with affinities in the nM range.

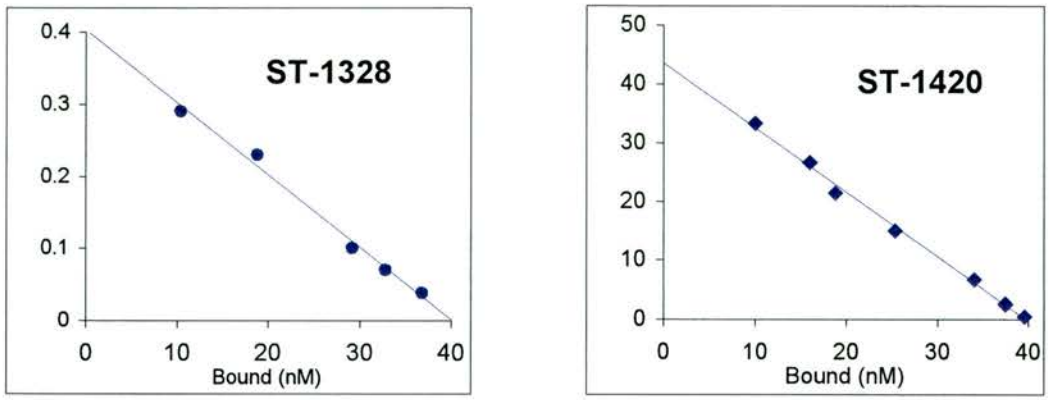

Figure 5.5: Scatchard plot analysis for the inhibition of COT by ST-1328 and ST-1420. The bound population was calculated from the fractional velocity and the concentration of the enzyme (30nM).

5.4 Inhibitory effect of C75 with COT

C75, an α-methylene-γ-butyrolactone, is a known inhibitor of fatty acid synthase (FAS) (Hu *et al.*, 2003). Treatment of mice with C75 alters the expression of hypothalamic neuropeptide, leading to reversible inanition and weight loss. In addition to its central action, C75 treatment causes changes in peripheral tissues, including inhibition of hepatic fatty acid synthesis, reduction of fatty liver, and diminution of adipose tissue mass. In addition to the increase of fatty acid oxidation and stimulation of carnitine palmitoyltransferase-1 (CPT-1) activity (Thupari *et al.*, 2002; Nicot *et al.*, 2004), we hypothesized that C75 might have effects on peroxisomal COT as well. The general chemical structure is given in figure 5.6.

The inhibition of COT was assayed with 5-200μM C75 with saturating concentrations of both decanoyl-CoA (50uM) and the L-carnitine (1mM). The IC_{50}

was 60uM and the remaining activity is expressed as percentage shows that the 96% inhibition was found at 100μM C75 even without pre-incubation of the enzyme (Figure 5.6).

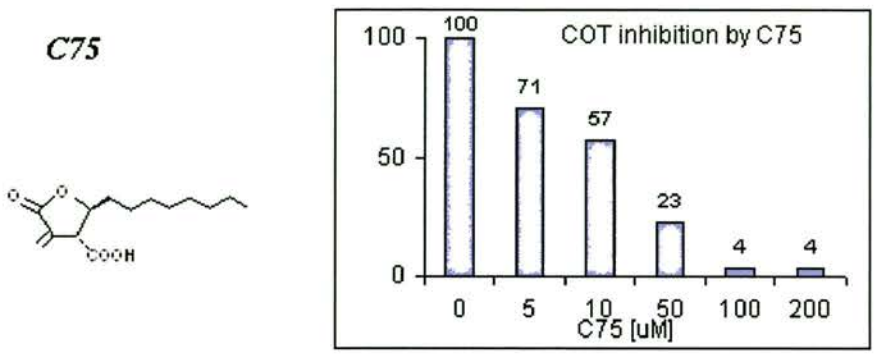

Figure 5.6: The structure of C75 and inhibition of human COT by C75 in the presence of saturating substrates without preincubation.

5.5 Inhibition of COT by etomoxiryl-CoA

5.5.1 Synthesis of Etomoxiryl-CoA from Etomoxir

Etomoxir-CoA was synthesised from etomoxir by *Mr.Gildas Deniau*, School of Chemistry, University of St Andrews. The final product was analysed by UV spectrum at 400-200nm where there is a difference between the etomoxir and etomoxiryl-CoA to confirm successful synthesis. Figure 5.7 shows the difference between the etomoxir and etomoxiryl-CoA.

5.5.2 Time-Dependent inhibition with etomoxiryl-CoA

The time and concentration dependence of the effect of etomoxiryl-CoA on COT was examined. Equal amounts of purified COT and etomoxiryl-CoA were incubated at 30°C in water bath and aliquots were assayed at different time intervals. The progressive inhibition compared to the control is shown in figure 5.8.

Irreversible reaction were tested by incubating COT (1.4μM) with 1μM

etomoxiryl-CoA for 5 minutes before diluting into assay mix containing 50 μM decanoyl-CoA and 1 mM carnitine. The activity was only 38% of the control despite the dilution of the inhibitor concentration to 20 nM in the cuvette where the enzyme was 28 nM.

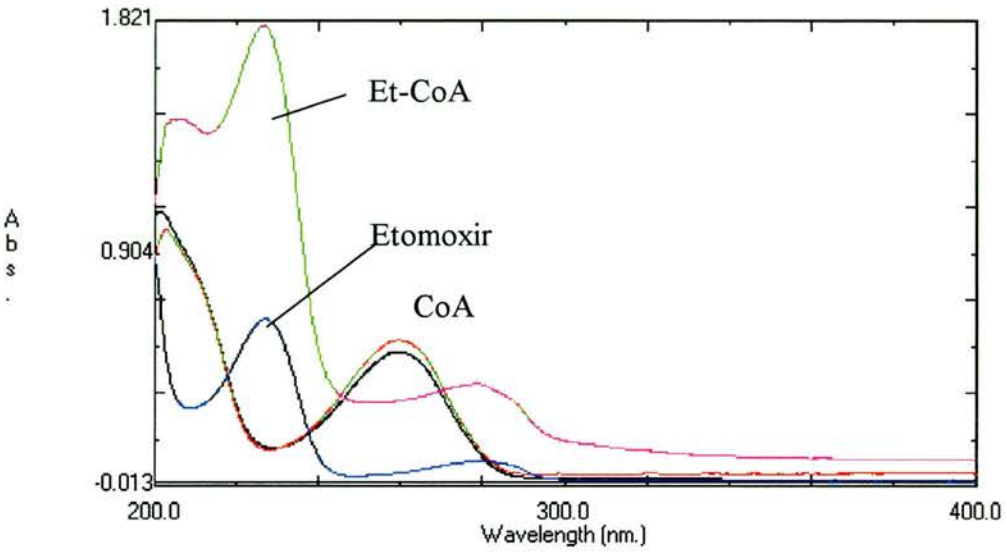

Figure 5.7: UV spectra of etomoxiryl-CoA, CoA and etomoxir. The peak at 260 nm represents the absorbance of CoA alone, as shown by the red curve for 5 mM CoA. Etomoxir alone (blue) peaks at 230 nm.

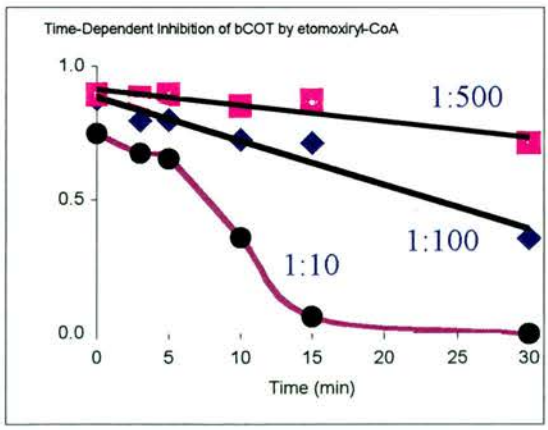

Figure 5.8: Time dependent inhibition of His-tagged hCOT by etomoxiryl-CoA. The assay determined the remaining activity after incubation of 100μg/ml COT (0.14μM) at 30°C with three different concentrations of etomoxiryl-CoA (stock, 0.1 mM). Substrates were added to start the reaction. The results are expressed as percentage of control activity over the time intervals in minutes.

5.6 Inactivation of COT by 2-bromoacetyl-L-carnitine

Formation of a "bridge compound" that dissociated from CAT with a half-life of 14 days suggested a strategy to help with crystallisation to immobilise the active site of COT (Chase and Tubbs, 1969). The same bridge compound was known to form in COT from the reaction of 2-bromopalmitoyl-CoA with L-carnitine in the active site of COT (Ramsay *et al.*, 1987).

The inhibitor 2-bromoacetyl-L-carnitine was obtained from Sigma Tau Pharmaceutical S.p.A., Italy. It was first confirmed that purified bovine COT was inactivated by 2-bromoacetyl-L-carnitine in the presence of CoA. Bovine COT was inactivated 100% at 1mM concentration of 2-bromoacetyl-L-carnitine in the presence of CoA over 120 minutes (Figure. 5.9). The enzyme alone lost 15% activity over an hour at 30°C indicating that the enzyme is not stable under the conditions of the incubation.

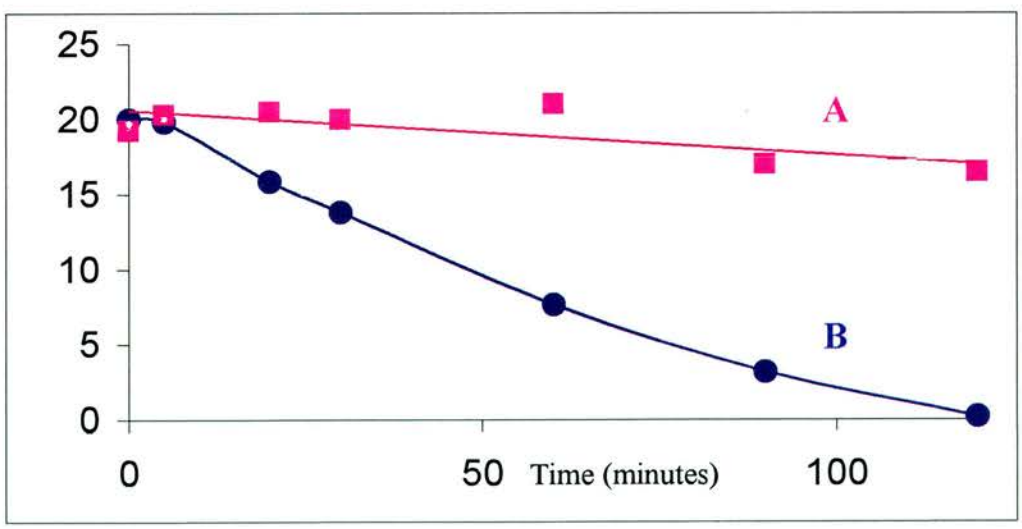

Figure 5.9: Time dependent inactivation of COT by 2-bromoacetyl L-carnitine. Purified COT (0.6mg/ml) was incubated without (**A**) and with 1mM 2-bromoacetyl-L-carnitine and 200μM CoA (**B**) at 30°C. The PDS assay for acyltransferase activity was performed at different time intervals.

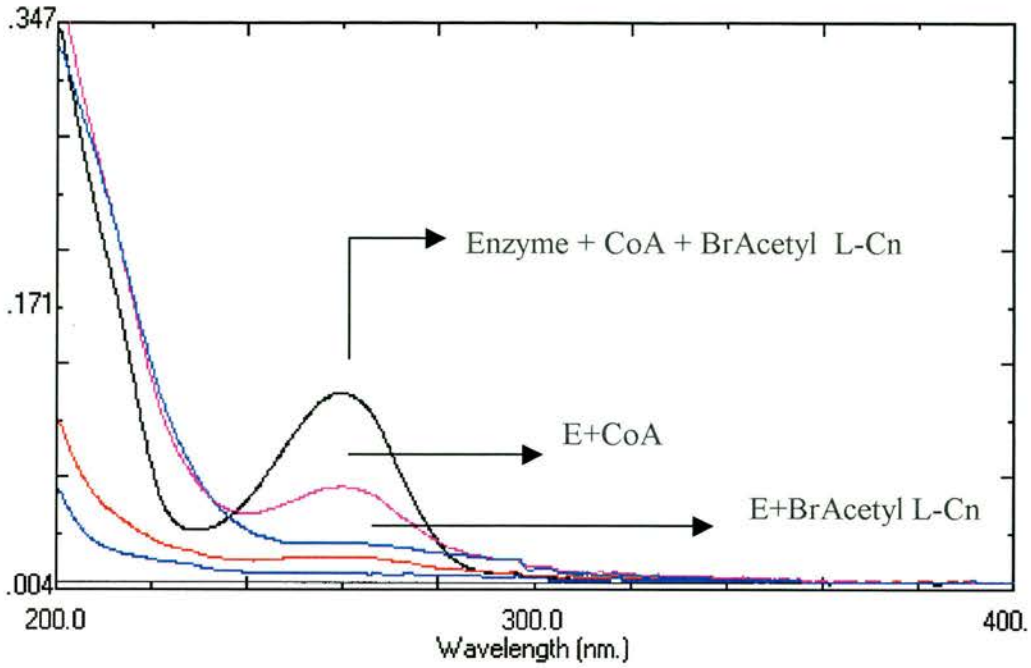

Figure 5.10: Spectrum of COT inactivated by 2-bromoacetyl-L-carnitine plus CoA. Purified COT (80nmol) was inactivated by incubating with 1mM 2-bromoacetyl L-carnitine and 200μM CoA. at 30°C for 1 hour. When activity was zero, the reagents were separated from the enzyme on a spin column of G50 Sephadex. The modified COT was assessed for incorporation of the CoA moiety by the UV spectrum at 400-200nM. Control incubations with either CoA or 2-bromoacetyl-l-carnitine alone were used to compare the results.

The inactivation was carried out by incubating 80nmols of enzyme with 1mM 2-bromoacetyl l-carnitine at 30°C, after which the sample was cooled on ice for 5 minutes. The volume was measured and the whole sample loaded onto a spin column of Sephadex G-50 and centrifuged at 3000xg for 2 minutes to separate the enzyme from free inhibitor and CoA. The effluent volume was measured and adjusted to 500μl with buffer. The sample was analysed by UV-spectrum (Figure 5.10), which shows that only the sample incubated with both substrates retained the CoA after

centrifugal gel filtration. It was hoped that the bridge compound would stabilise the COT to facilitate its crystallisation but it did not give any improvement.

6. CONCLUSIONS

Fatty acids represent a major energy source for mammals. Carnitine acyltransferases are important enzymes in fatty acid metabolism. These enzymes catalyse the reversible transfer of acyl group between CoA and L-carnitine. In addition to the major energy-yielding path in mitochondria, chain shortening of very long chain fatty acids takes place in the peroxisomes. Chain shortened fatty acids are exported from peroxisomes after transfer to carnitine by the action of carnitine octanoyltransferase (COT) and transported into the mitochondrial matrix for further β-oxidation with better energy conservation. CPT1 and CPT2 play a crucial role in the β-oxidation of long chain fatty acids in the mitochondria by facilitating their transport across the mitochondrial membrane. The function of CPT1 is regulated by malonyl-CoA, a crucial regulatory mechanism for fatty acid oxidation. Carnitine acetyltransferase (CAT) plays a role in the acetyl-CoA/CoA balance in the mitochondrial matrix and in the excretion of excess or harmful short chain acyl molecules as acylcarnitines. In the liver, oxidation of fatty acids produces ketone bodies that are an important fuel for extra-hepatic organs. Dysfunction or mutation of these enzymes have been linked to many serious human diseases.

Regulation of excessive mitochondrial fatty acid oxidation and hence ketogenesis is considered an important target for pharmaceutical intervention. Inhibition of CPT1 could be a way to achieve this (Anderson, 1998). The functional and structural studies of the carnitine acyltransferases will open the door to design effective and selective therapeutic agents for several human diseases, particularly non-insulin dependent diabetes (NIDDM).

COT proteins from different species were cloned and high levels of expression achieved. The purification of COT was successful and reproducible. The catalytic function of these COT proteins was analysed kinetically. The recombinant COT behaved as like the native form and kinetic constants are very similar. The cloned bovine COT showed kinetics consistent with the rapid equilibrium random mechanism previously established for COT (Nic a'Bhaird et al., 1998). In rapid equilibrium enzymes, Km is a good estimate of the binding constant Ks. The Km for all the COT proteins studied (human, rat, cow, and trout) dropped to about 0.5 μM above C10. The specificity constant for fatty acyl substrates >C10 was dependent on the catalytic efficacy (V). In human COT, decreased V for the longer acyl chains decreased the specificity constant, so that C10 remained the most efficient substrate. The greatest kinetic difference between bovine and human COT was that human COT had a maximum velocity for the reverse reaction (formation of acyl-CoA) three-fold higher than that for the forward reaction.

After multiple crystal screens, small bovine and human COT protein crystals were obtained but they did not grow bigger for diffraction. Neither ligands (substrates or inhibitors) present during crystallisation nor the generation of the "bridge" compound between acyl-carnitine in the active site improved the growth. However, purified CPT2 showed promising crystals grown in 3 days time and they were suitable for diffraction studies.

Mutational studies of COT were designed to explore the substrate specificity and malonyl-CoA inhibition properties. From the COT sequence, the larger methionine side group at 553 instead of glycine normally found at this site, blocked catalytic activity with any acyl chain except acetyl-CoA. However, saturable hydrolysis of the ester also occurred that was inhibited by decanoyl-CoA as expected

for CoA site occupancy. These experiments achieved two purposes. First, the alteration in the substrate specificity confirmed that the putative acyl binding tunnel proposed on the basis of the CAT structure (Jogl, G. and Tong, 2003) was present in COT and that blocking it prevented long chain acyl substrates from binding. The subsequent publication of the structure of COT confirmed this (Jogl, Gerwald et al., 2005). Secondly, it provides an explanation of why this mutation has deleterious consequences in the naturally occurring mutation G710E in CPT1 (Gobin et al., 2003).

Human COT is not sensitive to malonyl-CoA inhibition at physiologically relevant concentrations. When hCOT or rCOT was assayed with decanoyl-CoA and palmitoyl-CoA, no inhibition by malonyl-CoA was seen unless binding proteins such as bovine serum albumin or yeast membranes were added to decrease the concentration of the acyl-CoA substrate to below its Km value. When assayed with butyryl-CoA (for which concentrations around the Km are convenient), the hCOT and rCOT were competively inhibited by malonyl-CoA. The mutation of the Y340 in hCOT to the histidine found at that position in rCOT had no effect on the competitive inhibition nor on the inhibition in the presence of BSA. Thus, neither rat nor human COT is sensitive to malonyl-CoA regulation. Even when rCOT was expressed in yeast to allow its normal peroxisomal localisation and the membrane fraction (that retained only 1% of the total expressed activity) used in the assays, malonyl-CoA inhibition was observed only when the acyl-CoA substrate concentration was below Km.

Unlike malonyl-CoA, the amphipathic fatty acid synthesis inhibitor C75 is likely to permeate the peroxisomal membrane. The activation effect of C75 on CPT1 is independent of the malonyl-CoA binding site since it does not displace bound

malonyl-CoA and it also activates the malonyl-CoA insensitive isoenzyme, CPT2 (Nicot et al., 2004). In contrast to the activation of CPT1 and CPT2 shown in mitochondria isolated from yeast, the purified hCOT is inhibited by C75 with an IC_{50} of 60μM at saturating substrate concentrations. Thus, although increased mitochondrial breakdown of fats may be desirable, the potential side effect of decreasing the peroxisomal pathway would have to be considered in any drug development.

Constrained acetyl-L-carnitine and acyl-aminocarnitine analogues, prototype drugs provided by Sigma Tau S.p.A. inhibited bovine COT competitively. For antiketogenic drugs, it would be desirable to inhibit only CPT1 and leave all other carnitine acyltransferease isoenzymes active. The data here indicate that the conformationally constained analogues are competitive inhibitors with Ki values around 10μM. In contrast, the acyl-amino carnitine analogues, while acting competitively, are extremely potent inhibitors of COT. At the probable therapeutic concentrations that would inhibit CPT1, COT will also be completely inhibited. These acyl-amino carnitine derivatives could, however, be tools to explore the consequences of COT inhibition in cell culture.

7. APPENDIX

SEQUENCE ALIGHNMENT OF CARNITINE ACYLTRANSFERASES FROM DIFFERENT SPECIES

```
COT-Bovine          ------------------------------------------------------------
COT-Human           ------------------------------------------------------------
COT-Rat             ------------------------------------------------------------
CAT-Human           ------------------------------------------------------------
CAT-Mouse           ------------------------------------------------------------
CAT-Pigeon          ------------------------------------------------------------
CPT2-Rat            ------------------------------------------------------------
CPT2-Mouse          ------------------------------------------------------------
CPT2-Human          ------------------------------------------------------------
L-CPT1-Rat          ---------FQFTVTPDGIDLRLSHEALKQICLSGLHSWKKKFIRFKNGIITGVFPASPS 51
L-CPT1-Mouse        ---------FQFTVTPDGIDLRLSHEALKQICLSGLHSWKKKFIRFKNGIITGVFPASPS 51
L-CPT1-Human        MAEAHQAVAFQFTVTPDGIDLRLSHEALRQIYLSGLHSWKKKFIRFKNGIITGVYPASPS 60
M-CPT1-Rat          MAEAHQAVAFQFTVTPDGVDFRLSREALRHIYLSGINSWKKRLIRIKNGILRGVYPGSPT 60
M-CPT1-HouseMouse   MAEAHQAVAFQFTVTPDGVDFRLSREALRHIYLSGINSWKKRLIRIKNGILRGVYPGSPT 60
M-CPT1-Human        MAEAHQAVAFQFTVTPDGVDFRLSREALKHVYLSGINSWKKRLIRIKNGILRGVYPGSPT 60
BrainCPT1-Mouse     MAEAHQASSLLSSLSSDGAEVELSSPVWQEIYLCALRSWKRHLWRVWNDFLAGVVPATPL 60

COT-Bovine          ------------------------------------------------------------
COT-Human           ------------------------------------------------------------
COT-Rat             ------------------------------------------------------------
CAT-Human           ------------------------------------------------------------
CAT-Mouse           ------------------------------------------------------------
CAT-Pigeon          ------------------------------------------------------------
CPT2-Rat            ------------------------------------------------------------
CPT2-Mouse          ------------------------------------------------------------
CPT2-Human          ------------------------------------------------------------
L-CPT1-Rat          SWLIVVVGVISSMHTKVDPSLGMIAKINRTLDTTG--RMSSQTKNIVSGVLFGTGLWVAI 109
```

```
L-CPT1-Mouse          SWLIVVVGVISSMHTKVDPSLGMIAKINRTLDTTG--RMSSQTKNIVSGVLFGTGLWVAI 109
L-CPT1-Human          SWLIVVVGVMTTMYAKIDPSLGIIAKINRTLETAN--CMSSQTKNVVSGVLFGTGLWVAL 118
M-CPT1-Rat            SWLVVVMATVGSNYCKVDISMGLVHCIQRCLPTRYGSYGTPQTETLLSMVIFSTGVWATG 120
M-CPT1-HouseMouse     SWLVVVMATVGSNYCKVDISMGLVDCIQRCLPERYGHFGTPQTEALLSMVIFSTGVWATG 120
M-CPT1-Human          SWLVVIMATVGSSFCNVDISLGLVSCIQRCLPQGCGPYQTPQTRALLSMAIFSTGVWVTG 120
BrainCPT1-Mouse       SWLFLFSTIQLACLLQLDPSLGLMEKIKELLPDWGG--QHHQLQGFLSAAVFASCLWGAL 118

COT-Bovine            ------------------------MENQLAKSTEERTFQY---------QDSLPSLPVPS 27
COT-Human             ------------------------MENQLAKSTEERTFQY---------QDSLPSLPVPS 27
COT-Rat               ------------------------MENQLAKSIEERTFQY---------QDSLPPLPVPS 27
CAT-Human             ----------MLAFAARTVVKPLGFLKPFSLMKASSRFKAH--------QDALPRLPVPP 42
CAT-Mouse             ----------MLAFAARTVVKPLGLLKPSSLMKVSGRFKAH--------QDALPRLPVPP 42
CAT-Pigeon            ---------MDRKQKQAEKARPYGLLKPAALGKIPGRFQLH--------QEALPHLPVPP 43
CPT2-Rat              ----MMPRLLFRAWPRCPSLVLGAPSRPLSAVSGPDDYLQHSIVPTMHYQDSLPRLPIPK 56
CPT2-Mouse            ----MMPRLLLRDWPRCPSLVLGAPSRPLSAVSGPAEYLQHSIVPTMHYQDSLPRLPIPK 56
CPT2-Human            ----MVPRLLLRAWPRGPAVGPGAPSRPLSAGSGPGQYLQRSIVPTMHYQDSLPRLPIPK 56
L-CPT1-Rat            IMTMRYSLKVLLSYHGWMFAEHGKMSRSTRIWMAMVKVFSGRKPMLYSFQTSLPRLPVPA 169
L-CPT1-Mouse          IMTMRYSLKVLLSYHGWMFAEHGKMSRSTRIWMAMVKVFSGRKPMLYSFQTSLPRLPVPA 169
L-CPT1-Human          IVTMRYSLKVLLSYHGWMFTEHGKMSRATKIWMGMVKIFSGRKPMLYSFQTSLPRLPVPA 178
M-CPT1-Rat            IFLFRQTLKLLLSYHGWMFEMHSKTSHATKIWAICVRLLSSRRPMLYSFQTSLPKLPVPS 180
M-CPT1-HouseMouse     IFFFRQTLKLLLSYHGWMFEMHSKTSHATKIWAICVRLLSSRRPMLYSFQTSLPKLPVPS 180
M-CPT1-Human          IFFFRQTLKLLLCYHGWMFEMHGKTSNLTRIWAMCIRLLSSRHPMLYSFQTSLPKLPVPR 180
BrainCPT1-Mouse       IFTLHVALRLLLSHHGWLLEPHGAMSSPTKTWLALVRIFSGRHPRLFSFQRALPRQPVPS 178
                                                                 * :** *:*

COT-Bovine            LEESLKKYLESVKPFANEEEYKNTEAIVWKFQN--GIGEKLQQKLLQRAKGRRNWLEEWW 85
COT-Human             LEESLKKYLESVKPFANQEEYKKTEEIVQKFQS--GIGEKLHQKLLERAKGKRNWLEEWW 85
COT-Rat               LEESLKKYLESVKPFANEDEYKKTEEIVQKFQD--GVGKTLHQKLLERAKGKRNWLEEWW 85
CAT-Human             LQQSLDHYLKALQPIVSEEEWAHTKQLVDEFQASGGVGERLQKGLGRRARKTENWLSEWW 102
CAT-Mouse             LQQSLDYYLKALQPIVSEEEWAHTKQLVDEFQTSGGVGERLQKGLERRAKKMENWLSEWW 102
CAT-Pigeon            LQQTLDRYLLALQPIISEEELNHTQELVAEFRKPGGVGERLQKGLERRAKKTDNWLSDWW 103
CPT2-Rat              LEDTMKRYLNAQKPLLDDSQFRRTEALCKNFETGVGKELHAHLLAQDKQNKHTSYISGPW 116
CPT2-Mouse            LEDTMKRYLSAQKPLLNDSQFRKTEVLCKDFENGIGKELHAHLLAQDKQNKHTSYISGPW 116
CPT2-Human            LEDTIRRYLSAQKPLLNDGQFRKTEQFCKSFENGIGKELHEQLVALDKQNKHTSYISGPW 116
L-CPT1-Rat            VKDTVSRYLESVRPLMKEGDFQRMTALAQDFAVN--LGPKLQWYLKLKSWWATNYVSDWW 227
```

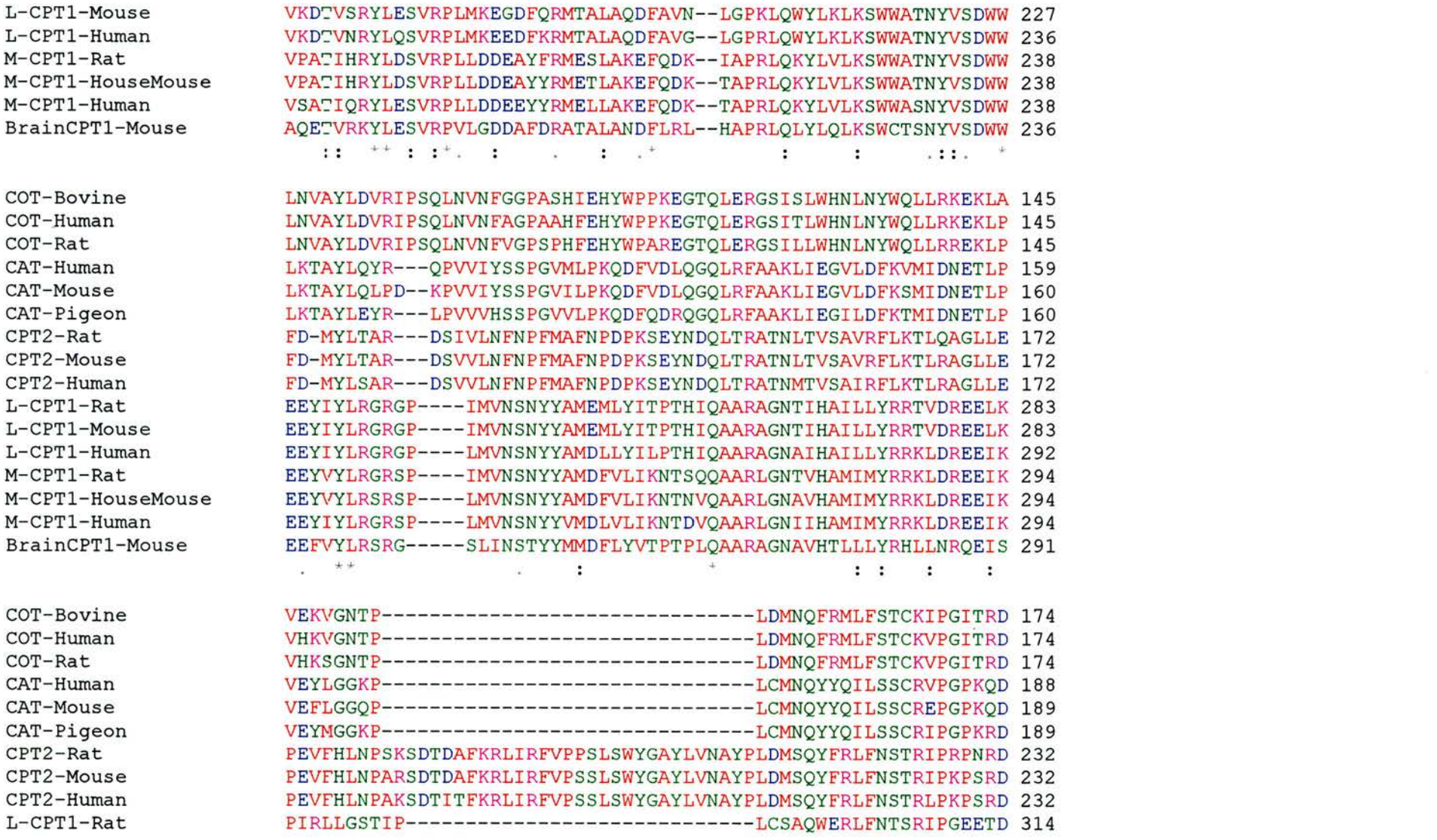
L-CPT1-Mouse VKDTVSRYLESVRPLMKEGDFQRMTALAQDFAVN--LGPKLQWYLKLKSWWATNYVSDWW 227
L-CPT1-Human VKDTVNRYLQSVRPLMKEEDFKRMTALAQDFAVG--LGPRLQWYLKLKSWWATNYVSDWW 236
M-CPT1-Rat VPATIHRYLDSVRPLLDDEAYFRMESLAKEFQDK--IAPRLQKYLVLKSWWATNYVSDWW 238
M-CPT1-HouseMouse VPATIHRYLDSVRPLLDDEAYYRMETLAKEFQDK--TAPRLQKYLVLKSWWATNYVSDWW 238
M-CPT1-Human VSATIQRYLESVRPLLDDEEYYRMELLAKEFQDK--TAPRLQKYLVLKSWWASNYVSDWW 238
BrainCPT1-Mouse AQETVRKYLESVRPVLGDDAFDRATALANDFLRL--HAPRLQLYLQLKSWCTSNYVSDWW 236
COT-Bovine LNVAYLDVRIPSQLNVNFGGPASHIEHYWPPKEGTQLERGSISLWHNLNYWQLLRKEKLA 145
COT-Human LNVAYLDVRIPSQLNVNFAGPAAHFEHYWPPKEGTQLERGSITLWHNLNYWQLLRKEKLP 145
COT-Rat LNVAYLDVRIPSQLNVNFVGPSPHFEHYWPAREGTQLERGSILLWHNLNYWQLLRREKLP 145
CAT-Human LKTAYLQYR---QPVVIYSSPGVMLPKQDFVDLQGQLRFAAKLIEGVLDFKVMIDNETLP 159
CAT-Mouse LKTAYLQLPD--KPVVIYSSPGVILPKQDFVDLQGQLRFAAKLIEGVLDFKSMIDNETLP 160
CAT-Pigeon LKTAYLEYR---LPVVVHSSPGVVLPKQDFQDRQGQLRFAAKLIEGILDFKTMIDNETLP 160
CPT2-Rat FD-MYLTAR---DSIVLNFNPFMAFNPDPKSEYNDQLTRATNLTVSAVRFLKTLQAGLLE 172
CPT2-Mouse FD-MYLTAR---DSVVLNFNPFMAFNPDPKSEYNDQLTRATNLTVSAVRFLKTLRAGLLE 172
CPT2-Human FD-MYLSAR---DSVVLNFNPFMAFNPDPKSEYNDQLTRATNMTVSAIRFLKTLRAGLLE 172
L-CPT1-Rat EEYIYLRGRGP----IMVNSNYYAMEMLYITPTHIQAARAGNTIHAILLYRRTVDREELK 283
L-CPT1-Mouse EEYIYLRGRGP----IMVNSNYYAMEMLYITPTHIQAARAGNTIHAILLYRRTVDREELK 283
L-CPT1-Human EEYIYLRGRGP----LMVNSNYYAMDLLYILPTHIQAARAGNAIHAILLYRRKLDREEIK 292
M-CPT1-Rat EEYVYLRGRSP----IMVNSNYYAMDFVLIKNTSQQAARLGNTVHAMIMYRRKLDREEIK 294
M-CPT1-HouseMouse EEYVYLRSRSP----LMVNSNYYAMDFVLIKNTNVQAARLGNAVHAMIMYRRKLDREEIK 294
M-CPT1-Human EEYIYLRGRSP----LMVNSNYYVMDLVLIKNTDVQAARLGNIIHAMIMYRRKLDREEIK 294
BrainCPT1-Mouse EEFVYLRSRG-----SLINSTYYMMDFLYVTPTPLQAARAGNAVHTLLLYRHLLNRQEIS 291
COT-Bovine VEKVGNTP--------------------------------LDMNQFRMLFSTCKIPGITRD 174
COT-Human VHKVGNTP--------------------------------LDMNQFRMLFSTCKVPGITRD 174
COT-Rat VHKSGNTP--------------------------------LDMNQFRMLFSTCKVPGITRD 174
CAT-Human VEYLGGKP--------------------------------LCMNQYYQILSSCRVPGPKQD 188
CAT-Mouse VEFLGGQP--------------------------------LCMNQYYQILSSCREPGPKQD 189
CAT-Pigeon VEYMGGKP--------------------------------LCMNQYYQILSSCRIPGPKRD 189
CPT2-Rat PEVFHLNPSKSDTDAFKRLIRFVPPSLSWYGAYLVNAYPLDMSQYFRLFNSTRIPRPNRD 232
CPT2-Mouse PEVFHLNPARSDTDAFKRLIRFVPSSLSWYGAYLVNAYPLDMSQYFRLFNSTRIPKPSRD 232
CPT2-Human PEVFHLNPAKSDTITFKRLIRFVPSSLSWYGAYLVNAYPLDMSQYFRLFNSTRLPKPSRD 232
L-CPT1-Rat PIRLLGSTIP--------------------------------LCSAQWERLFNTSRIPGEETD 314

```
L-CPT1-Mouse          PIRLLGSTIP----------------------------LCSAQWERLFNTSRIPGEETD 314
L-CPT1-Human          PIRLLGSTIP----------------------------LCSAQWERMFNTSRIPGEETD 323
M-CPT1-Rat            PVMALG-MVP----------------------------MCSYQMERMFNTTRIPGKETD 324
M-CPT1-HouseMouse     PVMALG-MVP----------------------------MCSYQMERMFNTTRIPGKETD 324
M-CPT1-Human          PVMALG-IVP----------------------------MCSYQMERMFNTTRIPGKDTD 324
BrainCPT1-Mouse       PTLLMG-MRP----------------------------LCSAQYERMFNTTRIPGVEKD 321
                                                            :   .   ::.: : .   .

COT-Bovine            SIINYFRTESEGHSPSHLAVLCRGRVFVFDVMH-EGYLMTAPEIQRQLTYIQKK-CHSEP 232
COT-Human             SIMNYFRTESEGRSPNHIVVLCRGRAFVFDVIH-EGCLVTPPELLRQLTYIHKK-CHSEP 232
COT-Rat               SIMNYFKTESEGHCPTHIAVLCRGRAFVFDVLH-DGCLITPPELLRQLTYIYQK-CWNEP 232
CAT-Human             TVSNFSKTKKP---PTHITVVHNYQFFELDVYHSDGTPLTADQIFVQLEKIWNS-SLQTN 244
CAT-Mouse             SVVNFLKSKRP---PTHITVVHNYQFFELDVYNSDGTPLTSDQIFVQLEKIWNS-SLQSN 245
CAT-Pigeon            SIVNYAKGKKQ---SRHITVVHNFQFFELDVYNSDGSPLTTDQLFIQLEKIWNT-SLQTN 245
CPT2-Rat              ELFTDTKAR-------HLLVLRKGHFYVFDVLDQDGNIVNPLEIQAHLKYILSD-SSPVP 284
CPT2-Mouse            ELFTDTKAR-------HLLVLRKGHFYVFDVLDQDGNIVNPSEIQAHLKYILSD-SSPVP 284
CPT2-Human            ELFTDDKAR-------HLLVLRKGNFYIFDVLDQDGNIVSPSEIQAHLKYILSD-SSPAP 284
L-CPT1-Rat            TIQHVKDSR-------HIVVYHRGRYFKVWLYH-DGRLLRPRELEQQMQQILDDTSEPQP 366
L-CPT1-Mouse          TIQHVKDSR-------HIVVYHRGRYFKVWLYH-DGRLLRPRELEQQMQQILDDTSEPQP 366
L-CPT1-Human          TIQHMRDSK-------HIVVYHRGRYFKVWLYH-DGRLLKPREMEQQMQRILDNTSEPQP 375
M-CPT1-Rat            LLQHLSESR-------HVAVYHKGRFFKVWLYE-GSCLLKPRDLEMQFQRILDDTSPPQP 376
M-CPT1-HouseMouse     LLQHLSESR-------HVAVYHKGRFFKVWLYE-GSRLLKPRDLEMQFQRILDDPSPPQP 376
M-CPT1-Human          VLQHLSDSR-------HVAVYHKGRFFKLWLYE-GARLLKPQDLEMQFQRILDDPSPPQP 376
BrainCPT1-Mouse       HLRHLQDSR-------HVAVFHRGRFFRVGTHS-PNGLLSPRALEQQFQDILDDPSPACP 373
                       :      .       .: .  . . : .         : .  :  ::  .  .  .

COT-Bovine            DGPGVAALTTEERTRWAKAREYLISLNPENLTILEKIQSSLLVFCLDDDS---PHVTP-E 288
COT-Human             DGPGIAALTSEERTRWAKAREYLIGLDPENLALLEKIQSSLLVYSMEDSS---PHVTP-E 288
COT-Rat               VGPSIAALTSEERTRWAKAREYLIGLDPENLTLLEKIQSSLFVYSIEDTS---PHATP-E 288
CAT-Human             KEP-VGILTSNHRNSWAKAYNTLIKDK-VNRDSVRSIQKSIFTVCLDATM---PRVSEDV 299
CAT-Mouse             KEP-VGILTSNHRNTWAKAYNNLIKDK-VNRESVNSIQKSIFTVCLDKQV---PRVSDDV 300
CAT-Pigeon            KEP-VGILTTNHRNSWAKAYNNLLKDK-TNKESVRTIEKSICTICLDAPM---PRVSDDI 300
CPT2-Rat              EFP-VAYLTSENRDVWAELRQKLIFD--GNEETLKKVDSAVFCLCLDDFP---MKD---- 334
CPT2-Mouse            EFP-LAYLTSENRDVWAELRQKLIHG--GNEETLRKVDSAVFCLCLDDFP---MKD---- 334
CPT2-Human            EFP-LAYLTSENRDIWAELRQKLMSS--GNEESLRKVDSAVFCLCLDDFP---IKD---- 334
L-CPT1-Rat            GEAKLAALTAADRVPWAKCRQTCFAR-GKNKQSLDAVEKAAFFVTLDESEQGYREEDPEA 425
```

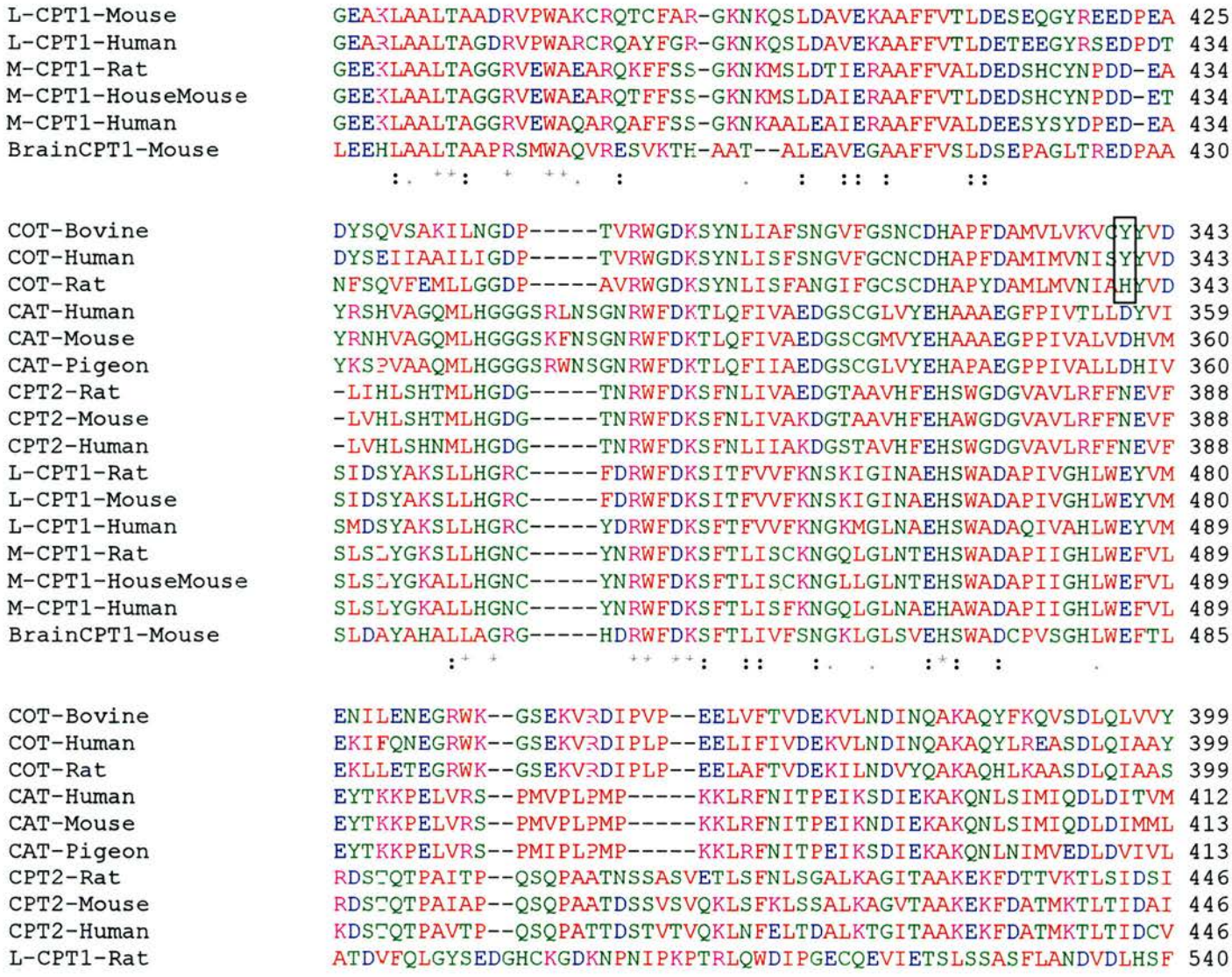
L-CPT1-Mouse GEAKLAALTAADRVPWAKCRQTCFAR-GKNKQSLDAVEKAAFFVTLDESEQGYREEDPEA 425
L-CPT1-Human GEARLAALTAGDRVPWARCRQAYFGR-GKNKQSLDAVEKAAFFVTLDETEEGYRSEDPDT 434
M-CPT1-Rat GEEKLAALTAGGRVEWAEARQKFFSS-GKNKMSLDTIERAAFFVALDEDSHCYNPDD-EA 434
M-CPT1-HouseMouse GEEKLAALTAGGRVEWAEARQTFFSS-GKNKMSLDAIERAAFFVTLDEDSHCYNPDD-ET 434
M-CPT1-Human GEEKLAALTAGGRVEWAQARQAFFSS-GKNKAALEAIERAAFFVALDEESYSYDPED-EA 434
BrainCPT1-Mouse LEEHLAALTAAPRSMWAQVRESVKTH-AAT--ALEAVEGAAFFVSLDSEPAGLTREDPAA 430
COT-Bovine DYSQVSAKILNGDP-----TVRWGDKSYNLIAFSNGVFGSNCDHAPFDAMVLVKVCYYVD 343
COT-Human DYSEIIAAILIGDP-----TVRWGDKSYNLISFSNGVFGCNCDHAPFDAMIMVNISYYVD 343
COT-Rat NFSQVFEMLLGGDP-----AVRWGDKSYNLISFANGIFGCSCDHAPYDAMLMVNIAHYVD 343
CAT-Human YRSHVAGQMLHGGGSRLNSGNRWFDKTLQFIVAEDGSCGLVYEHAAAEGFPIVTLLDYVI 359
CAT-Mouse YRNHVAGQMLHGGGSKFNSGNRWFDKTLQFIVAEDGSCGMVYEHAAAEGPPIVALVDHVM 360
CAT-Pigeon YKSPVAAQMLHGGGSRWNSGNRWFDKTLQFIIAEDGSCGLVYEHAPAEGPPIVALLDHIV 360
CPT2-Rat -LIHLSHTMLHGDG-----TNRWFDKSFNLIVAEDGTAAVHFEHSWGDGVAVLRFFNEVF 388
CPT2-Mouse -LVHLSHTMLHGDG-----TNRWFDKSFNLIVAKDGTAAVHFEHAWGDGVAVLRFFNEVF 388
CPT2-Human -LVHLSHNMLHGDG-----TNRWFDKSFNLIIAKDGSTAVHFEHSWGDGVAVLRFFNEVF 388
L-CPT1-Rat SIDSYAKSLLHGRC-----FDRWFDKSITFVVFKNSKIGINAEHSWADAPIVGHLWEYVM 480
L-CPT1-Mouse SIDSYAKSLLHGRC-----FDRWFDKSITFVVFKNSKIGINAEHSWADAPIVGHLWEYVM 480
L-CPT1-Human SMDSYAKSLLHGRC-----YDRWFDKSFTFVVFKNGKMGLNAEHSWADAQIVAHLWEYVM 489
M-CPT1-Rat SLSLYGKSLLHGNC-----YNRWFDKSFTLISCKNGQLGLNTEHSWADAPIIGHLWEFVL 489
M-CPT1-HouseMouse SLSLYGKALLHGNC-----YNRWFDKSFTLISCKNGLLGLNTEHSWADAPIIGHLWEFVL 489
M-CPT1-Human SLSLYGKALLHGNC-----YNRWFDKSFTLISFKNGQLGLNAEHAWADAPIIGHLWEFVL 489
BrainCPT1-Mouse SLDAYAHALLAGRG-----HDRWFDKSFTLIVFSNGKLGLSVEHSWADCPVSGHLWEFTL 485
ENILENEGRWK--GSEKVRDIPVP--EELVFTVDEKVLNDINQAKAQYFKQVSDLQLVVY 399
COT-Human EKIFQNEGRWK--GSEKVRDIPLP--EELIFIVDEKVLNDINQAKAQYLREASDLQIAAY 399
COT-Rat EKLLETEGRWK--GSEKVRDIPLP--EELAFTVDEKILNDVYQAKAQHLKAASDLQIAAS 399
CAT-Human EYTKKPELVRS--PMVPLPMP-----KKLRFNITPEIKSDIEKAKQNLSIMIQDLDITVM 412
CAT-Mouse EYTKKPELVRS--PMVPLPMP-----KKLRFNITPEIKNDIEKAKQNLSIMIQDLDIMML 413
CAT-Pigeon EYTKKPELVRS--PMIPLPMP-----KKLRFNITPEIKSDIEKAKQNLNIMVEDLDVIVL 413
CPT2-Rat RDSTQTPAITP--QSQPAATNSSASVETLSFNLSGALKAGITAAKEKFDTTVKTLSIDSI 446
CPT2-Mouse RDSTQTPAIAP--QSQPAATDSSVSVQKLSFKLSSALKAGVTAAKEKFDATMKTLTIDAI 446
CPT2-Human KDSTQTPAVTP--QSQPATTDSTVTVQKLNFELTDALKTGITAAKEKFDATMKTLTIDCV 446
L-CPT1-Rat ATDVFQLGYSEDGHCKGDKNPNIPKPTRLQWDIPGECQEVIETSLSSASFLANDVDLHSF 540

```
L-CPT1-Mouse          ATDVFQLGYSEDGHCKGDKNPNIPKPTRLQWDIPGECQEVIETSLSSASFLANDVDLHSF 540
L-CPT1-Human          SIDSLQLGYAEDGHCKGDINPNIPYPTRLQWDIPGECQEVIETSLNTANLLANDVDFHSF 549
M-CPT1-Rat            ATDTFHLGYTETGHCVGEPNTKLPPPQRMQWDIPEQCQTAIENSYQVAKALADDVELYCF 549
M-CPT1-HouseMouse     GTDTFHLGYTETGHCVGEPNTTLPPPQRLPWDIPEQCREAIENSYQVAKALADDVELYCF 549
M-CPT1-Human          GTDSFHLGYTETGHCLGKPNPALAPPTRLQWDIPKQCQAVIESSYQVAKALADDVELYCF 549
BrainCPT1-Mouse       ATECFQLGYATDGHCKGHPDPTLPQPQRLQWDLPEQIQPSISLALRGAKTLSGNIDCHVF 545
                                                 : : :       :  :          :

COT-Bovine            AFTSFGKKLTKEKQLHPDTFIQLALQLAYYRLHGRPGCCYETAMTRLFYHGRTETVRPCT 459
COT-Human             AFTSFGKKLTKNKMLHPDTFIQLALQLAYYRLHGHPGCCYETAMTRHFYHGRTETMRSCT 459
COT-Rat               TFTSFGKKLTKKEALHPDTFIQLALQLAYYRLHGRPGCCYETAMTRYFYHGRTETVRSCT 459
CAT-Human             VFHHFGKDFPKSEKLSPDAFIQMALQLAYYRIYGQACATYESASLRMFHLGRTDTIRSAS 472
CAT-Mouse             TFHHFGKDFPKSEKLSPDAFIQVALQLAYYRIYGQACATYESASLRMFHLGRTDTIRSAS 473
CAT-Pigeon            VFHQFGKNYPKSEKISPDAFIQLALQLAYYRMYGHSCATYESASLRMFRLGRTDTIRSTS 473
CPT2-Rat              QFQRGGKEFLKKKQLSPDAVAQLAFQMAFLRQYGQTVATYESCSTAAFKHGRTETIRPAS 506
CPT2-Mouse            QFQRGGKEFLKKKKLSPDAVAQLAFQMAFLRQYGQTVATYESCSTAAFKHGRTETICPAS 506
CPT2-Human            QFQRGGKEFLKKQKLSPDAVAQLAFQMAFLRQYGQTVATYESCSTAAFKHGRTETIRPAS 506
L-CPT1-Rat            PFDTFGKGLIKKCRTSPDAFIQLALQLAHYKDMGKFCLTYEASMTRLFREGRTETVRSCT 600
L-CPT1-Mouse          PFDTFGKGLIKKCRTSPDAFIQLALQLAHYKDMGKFCLTYEASMTRLFREGRTETVRSCT 600
L-CPT1-Human          PFVAFGKGIIKKCRTSPDTFVQLALQLAHYKDMGKFCLTYEASMTRLFREGRTETVRSCT 609
M-CPT1-Rat            QFLPFGKGLIKKCRTSPDAFVQIALQLAHFRDKGKFCLTYEASMTRMFREGRTETVRSCT 609
M-CPT1-HouseMouse     QFLPFGKGLIKKCRTSPDAFVQIALQLAHFRDKGKFCLTYEASMTRMFREGRTETVRSCT 609
M-CPT1-Human          QFLPFGKGLIKKCRTSPDAFVQIALQLAHFRDRGKFCLTYEASMTRMFREGRTETVRSCT 609
BrainCPT1-Mouse       PFSHFGKSFIKCCHVSSDSFIQLVLQLAHFRDRGQFCLTYESAMTRLFLEGRTETVRSCT 605
                        *   **   *     .*:. *:.:*:*. :  *:    **:.    *  ***:*: . :

COT-Bovine            VEAVNWCQSMQ--NPSTSLLERKHMMLEAFAKHNKMMKDCSTGKGFDRHLLGLSLIAKEE 517
COT-Human             VEAVRWCQSMQ--DPSVNLRERQQKMLQAFAKHNKMMKDCSAGKGFDRHLLGLLLIAKEE 517
COT-Rat               VEAVRWCQSMQ--DPSASLLERQQKMLDAFAKHNKMMRDCSHGKGFDRHLLGLLLIAKEE 517
CAT-Human             MDSLTFVKAMD--DSSVTEHQKVELLRKAVQAHRGYTDRAIRGEAFGRHLLGLKLQAIED 530
CAT-Mouse             IDSLAFVKGMG--DSTVPEQQKVELLRKAVQAHRAYTDRAIRGEAFDRHLLGLKLQAIED 531
CAT-Pigeon            IESHKFVQSMD--SPDKSDQEKADLLRRATQAHKEYTNMAIQGNAIDRHLLGLKLQAIED 531
CPT2-Rat              IFTKRCSEAFVRDPSKHSVGELQHMMAECSKYHGQLTKEAAMGQGFDRHLYALRYLATAR 566
CPT2-Mouse            IFTKRCSEAFVREPSKHSVGELQHMMAECSKYHGQLTKEAAMGQGFDRHLFALRYLAAAR 566
CPT2-Human            VYTKRCSEAFVREPSRHSAGELQQMMVECSKYHGQLTKEAAMGQGFDRHLFALRHLAAAK 566
L-CPT1-Rat            TESCNFVLAMMDPTTTAE--QRLKLFKIACEKHQHLYRLAMTGAGIDRHLFCLYVVSKYL 658
```

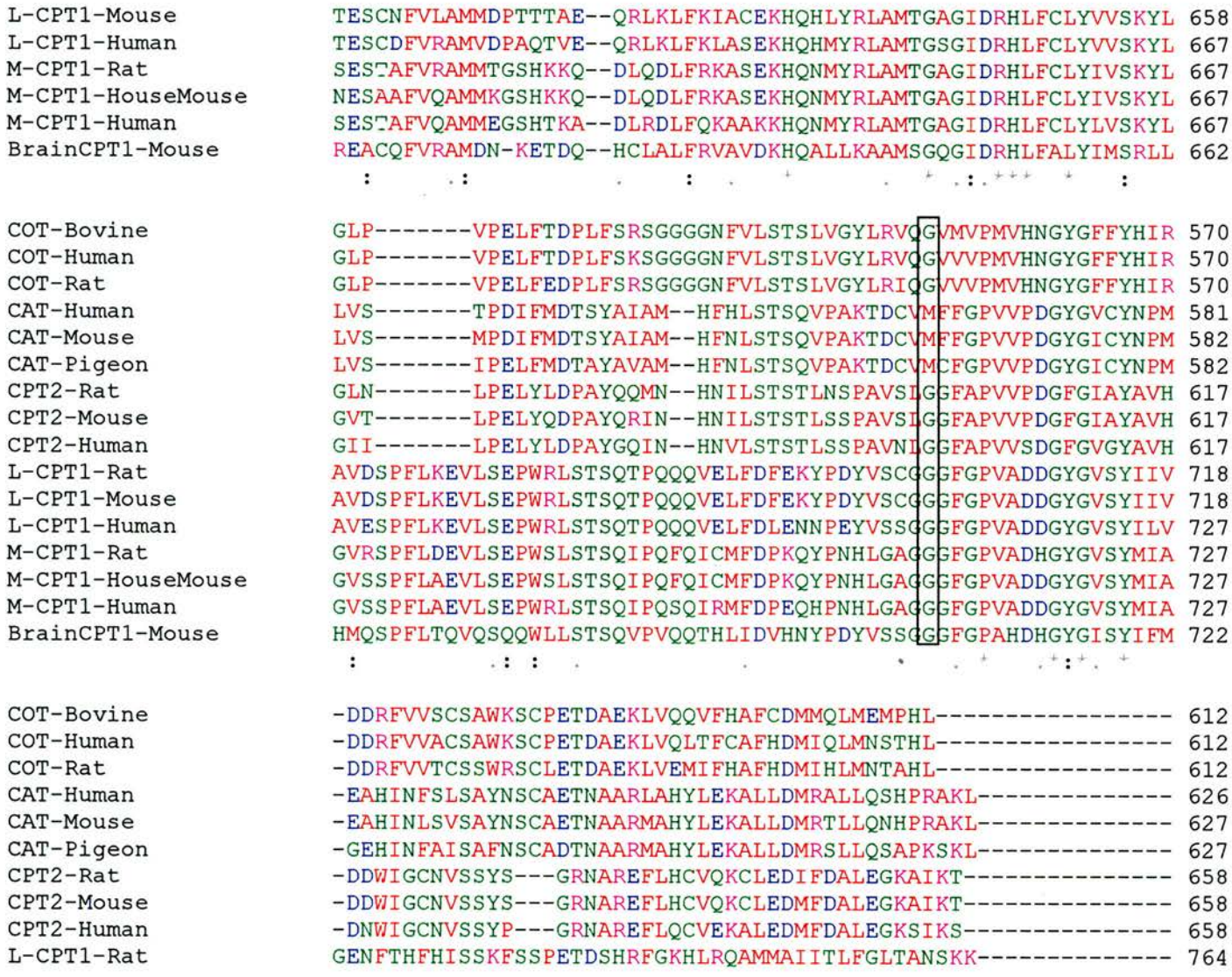
L-CPT1-Mouse TESCNFVLAMMDPTTTAE--QRLKLFKIACEKHQHLYRLAMTGAGIDRHLFCLYVVSKYL 658
L-CPT1-Human TESCDFVRAMVDPAQTVE--QRLKLFKLASEKHQHMYRLAMTGSGIDRHLFCLYVVSKYL 667
M-CPT1-Rat SESTAFVRAMMTGSHKKQ--DLQDLFRKASEKHQNMYRLAMTGAGIDRHLFCLYIVSKYL 667
M-CPT1-HouseMouse NESAAFVQAMMKGSHKKQ--DLQDLFRKASEKHQNMYRLAMTGAGIDRHLFCLYIVSKYL 667
M-CPT1-Human SESTAFVQAMMEGSHTKA--DLRDLFQKAAKKHQNMYRLAMTGAGIDRHLFCLYLVSKYL 667
BrainCPT1-Mouse REACQFVRAMDN-KETDQ--HCLALFRVAVDKHQALLKAAMSGQGIDRHLFALYIMSRLL 662
COT-Bovine GLP-------VPELFTDPLFSRSGGGGNFVLSTSLVGYLRVQGVMVPMVHNGYGFFYHIR 570
COT-Human GLP-------VPELFTDPLFSKSGGGGNFVLSTSLVGYLRVQGVVVPMVHNGYGFFYHIR 570
COT-Rat GLP-------VPELFEDPLFSRSGGGGNFVLSTSLVGYLRIQGVVVPMVHNGYGFFYHIR 570
CAT-Human LVS-------TPDIFMDTSYAIAM--HFHLSTSQVPAKTDCVMFFGPVVPDGYGVCYNPM 581
CAT-Mouse LVS-------MPDIFMDTSYAIAM--HFNLSTSQVPAKTDCVMFFGPVVPDGYGICYNPM 582
CAT-Pigeon LVS-------IPELFMDTAYAVAM--HFNLSTSQVPAKTDCVMCFGPVVPDGYGICYNPM 582
CPT2-Rat GLN-------LPELYLDPAYQQMN--HNILSTSTLNSPAVSLGGFAPVVPDGFGIAYAVH 617
CPT2-Mouse GVT-------LPELYQDPAYQRIN--HNILSTSTLSSPAVSLGGFAPVVPDGFGIAYAVH 617
CPT2-Human GII-------LPELYLDPAYGQIN--HNVLSTSTLSSPAVNLGGFAPVVSDGFGVGYAVH 617
L-CPT1-Rat AVDSPFLKEVLSEPWRLSTSQTPQQQVELFDFEKYPDYVSCGGGFGPVADDGYGVSYIIV 718
L-CPT1-Mouse AVDSPFLKEVLSEPWRLSTSQTPQQQVELFDFEKYPDYVSCGGGFGPVADDGYGVSYIIV 718
L-CPT1-Human AVESPFLKEVLSEPWRLSTSQTPQQQVELFDLENNPEYVSSGGGFGPVADDGYGVSYILV 727
M-CPT1-Rat GVRSPFLDEVLSEPWSLSTSQIPQFQICMFDPKQYPNHLGAGGGFGPVADHGYGVSYMIA 727
M-CPT1-HouseMouse GVSSPFLAEVLSEPWSLSTSQIPQFQICMFDPKQYPNHLGAGGGFGPVADDGYGVSYMIA 727
M-CPT1-Human GVSSPFLAEVLSEPWRLSTSQIPQSQIRMFDPEQHPNHLGAGGGFGPVADDGYGVSYMIA 727
BrainCPT1-Mouse HMQSPFLTQVQSQQWLLSTSQVPVQQTHLIDVHNYPDYVSSGGGFGPAHDHGYGISYIFM 722
COT-Bovine -DDRFVVSCSAWKSCPETDAEKLVQQVFHAFCDMMQLMEMPHL---------- 612
COT-Human -DDRFVVACSAWKSCPETDAEKLVQLTFCAFHDMIQLMNSTHL---------- 612
COT-Rat -DDRFVVTCSSWRSCLETDAEKLVEMIFHAFHDMIHLMNTAHL---------- 612
CAT-Human -EAHINFSLSAYNSCAETNAARLAHYLEKALLDMRALLQSHPRAKL---------- 626
CAT-Mouse -EAHINLSVSAYNSCAETNAARMAHYLEKALLDMRTLLQNHPRAKL---------- 627
CAT-Pigeon -GEHINFAISAFNSCADTNAARMAHYLEKALLDMRSLLQSAPKSKL---------- 627
CPT2-Rat -DDWIGCNVSSYS---GRNAREFLHCVQKCLEDIFDALEGKAIKT---------- 658
CPT2-Mouse -DDWIGCNVSSYS---GRNAREFLHCVQKCLEDMFDALEGKAIKT---------- 658
CPT2-Human -DNWIGCNVSSYP---GRNAREFLQCVEKALEDMFDALEGKSIKS---------- 658
L-CPT1-Rat GENFTHFHISSKFSSPETDSHRFGKHLRQAMMAIITLFGLTANSKK---------- 764

```
L-CPT1-Mouse          GENFTHFHISSKFSSPETDSHRFGKHLRQAMMAIITLFGLTANSKK-------------- 764
L-CPT1-Human          GENLINFHISSKFSCPETDSHRFGRHLKEAMTDIITLFGLSSNSKK-------------- 773
M-CPT1-Rat            GENIMFFHVSSKLSSSETNALRFGNHIRQALLDIADLFKISKTDS--------------- 772
M-CPT1-HouseMouse     GENIMFFHISSKYSSSETNAQRFGNHIRQALLDIAELFKISKTDS--------------- 772
M-CPT1-Human          GENIIFFHISSKFSSSETNAQRFGNHIRKALLDIADLFQVPKAYS--------------- 772
BrainCPT1-Mouse       GENAITFHISSKKSSTETDSHRLGQHIENALLDVASLFRVGQHFKRQFRGENSDYRYNFL 782
                             *:       :: .: .    .:  :   :

COT-Bovine            ----------------
COT-Human             ----------------
COT-Rat               ----------------
CAT-Human             ----------------
CAT-Mouse             ----------------
CAT-Pigeon            ----------------
CPT2-Rat              ----------------
CPT2-Mouse            ----------------
CPT2-Human            ----------------
L-CPT1-Rat            ----------------
L-CPT1-Mouse          ----------------
L-CPT1-Human          ----------------
M-CPT1-Rat            ----------------
M-CPT1-HouseMouse     ----------------
M-CPT1-Human          ----------------
BrainCPT1-Mouse       SCKTVDPNTPTSSTNL 798
```

8. REFERENCES

Anderson RC, (1998). Carnitine palmitoyltransferase: A viable target for the treatment of NIDDM? *Curr. Pharm. Design.* **4**: 1-16

Anderson RC, Balestra M, Bell PA, Deems RO, Fillers WS, Foley JE, Fraser JD, Mann WR, Rudin M, Villhauer EB (1995). Antidiabetic agents - a new class of reversible carnitine palmitoyltransferase-I Inhibitors. *J. Med. Chem.* **38**: 3448-3450

Aoyama T, Tsushima K, Souri M, Kamijo T, Suzuki Y, Shimozawa N, Orii T, Hashimoto T. (1994). Molecular cloning and functional expression of a human peroxisomal acyl-coenzyme A oxidase. *Biochem Biophys Res Commun* **198**: 1113-18.

Bartels GL, Remme WJ, Holwerda KJ (1996). Anti-ischaemic efficacy of L-propionyl-carnitine promising novel metabolic approach to ischaemia? *Eur Heart J.* **17**: 414–420.

Benvenga S, Ruggeri RM, Russo A, Lapa D, Campenni A, Trimarchi F (2001). Usefulness of L-carnitine, a naturally occurring peripheral antagonist of thyroid hormone action, in iatrogenic hyperthyroidism: a randomized, double-blind, placebo-controlled clinical trial. *J Clin Endocrinol Metab.* **86**(8):3579-94.

Berg, J. M., Stryer, L., and Tymoczko, J. L (2002). Biochemistry, W.H Freeman, New York.

Bieber, L. L (1988).Carnitine. Annual Review of Biochemistry **57**: 261-283.

Bieber, L. L., Emaus, R., Valkner, S. (1982). Possible functions of short-chain and medium-chain carnitine acyltransferases. *Fed. Proc.*, **41**: 2858-2861.

Bolognesi M, Amodio P, Merkel C, Godi L, Gatta A (1995). Effect of 8-day therapy with propionyl-L-carnitine on muscular and subcutaneous blood flow of the lower limbs in patients with peripheral arterial disease. *Clin Physiol.* **15**(5):417- 3.

Bonnefont J. P., Taroni F., Cavadini P., Cepanec C., Brivet M., Saudubray J. M., Leroux J. P., Demaugre F (1996). Molecular analysis of carnitine palmitoyltransferase II deficiency with hepatocardiomuscular expression. Am. *J. Hum. Genet.* **58**: 971-978.

Bonnefont, J. P., Demaugre, F., Prip-Buus, C., Saudubray, J. M., Brivet, M., Abadi, N., and Thuillier, L (1999). Carnitine palmitoyltransferase deficiencies. *Molecular Genetics and Metabolism* **68** (4): 424-440.

Brandt J. M., Djouadi F., Kelly D. P (1998). Fatty acids activate transcription of the muscle carnitine palmitoyltransferase I gene in cardiac myocytes via the peroxisome proliferator activated receptor α. *J. Biol. Chem.***273**: 23786-23792

Bremer, J (1983). Carnitine metabolism and function. *Phisiol. Rev.*, **63** (4), 1420-1480.

Brevetti G, Perna S, Sabba C, Martone VD, Condorelli M (1995). Propionyl-L-carnitine in intermittent claudication: double-blind, placebo-controlled, dose titration, multicenter study. *J Am Coll Cardiol.***26**(6):1411-6.

Calvani M, Carta A, Caruso G, Benedetti N, Iannuccelli M (1992). Action of acetyl-L-carnitine in neurodegeneration and Alzheimer's disease. *Ann N Y Acad Sci,* **21**;663:483-6.

Caponnetto S, Canale C, Masperone MA, Terracchini V, Valentini G, Brunelli C (1994). Efficacy of L-propionylcarnitine treatment in patients with left ventricular dysfunction. *Eur Heart J.* **15**(9):1267-73.

Chase JF, Tubbs PK (1970). Specific alkylation of a histidine residue in carnitine acetyltransferase by bromoacetyl-L-carnitine. *Biochem J.* **116**(4):713-20.

Chase JFA, Tubbs PK. (1966). *Biochem. J.* **99**: 32-40

Chase JFA, Tubbs PK. (1969) Conditions for the self-catalysed inactivation of carnitine acetyltransferase. *Biochem. J.* **111:** 225-235

Chatterjee B, Song CS, Kim JM, Roy AK (1988). Cloning, sequencing, and regulation of rat liver carnitine octanoyltransferase: transcriptional stimulation of the enzyme during peroxisome proliferation. *Biochemistry.* **27**(25): 9000-6.

Cherchi A, Lai C, Angelino F, Trucco G, Caponnetto S, Mereto PE, Rosolen G, Manzoli U, Schiavoni G, Reale A (1985). Effects of L-carnitine on exercise tolerance in chronic stable angina: a multicenter, double-blind, randomized, placebo controlled crossover study. *Int J Clin Pharmacol Ther Toxicol* **23**(10):569-72.

Choi YR, Fogle PJ, Clarke PR, Bieber LL (1977). Quantitation of water-soluble acylcarnitines and carnitine acyltransferases in rat tissues. *J Biol Chem* **252**(22):7930-1.

Choi, S. J., Oh, D. H., Song, C. S., Roy, A. K., and Chatterjee, B (1995). Molecular-cloning and sequence analysis of the rat liver carnitine octanoyltransferase cDNA, Its natural gene and the gene promoter. *Biochimica Et Biophysica Acta*-Gene Structure and Expression **1264** (2)**:** 215-222.

Clarke PRH, Bieber LL. (1981) Isolation and purification of mitochondrial carnitine octanoyltransferase activities from beef heart. *J. Biol. Chem.* **256**: 9861-9868

Colucci WJ, Gandour RD. (1988) Carnitine Acetyltransferase - a Review of Its biology, enzymology and bioorganic chemistry. *Bioorganic Chem.* **16:** 307-334

Corr PB, Yamada KA (1995). Selected metabolic alterations in the ischemic heart and their contributions to arrhythmogenesis. *Herz.* **20**(3):156-68.

Cox RA, Hoppel CL (1973). Biosynthesis of carnitine and 4-N-trimethylaminobutyrate from 6-N-trimethyl-lysine. *Biochem J.* **136**(4):1083-90.

Cronin, C. N (1997a). cDNA cloning, recombinant expression, and site-directed mutagenesis of bovine liver carnitine octanoyltransferase - Arg505 binds the carboxylate group of carnitine. *European Journal of Biochemistry* **247** (3)**:** 1029-1037.

Cronin, C. N (1997b). The conserved serine-threonine-serine motif of the carnitine acyltransferases is involved in carnitine binding and transition-state stabilization: A site-directed mutagenesis study. *Biochemical and Biophysical Research Communications* **238** (3)**:** 784-789.

Dal Negro R, Pomari G, Zoccatelli O, Turco P (1986). L-carnitine and rehabilitative respiratory physiokinesitherapy: metabolic and ventilatory response in chronic respiratory insufficiency. *Int J Clin Pharmacol Ther Toxicol.* **24**(8):453-6.

Davini P, Bigalli A, Lamanna F, Boem A (1992). Controlled study on L-carnitine therapeutic efficacy in post-infarction. *Drugs Exp Clin Res.* **18**(8):355-65.

Derrick, J. P., and Ramsay, R. R (1989). L-Carnitine Acyltransferase in intact peroxisomes is inhibited by malonyl-CoA. *Biochemical Journal* **262** (3)**:** 801-806.

Farrell SO, Fiol CJ, Reddy JK, Bieber LL. (1984) Properties of purified carnitine acyltransferases of mouse liver peroxisomes. *J. Biol. Chem.* **259**: 3089-3095

Faye A, Borthwick K, Esnous C, Price NT, Gobin S, Jackson VN, Zammit VA,Girard J, Prip-Buus C (2005). Demonstration of N- and C-terminal domain intramolecular interactions in rat liver carnitine palmitoyltransferase 1 that determine its degree of malonyl-CoA sensitivity. *Biochem J.* **387**(1):67-76

Ferdinandusse S, Mulders J, Ijlst L, Denis S, Dacremont G, Waterham HR, Wanders RJA. (1999). Molecular cloning and expression of human carnitine octanoyltransferase: Evidence for its role in the peroxisomal beta-oxidation of branched-chain fatty acids. *Biochem. Biophys. Res. Commun.* **263**: 213-218

Fraser F., Corstorphine C. G., Zammit V. A (1997). Topology of carnitine palmitoyltransferase I in the mitochondrial outer membrane. *Biochem. J.* **323**:711-718

Fritz IB (1963). Carnitine and its role in fatty acid metabolism. *Adv Lipid Res.* **64**:285-334.

Fritz IB, Marquis NR.(1965). The role of acylcarnitine esters and carnitine palmityltransferase in the transport of fatty acyl groups across mitochondrial membranes. *Proc Natl Acad Sci U S A.***54** (4):1226-33.

Gandour RD, Blackwell NL, Colucci WJ, Chung C, Bieber LL, Ramsay RR, Brass EP, Fronczek FR. (1992) Syntheses, structures and enzymatic evaluations

of hemiacylcarnitiniums, a new class of carnitine acyltransferase inhibitors. *J. Org. Chem.* **57:** 3426-3431

Gandour RD, Colucci WJ, Stelly TC, Brady PS, Brady LJ. (1986) Active-site probes of carnitine acyltransferases: Inhibition of carnitine acetyltransferase by hemiacetylcarnitinium, a reaction intermediate analog. *Biochem. Biophys. Res. Commun.* **138:** 735-741

Garland, P. B., D. Shepherd, D. G. Nicholls, D. W. Yates, and P. A. Light (1969). Interactions between fatty acid oxidation and the tricarboxylic acid cycle. In Citric Acid Cycle. M. Lowenstein, editor. Marcel Dekker, New York. 163-212.

Garzya G, Corallo D, Fiore A, Lecciso G, Petrelli G, Zotti C (1990). Evaluation of the effects of L-acetylcarnitine on senile patients suffering from depression. Drugs *Exp Clin Res,* **16**(2):101-6.

Giannessi F, Chiodi P, Marzi M, Minetti P, Pessotto P, De Angelis F, Tassoni E, Conti R, Giorgi F, Mabilia M, Dell'Uomo N, Muck S, Tinti MO, Carminati P, Arduini A. (2001) Reversible carnitine palmitoyltransferase inhibitors with broad chemical diversity as potential antidiabetic agents. *J. Med. Chem.* **44:** 2383-2386

Gobin S, Thuillier L, Jogl G, Faye A, Tong L, Chi M, Bonnefont JP, Girard J, Prip-Buus C. (2003) Functional and structural basis of carnitine palmitoyltransferase 1A deficiency. *J. Biol. Chem.* **278:** 50428-50434

Harano, Y., J. Kowal, R. Yamazaki, L. Lavine, and M. Miller (1972). Carnitine palmitoyltransferase activities (1and 2) and the rate of palmitate oxidation in liver mitochondria from diabetic rats. *Archi. Biochemi. Biophys.***153**: 426-437.

Heinonen OJ (1996). Carnitine and physical exercise. *Sports Med.* **22**:109–132.

Horne DW, Broquist HP(1973). Role of lysine and -N-trimethyllysine in carnitine biosynthesis. I. Studies in Neurospora crassa. *J Biol Chem*; **248**(6):2170-5.

Hu ZY, Cha SH, Chohnan S, Lane MD. (2003) Hypothalamic malonyl-CoA as a mediator of feeding behavior. *Proc. Natl. Acad. Sci. U. S. A.* **100:** 12624-12629

Iliceto S, Scrutinio D, Bruzzi P, D'Ambrosio G, Boni L, Di Biase M, Biasco G, Hugenholtz PG, Rizzon P (1995). Effects of L-carnitine administration on left ventricular remodeling after acute anterior myocardial infarction: the L-Carnitine Ecocardiografia Digitalizzata Infarto Miocardico (CEDIM) Trial. *J Am Coll Cardiol.* **26**(2):380-7.

Jenkins DL, Griffith OW. (1986) Antiketogenic and Hypoglycemic Effects of Aminocarnitine and Acylaminocarnitines. *Proc. Natl. Acad. Sci. U. S. A.* **83:** 290-294

Jogl G, Hsiao Y-S, Tong L. (2005) Crystal structure of mouse carnitine octanoyltransferase and molecular determinants of substrate selectivity. *J. Biol. Chem.* **280**: 738-744

Jogl G, Tong L. (2003) Crystal structure of carnitine acetyltransferase and implications for the catalytic mechanism and fatty acid transport. *Cell* **112**: 113-122

Kopec B, Fritz IB (1971). Properties of a purified carnitine palmitoyltransferase, and evidence for the existence of other carnitine acyltransferases. *Can J Biochem.* **49**(8):941-8

Leenders F, Tesdorpf JG, Markus M, Engel T, Seedorf U, Adamski J (1996). Porcine 80 kDa protein reveals intrinsic 17 beta-hydroxysteroid dehydrogenase, fatty

acyl-CoA hydratase/dehydrogenase, and sterol transfer activities. *J Biol Chem* **271**: 5438-42.

Linding R, Russell RB, Neduva V, Gibson TJ.(2003). GlobPlot: Exploring protein sequences for globularity and disorder. *Nucleic Acids Res.***31**(13):3701-8.

Loster H, Miehe K, Punzel M (1999). Prolonged oral L-carnitine substitution increases bicycle ergometer performance in patients with severe, ischemically induced cardiac insufficiency. *Cardiovasc Drugs Ther.* **13**: 537–546.

Markwell MA, Tolbert NE, Bieber LL (1976). Comparison of the carnitine acyltransferase activites from rat liver peroxisomes and microsomes. *Arch Biochem Biophys.* **176**(2):497-88.

Mascaro C., Acosta E., Ortiz J. A., Marrero P. F., Hegardt F. G., Haro D (1998). Control of human muscle type carnitine palmitoyltransferase I gene transcription by peroxisome proliferator activated receptor. *J. Biol. Chem.* **273**:8560-8563

McGarry JD, Brown NF(1997). The mitochondrial carnitine palmitoyltransferase system. From concept to molecular analysis. *Eur J Biochem.* **244**(1):1-14.

McGarry JD, Foster DW (1974). The metabolism of octanoylcarnitine in perfused livers from fed and fasted rats. Evidence for a possible regulatory role of carnitine acyltransferase in the control of ketogenesis. *J Biol Chem.* **249**(24):7984-90

McGarry, J. D., and D. W. Foster (1972). Regulation of ketogenesis and clinical aspects of the ketotic state. *Metab. Clin. Exp.* **21**: 471-489.

McGarry, J. D., Leatherman, G. F., and Foster, D. W (1978). The site of inhibition of fatty acid oxidation by malonyl-CoA. Journal of Biological Chemistry **253:** 4128-4136.

Miyazawa S, Ozasa H, Osumi T, Hashimoto T. (1983) Purification and properties of carnitine octanoyltransferase and carnitine palmitoyltransferase from rat liver. *J. Biochem.* **94**: 529-542

Morillas M, Clotet J, Rubi B, Serra D, Asins G, Arino J, Hegardt FG. (2000) Identification of the two histidine residues responsible for the inhibition by malonyl-CoA in peroxisomal carnitine octanoyltransferase from rat liver. *FEBS Lett.* **466:** 183-186

Morillas, M., Gomez-Puertas, P., Roca, R., Serra, D., Asins, G., Valencia, A. and Hegardt, F.G., (2001). Related articles, links structural model of the catalytic core of carnitine palmitoyltransferase I and carnitine octanoyltransferase (COT): mutation of CPT I histidine 473 and alanine 381 and COT alanine 238 impairs the catalytic activity. *J. Biol. Chem.* **276**: 45001–45008

Morillas, M., Lopez-Vinas, E., Valencia, A., Serra, D., Gomez-Puertas, P., Hegardt, F. G., and Asins, G (2004). Structural model of carnitine palmitoyltransferase I based on the carnitine acetyltransferase crystal. *Biochemical Journal* **379:** 777-784.

Murthy MSR, Ramsay RR, Pande SV. (1990) Acyl-CoA Chain-Length Affects the Specificity of Various Carnitine Palmitoyltransferases with Respect to Carnitine Analogs - Possible Application in the Discrimination of Different Carnitine Palmitoyltransferase Activities. *Biochem. J.* **267:** 273-276

Nic a'Bhaird N, Kumaravel G, Gandour RD, Krueger MJ, Ramsay RR. (1993) Comparison of the Active-Sites of the Purified Carnitine Acyltransferases from Peroxisomes and Mitochondria by Using a Reaction-Intermediate Analog. *Biochem. J.* **294:** 645-651

Nic a'Bhaird N, Ramsay RR. (1992) Malonyl-Coa Inhibition of Peroxisomal Carnitine Octanoyltransferase. *Biochem. J.* **286**: 637-640

Nic a'Bhaird N, Yankovskaya V, Ramsay RR. (1998) Active sites residues of beef liver carnitine octanoyltransferase (COT) and carnitine palmitoyltransferase (CPT-II). *Biochem. J.* **330:** 1029-1036

Nic a'Bhaird, N., and Ramsay, R. R (1992). Malonyl-CoA inhibition of Peroxisomal Carnitine Octanoyltransferase. *Biochemical Journal* **286:** 637-640.

Nic a'Bhaird, N., Kumaravel, G., Gandour, R. D., Krueger, M. J., and Ramsay, R. R (1993). Comparison of the active sites of the purified carnitine acyltransferases from peroxisomes and mitochondria by using a reaction-intermediate analog. *Biochemical Journal,* **294:** 645-651.

Nicot C, Napal L, Relat J, Gonzalez S, Llebaria A, Woldegiorgis G, Marrero PF, Haro D. (2004) C75 activates malonyl-CoA sensitive and insensitive components of the CPT system. *Biochem. Biophys. Res. Commun.* **325:** 660-664

Nicot C, Napal L, Relat J, Gonzalez S, Llebaria A, Woldegiorgis G, Marrero PF, Haro D. (2004) C75 activates malonyl-CoA sensitive and insensitive components of the CPT system. *Biochem. Biophys. Res. Commun.* **325:** 660-664

Prentki M, Corkey BE. Are the beta-cell signaling molecules malonyl-CoA and cystolic long-chain acyl-CoA implicated in multiple tissue defects of obesity and NIDDM? *Diabetes.* **45**(3):273-83

Price, N.T., van der Leij, F.R., Jackson, V.N., Corstorphine, C.G., Thomson, R., Sorensen, A. and Zammit, V., (2002). A novel brain-expressed protein related to carnitine palmitoyltransferase 1. *Genomics* **80**: 433–442

Quatraro A, Roca P, Donzella C, Acampora R, Marfella R, Giugliano D (1995). Acetyl-L-carnitine for symptomatic diabetic neuropathy. *Diabetologia.* **38**(1):123

Ramsay RR, Derrick JP, Friend AS, Tubbs PK. (1987) Purification and properties of the Soluble Carnitine Palmitoyltransferase from bovine liver mitochondria. *Biochem. J.* **244:** 271-278

Ramsay RR, Naismith JH. (2003) A snapshot of carnitine acetyltransferase. *Trends Biochem.Sci.* **28**: 343-346

Ramsay RR, Zammit VA (2004). Carnitine acyltransferases and their influence on CoA pools in health and disease.*Mol Aspects Med.* **25,**(5-6):475-93.

Ramsay RR. (2000). The carnitine acyltransferases: modulators of acyl-CoA-dependent reactions. *Biochem Soc Trans.***28** (2):182-6.

Ramsay, R. R (1988). The soluble carnitine palmitoyltransferase from bovine liver - a comparison with the enzymes from peroxisomes and from the mitochondrial inner membrane. *Biochemical Journal* **249** (1)**:** 239-245.

Ramsay, R. R (1999). The role of the carnitine system in peroxisomal fatty acid oxidation. *American Journal of the Medical Sciences* **318** (1)**:** 28-35.

Ramsay, R. R., and Bhaird,N, (1992). Malonyl-CoA inhibits purified peroxisomal carnitine octanoyltransferase at the active site. *Faseb Journal* **6** (4)**:** A1383-A1383.

Ramsay, R. R., and Gandour, R. D (1999). Selective modulation of carnitine long-chain acyltransferase activities - kinetics, inhibition and active sites of COT and CPT-II. *Adv Med Biol.* **466**: 103-109.

Ramsay, R. R., Gandour, R. D., and van der Leij, F. R (2001). Molecular enzymology of carnitine transfer and transport. *Biochimica Biophysica Acta* **1546** (1)**:** 21-43.

Richards EW, Hamm MW, Fletcher JE, Otto DA. (1990) The Binding of Palmitoyl-CoA to Bovine Serum-Albumin. *Biochimica Et Biophysica Acta* **1044**: 361-367

Sabba C, Berardi E, Antonica G, Ferraioli G, Buonamico P, Godi L, Brevetti G, Albano O (1994). Comparison between the effect of L-propionylcarnitine, L-acetylcarnitine and nitroglycerin in chronic peripheral arterial disease: a haemodynamic double blind echo-Doppler study. *Eur Heart J.* **15**(10):1348-52.

Seedorf U, Brysch P, Engel T, Schrage K, Assmann G (1994). Sterol carrier protein X is peroxisomal 3-oxoacyl coenyzme A thiolase with intrinsic sterol carrier and lipid transfer activity. *J Biol Chem* **269**: 21277-83.

Shepherd, D., D. W. Yates, and P. B. Garland (1966). The rate limiting step in the oxidation of palmitate or palmitoyl-Coenzyme A by rat-liver mitochondria. *Biochem .J.* **98**: 3c-4c.

Sitheswaran N, Price NT, Ramsay RR. (2005) The G553M mutant of peroxisomal carnitine octanoyltransferase catalyses acetyl transfer and acetyl-CoA hydrolysis. *Chemical Monthly, **136**,(8), 1341-1349.*

Solberg HE (1971). Carnitine octanoyltransferase. Evidence for a new enzyme in mitochondria. *FEBS Lett.* **12**(3):134-136.

Tanphaichitr V, Horne DW, Broquist HP (1971). Lysine, a precursor of carnitine in the rat. *J Biol Chem.***246**(20):6364-6.

Taroni, F., Verderio, E., Fiorucci, S., Cavadini, P., Finocchiaro, G., Uziel, G., Lamantea, E., Gellera, C., and Didonato, S (1992). Molecular Characterization of Inherited Carnitine Palmitoyltransferase-Ii Deficiency. *Proceedings of the National Academy of Sciences of the United States of America.* **89** (18)**:** 8429-8433.

Thal LJ, Calvani M, Amato A (2000). A 1-year controlled trial of acetyl-l-carnitine in early-onset AD. *Neurology*. **55**: 805–810.

Thupari JN, Landree LE, Ronnett GV, Kuhajda FP. (2002) C75 increases peripheral energy utilization and fatty acid oxidation in diet-induced obesity. *Proc. Natl. Acad. Sci. U. S. A.* **99:** 9498-9502

Van der Leij FR, Huijkman NC, Boomsma C, Kuipers JR, Bartelds B (2000). Genomics of the human carnitine acyltransferase genes. *Mol Gene Metab*. **71** (1-2): 139-153.

van Roermund CWT, Elgersma Y, Singh N, Wanders RJA, Tabak HF. (1995) The Membrane of Peroxisomes in Saccharomyces-Cerevisiae Is Impermeable to NADH and Acetyl-CoA under in-Vivo Conditions. *EMBO J.* **14**: 3480-3486

van Roermund CWT, Hettema EH, van den Berg M, Tabak HF, Wanders RJA. (1999) Molecular characterization of carnitine-dependent transport of acetyl-CoA from peroxisomes to mitochondria in Saccharomyces cerevisiae and identification of a plasma membrane carnitine transporter, Agp2p. *EMBO J.* **18**: 5843-5852

Verhoeven NM, Schor DS, Roe CR, Wanders RJ, Jakobs C (1998). Pristanic acid beta-oxidation in peroxisomal disorders: studies in cultured human fibroblasts. *Biochim Biophys Acta.* **1391**(3):351-6.

Wanders RJ, Denis S, van Roermund CW, (1992). Characteristics and subcellular localization of pristanoyl-CoA synthetase in rat liver. *Biochim Biophys Acta* **1125**: 274-9.

Wanders, R. J. A., Vreken, P., Ferdinandusse, S., Jansen, G. A., Waterham, H. R., van Roermund, C. W. T., and Van Grunsven, E. G (2001). Peroxisomal fatty acid alpha- and beta-oxidation in humans: enzymology, peroxisomal metabolite transporters and peroxisomal diseases. *Biochemical Society Transactions* **29:** 250-267.

Williamson JR, Walajtys-Rode E, Coll KE (1979). Effects of branched chain alpha-ketoacids on the metabolism of isolated rat liver cells. I. Regulation of branched chain alpha-ketoacid metabolism. *J Biol Chem.* **254**(22):11511-20.

Yamazaki, N., Shinohara, Y., Shima, A. and Terada, H., (1995). High expression of a novel carnitine palmitoyltransferase I-like protein in rat brown adipose tissue and heart: isolation and characterization of its cDNA clone. *FEBS Lett.* **363**, 41–45

Young MJ, Boulton AJM, Macleod AF (1993) A multicentre study of the prevalence of diabetic peripheral neuropathy in the United Kingdom hospital clinic population. *Diabetalogica,* **36**:150-154.

Yu G. S., Lu Y.C., Gulick T (1998). Expression of novel isoforms of carnitine palmitoyltransferase I (CPT-I) generated by alternative splicing of the CPTI-Iß gene. *Biochem. J.* **334**:225-231

Zammit V. A. (1999). Carnitine acyltransferases: functional significance of subcellular distribution and membrane topology. *Prog. Lipid Res.*, **38**, 199-224.